

UNCLASSIFIED

AD NUMBER

ADB015615

LIMITATION CHANGES

TO:

Approved for public release; distribution is unlimited.

FROM:

Distribution authorized to U.S. Gov't. agencies only; Test and Evaluation; DEC 1976. Other requests shall be referred to Air Force Propulsion Lab., Edwards AFB, CA.

AUTHORITY

AFRPL ltr 15 May 1986

THIS PAGE IS UNCLASSIFIED

AD B0 15-615-

AUTHORITY:

AFRPL

15 MAR 86



AD NO. 9

DDC FILE COPY

AD B015615

AFRPL-TR-76-8

## ► CHEMICAL LASER SOLID FUELS PROGRAM

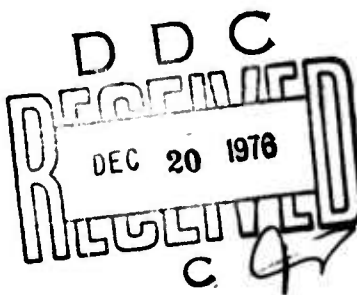
## FINAL REPORT

**AUTHORS: CAPT. JOHN E. O'PRAY  
CAPT. RONALD E. CHANNELL  
OR. FRANCISCO Q. ROBERTO**

DECEMBER 1976

**DISTRIBUTION LIMITED TO U.S. GOVT. AGENCIES ONLY. TEST AND EVALUATION  
5 OCTOBER 1976. OTHER REQUESTS FOR THIS DOCUMENT MUST BE REFERRED  
TO AFRPL (STINFO)/DOZ, EDWARDS AFB CALIFORNIA 93523.**

**AIR FORCE ROCKET PROPULSION LABORATORY  
DIRECTOR OF SCIENCE AND TECHNOLOGY  
AIR FORCE SYSTEMS COMMAND  
EDWARDS AFB, CALIFORNIA 93523**



## NOTICES

When U.S. Government drawings, specifications, or other data are used for any purpose other than a definitely related government procurement operation, the Government thereby incurs no responsibility nor any obligation whatsoever, and the fact that the Government may have formulated, furnished, or in any way supplied the said drawings, specifications or other data, is not to be regarded by implication or otherwise, or in any manner licensing the holder or any other person or corporation, or conveying any rights or permission to manufacture, use, or sell any patented invention that may in any way be related thereto.

## FOREWORD

This report was prepared by the Air Force Rocket Propulsion Laboratory, Edwards AFB, California 93523 under JON 332606ML.

This technical report is approved for release and distribution in accordance with the distribution statement on the cover and on the DD Form 1473.

*John E O'Pray*  
JOHN E. O'PRAY, CAPT., USAF  
Author

*Ronald E. Channell*  
RONALD E. CHANNELL, CAPT., USAF  
Author

*Francisco Q. Roberto*  
Dr. FRANCISCO Q. ROBERTO  
Author

*Calvin R. Dexter*  
CALVIN R. DEXTER, MAJOR, USAF, Chief  
Components & Design Branch

FOR THE COMMANDER

*Charles R. Cooke*  
CHARLES R. COOKE, Director  
Solid Rocket Division



## UNCLASSIFIED

SECURITY CLASSIFICATION OF THIS PAGE (When Data Entered)

14) REPORT DOCUMENTATION PAGE		READ INSTRUCTIONS BEFORE COMPLETING FORM
1. REPORT NUMBER AFRPL-TR-76-82	2. GOVT ACCESSION NO. 9 3. SUBJEC <sup>9</sup> T CATALOG NUMBER	4. TYPE OF REPORT & PERIOD COVERED November 1971 - October 75
5. TITLE (and subtitle) 6) Chemical Laser Solid Fuels Program	6. PERFORMING ORG. REPORT NUMBER	7. AUTHOR(s) Capt John E. O'Pray, Capt Ronald E. Channell Dr. Francisco Q. Roberto
8. CONTRACT OR GRANT NUMBER(s)	9. PERFORMING ORGANIZATION NAME AND ADDRESS Air Force Rocket Propulsion Laboratory/AFSC Edwards AFB, California 93523	10. PROGRAM ELEMENT, PROJECT, TASK AREA & WORK UNIT NUMBERS 11) 332606ML 12) 06
11. CONTROLLING OFFICE NAME AND ADDRESS	12. REPORT DATE 11) December 1976	13. NUMBER OF PAGES 177 12) 181
14. MONITORING AGENCY NAME & ADDRESS (if different from Controlling Office)	15. SECURITY CLASS. FOR THIS REPORT UNCLASSIFIED	15a. DECLASSIFICATION/DOWNGRADING SCHEDULE
16. DISTRIBUTION STATEMENT (of this Report) Distribution limited to U.S. Govt. agencies only. Test and Evaluation 5 October 1976. Other requests for this document must be referred to AFRPL(STINFO)/DOZ, Edwards AFB, California 93523.	17. DISTRIBUTION STATEMENT (of the abstract entered in Block 20, if different from Report) Approved for public release: Distribution unlimited	
18. SUPPLEMENTARY NOTES		
19. KEY WORDS (Continue on reverse side if necessary and identify by block number) Laser Deuterium Fluoride Deuterium Generator Chemical Laser Chemical Laser Fluorine generator Solid Fuel Laser Gas generator Nitrogen generator Solid Propellant Laser Solid Prop. Gas Generator Hydrogen generator		
20. ABSTRACT (Continue on reverse side if necessary and identify by block number) The first successful demonstrations of solid propellant gas generators for chemical lasers were carried out under this in-house program conducted jointly by the Air Force Rocket Propulsion Laboratory and the Air Force Weapons Laboratory. Because of their inherent storability and simplicity, solid propellant gas generators have potential advantages as reactant sources for chemical lasers compared to the alternatives of reactant storage as high pressure gases or cryogenic liquids. Solid propellant gas generators which can supply all of the		

**UNCLASSIFIED**

SECURITY CLASSIFICATION OF THIS PAGE(When Data Entered)

reactants for a deuterium fluoride (DF) chemical laser were developed. The reactants required by the laser were generated from separate solid propellant gas generators and then fed into a conventional, combustion-driven, super-sonic flow DF laser. The deuterium laser cavity fuel, the nitrogen trifluoride plus fluorine oxidizer, the hydrogen precombustor fuel and the nitrogen diluent were supplied from four separate solid propellant gas generators. In addition to the low power lasing demonstrations conducted with all four types of gas generators, the solid propellant deuterium generators were scaled-up to the flow rates required for multi-hundred watt DF lasers.

**UNCLASSIFIED**

SECURITY CLASSIFICATION OF THIS PAGE(When Data Entered)

## CONTENTS

<u>Section</u>		<u>Page</u>
I	Introduction .....	7
II	Deuterium and Hydrogen Generators .....	14
	A. Deuterium and Hydrogen Generator Formulations .....	14
	B. Deuterium and Hydrogen Generator Formulation Processing Scaleup and Hazards Testing.....	34
	C. Deuterium and Hydrogen Gas Generators.....	48
III	Fluorine Gas Generators.....	73
	A. Fluorine Generator Formulations .....	73
	B. Fluorine Generator Formulation Processing.....	100
	C. $\text{NF}_3 + \text{F}_2$ Gas Generator .....	102
IV	Nitrogen Gas Generators.....	109
	A. Nitrogen Generator Formulations .....	109
	B. Nitrogen Generator Formulation Processing.....	113
	C. Nitrogen Gas Generators.....	114
V	Lasing Demonstrations with Solid Propellant Gas Generators .....	119
	A. Hydrogen Generator Lasing Demonstration at AFWL.....	120
	B. Deuterium and Nitrogen Generator Lasing Demonstrations Using AFRPL Laser with Throat Injection Nozzle.....	125
	C. Nitrogen Trifluoride Plus Fluorine, Deuterium, Hydrogen, and Nitrogen Gas Generator Lasing Demonstrations Using AFRPL XCL5 IF Laser .....	144
	D. High Power DF Lasing Demonstration at AFWL Using AFRPL Mod 2 High Flow Rate Deuterium Generators .....	170
	References .....	176

## ILLUSTRATIONS

<u>Figure</u>	<u>Page</u>
1 Solid Propellant Gas Generators for DF Chemical Lasers.....	10
2 Effect of LiAlH <sub>4</sub> to NH <sub>4</sub> Cl Ratio on Combustion Temperature and H <sub>2</sub> Weight Yield .....	16
3 Effect of Fe <sub>2</sub> O <sub>3</sub> Content on Combustion Temperature and H <sub>2</sub> Weight Yield .....	17
4 Effect of Fe <sub>2</sub> O <sub>3</sub> Content on Burning Rate.....	19
5 Packing Pressure Effect in Grain Density - 3LAD2 Formulation .....	30
6 Burning Rate Versus Pressure, D <sub>2</sub> Generator Formulations .....	32
7 "Walk-In" Drybox for Processing Scaleup Batches of Deuterium and Hydrogen Generator Formulations .....	37
8 Formulation Mixer and Hydraulic Grain Press Inside Drybox .....	39
9 Thermal Stability Test Grain of 3LAH2 Formulation After 24 Hours at 75°C in Air Beside Baseline Grain .....	46
10 Evaluation of Deuterium Gas Generators .....	49
11 Mod 1 Deuterium Generator - Schematic .....	52
12 Mod 1 Deuterium Gas Generator - Detailed Cross Section .....	55
13 Deuterium Metering Nozzle Assembly .....	59
14 Oscillograph Data Traces for Two Tests of Grains of 3LAD2 Formulation with Different Ingredient Particle Sizes in Mod 1 Deuterium Generator .....	62
Figure 14a. Test 532, Particle Size < 74 $\mu\text{m}$	
Figure 14b. Test 533, Particle Size < 105 $\mu\text{m}$	
15 Combustion Noise Comparison Between Grains of 3LAD2 Formulation with Ingredient Particle sizes < 74 $\mu\text{m}$ and < 105 $\mu\text{m}$ .....	64
Figure 15a. Test 531, Particle Size < 74 $\mu\text{m}$ .	
Figure 15b. Test 535, Particle Size < 105 $\mu\text{m}$ .	

ILLUSTRATIONS (Continued)

<u>Figure</u>		<u>Page</u>
16	Cross Section of Mod 2 High Flow Rate Deuterium Generator.....	67
17	Mod 2 High Flow Rate Deuterium Generator with Grain of 3LAD2 Formulation .....	69
18	Oscillograph Data Traces for Mod 2 Deuterium Generator Test with 3LAD2 Grain .....	71
19	Comparison of Fluorine Generator Approaches .....	75
20	Theoretical Combustion Properties of $\text{NF}_4\text{BF}_4$ /Polytetra-fluoroethylene Formulations .....	94
21	$\text{NF}_3 + \text{F}_2$ Gas Generator .....	103
22	Burning Rate Data for $\text{NF}_3\text{SbF}_6/\text{CsF}/\text{AlN}$ Formulation from Tests of 2.54 cm (1.0 in) Diameter Grains in $\text{NF}_3 + \text{F}_2$ Gas Generator .....	108
23	Pressure Trace for Nitrogen Generator Test (No. 502) .....	117
24	AFRPL First Generation Hydrogen Generator Coupled to AFWL Subsonic Flow HF Laser for the First Lasing Demonstration .....	121
25	Comparison of Laser Output Power Using Hydrogen From Solid Propellant Gas Generator and From Compressed Gas Feed System.....	124
26	Cryopump System for AFRPL Laser Tests .....	127
27	Cross Section of AFRPL Low Power DF- $\text{CO}_2$ or DF Chemical Laser with Throat Injection Nozzle .....	132
28	Throat Injection Nozzle Assembly Looking Upstream Toward Throat.....	134
29	Secondary Injection Orifices Along Nozzle Throat .....	135
30	Spraybar Combustor Injector for AFRPL Laser with Throat Injection Nozzle .....	136
31	AFRPL Low Power DF- $\text{CO}_2$ or DF Laser with Throat Injection Nozzle .....	137
32	Cross Section of AFRPL "XCL5" Low Power DF Chemical Laser .....	146
33	XCL5 Nozzle Assembly from Laser Cavity Side .....	148

ILLUSTRATIONS (Continued)

<u>Figure</u>		<u>Page</u>
34	XCL5 Combustor Injector .....	150
35	Overall View of XCL5 Laser System .....	151
36	Oscillograph Data for XCL5 Compressed Gas Baseline Lasing Test No. 450 .....	158
37	Nitrogen, "Fluorine" ( $NF_3 + F_2$ ), Deuterium, and Hydrogen Gas Generators Used for Lasing Demonstration on the XCL5 Laser .....	160
38	Oscillograph Record of XCL5 Lasing Test No. 451 with Mod 1 Deuterium Generator .....	162
39	"Fluorine" ( $NF_3 + F_2$ ), Deuterium, and Hydrogen Gas Generators Coupled to XCL5 Laser .....	163
40	Oscillograph Record of XCL5 Compressed Gas Baseline Lasing Test No. 500-2 .....	165
41	Oscillograph Record of First Lasing Test with $NF_3 + F_2$ Gas Generator (Test No. 501) .....	166
42	Oscillograph Record of Multiple Gas Generator Test No. 542 .....	169
43	AFRPL Mod 2 Deuterium Generator Coupled to AFWL Supersonic Flow DF Laser for High Power Lasing Demonstration .....	171
44	Laser Power and Deuterium Mass Flow Rate Histories for the First Mod 2 Deuterium Generator Lasing Test on the AFWL DF Laser.....	173

## TABLES

<u>Table</u>		<u>Page</u>
1	Theoretical Combustion Products of Hydrogen Generating Formulations With and Without Hydrocarbon Binder .....	21
2	Mass Spectrometer Analysis of Hydrogen and Deuterium Generator Gas Samples .....	24
3	Deuterium Generator Gas Sampling Data .....	27
4	AFRPL Deuterium and Hydrogen Generator Scaleup Formulations 3LAD2 ( $D_2$ ) and 3LAH2 ( $H_2$ ).....	31
5	Deuterium Generator Formulation Isotopic Purity Throughout the Processing Cycle .....	41
6	Comparison of Experimental and Theoretical Combustion Products from $NF_4BF_4$ /Polytetrafluoroethylene Formulations.....	96
7	Comparison of Combustion Product Properties for $F_2$ , $NF_3$ , and $NF_4BF_4$ Oxidizers .....	155
8	Effect of Combustor Gas Properties on the Power Output of the XCL5 Laser .....	156

## SECTION I

### INTRODUCTION

The first successful demonstration of solid propellant gas generators for chemical lasers was carried out under this in-house program which was supported jointly by the Air Force Rocket Propulsion Laboratory (AFRPL) and the Air Force Weapons Laboratory (AFWL). The overall objective of this interlaboratory program was to demonstrate the feasibility of using solid propellant gas generators to supply the reactants for deuterium fluoride (DF) chemical lasers. The solid propellant gas generator development was conducted at the Rocket Propulsion Laboratory, and lasing demonstrations were conducted at both laboratories.

There are three primary motivations for developing solid propellant gas generators for chemical lasers. The first is the inherent storability and simplicity of solid propellant gas generators compared to the alternatives of storing the reactants as high pressure, ambient temperature gases or as cryogenic liquids. The second incentive is the elimination of the hazards of handling elemental fluorine which is extremely reactive either as high pressure gas or a cryogenic liquid and which was the original baseline oxidizer for DF chemical lasers before the far less

hazardous oxidizer nitrogen trifluoride was available in sufficient quantities. The third motivation is minimization of the volume required for storage of the laser's deuterium and hydrogen, both of which have low density even as cryogenic liquids.

The overall approach for this initial feasibility demonstration program was to identify and formulate promising gas generating solid compositions, to design and test small gas generators using these formulations, and then to conduct low power lasing demonstrations using reactants supplied from these gas generators. An overall constraint was that the gas generators should match demonstrated chemical laser operating conditions. Thus, the propellant development effort emphasized those formulations which could supply reactants at pressures, temperatures, and purities which were compatible with demonstrated chemical laser designs. Each of the laser reactants is supplied from a separate gas generator.

The possibility of using a single solid propellant gas generator to supply a nonequilibrium gas mixture suitable for chemical lasing was investigated during the initial phase of this interlaboratory program. As is described in Reference 1, all attempts to devise a chemical laser operating from a single solid propellant gas generator were unsuccessful. Therefore, the multiple gas generator approach was adopted.

As shown in Figure 1, a typical combustion-driven, supersonic-flow cold-reaction DF chemical laser requires four separate reactant gases. The laser combustor thermally generates the fluorine atoms required for the lasing reaction by combusting a fluorinated oxidizer such as elemental fluorine or nitrogen trifluoride with a fuel such as hydrogen or a hydrocarbon. A diluent is also injected into the combustor. Typically, DF lasers operate with helium diluent for maximum specific power. Nitrogen diluent, which can be generated from a solid formulation, can also be used although the laser performance is significantly degraded with nitrogen instead of helium diluent. The mixture of fluorine atoms, diluent, and precombustion products expands through an array of supersonic nozzles into the low pressure laser cavity region. Molecular deuterium is injected through a separate array of nozzles, and the vibrationally excited DF lasing molecules are formed in the reaction zones between the two sets of supersonic gas streams.

Developing the four types of gas generating formulations required to feed such a DF laser was a difficult task. The first problem is that chemical laser performance is very sensitive to contaminants in the reactant gases. Relatively small concentrations of contaminants which have high deactivation rates for vibrationally excited DF can seriously degrade the laser performance. Unfortunately, "conventional" solid rocket propellants in which all of the combustion products are gaseous

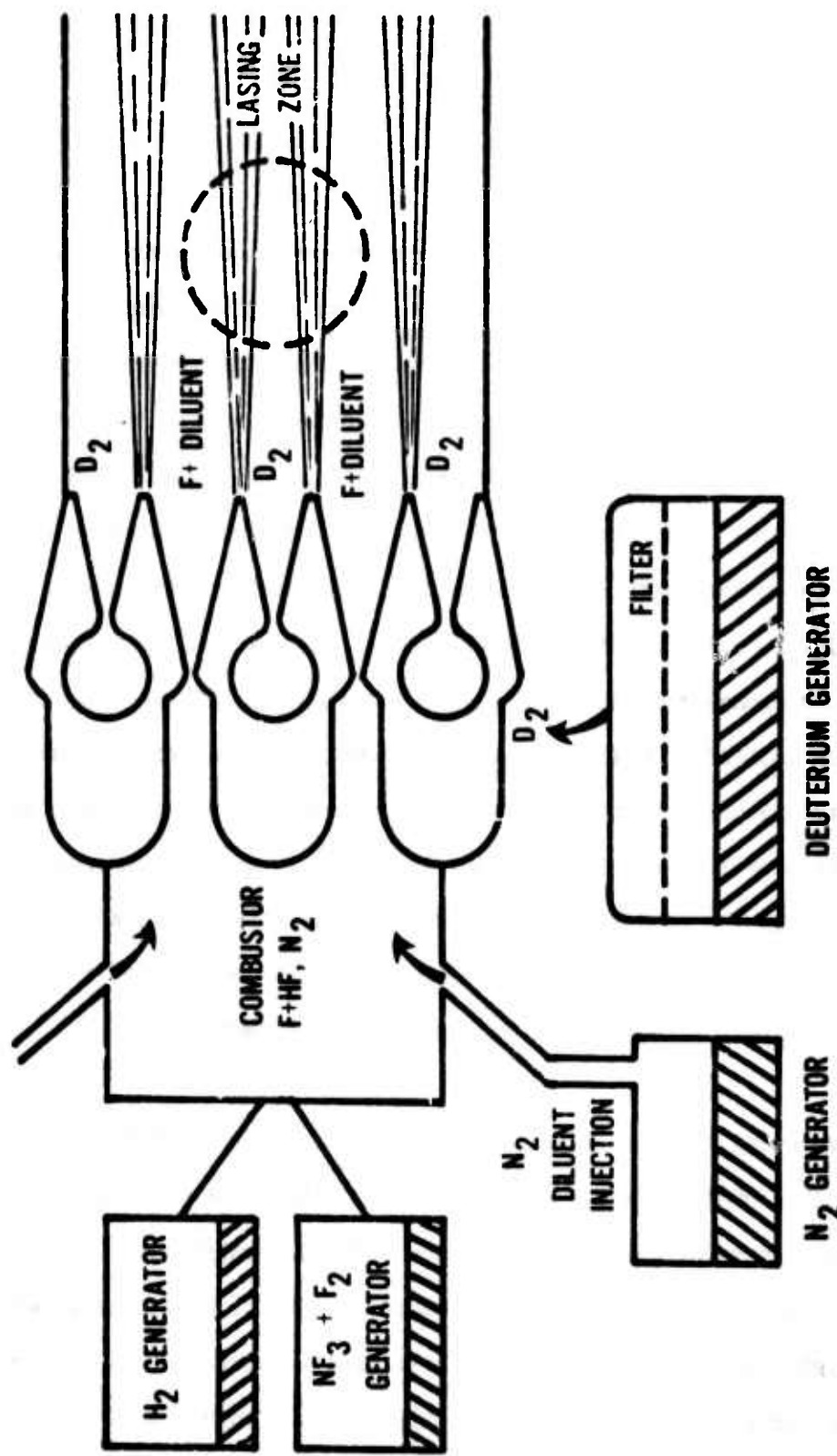


Figure 1. Solid Propellant Gas Generators for DF Chemical Lasers

generate multi-component, heavily contaminated combustion product mixtures. Therefore, generating high purity reactants suitable for chemical lasers requires highly unconventional solid formulations. Thus, even though the term "propellant" is frequently used when referring to the solid formulations developed for laser gas generators, these formulations have very little resemblance to conventional solid rocket propellants.

There were two aspects of the problem of developing solid formulations which produce reactants pure enough for laser applications. The first aspect was the identification of deactivating species which should be excluded from the gaseous combustion products. The primary data input for this aspect of the propellant development problem was from the AFWL-sponsored HF and DF deactivation rate measurements. Additional deactivation kinetics data on potential constituents was obtained from the general kinetics literature.

The second aspect of the problem, once undesirable molecular species were identified, was the identification of formulations which could supply maximum concentrations of laser reactants with minimum concentrations of deactivating secondary constituents. The first step in the formulation process was the usual equilibrium thermochemistry analysis. However, this was only the first step, particularly where highly unconventional formulations were concerned. The second step was combustion

characterization at the gram scale. This combustion characterization included obtaining burn rate and pressure exponent data as a function of composition. An essential third step in the formulation development process was actual sampling of the combustion products from promising formulations. A major asset for this interlaboratory project was a unique molecular beam type mass spectrometer which is described in Reference 2. This instrument is capable of direct sampling of reactive species from atmospheric pressure flames. It identifies highly reactive or condensable species, such as fluorine atoms or sodium vapor, which are important in laser gas generator formulations. Sampling data of this quality provided a sound basis for concluding that a formulation was indeed suitable for use in a laser gas generator.

The next step in demonstrating the feasibility of each laser gas generator formulation was to conduct a lasing demonstration using the reactant gas supplied from the solid propellant gas generator. For most of the initial lasing demonstrations, only one solid propellant gas generator was used, and the other laser reactants were fed from conventional compressed gas reactant supply systems. However, lasing was also demonstrated with up to three of the four reactants required for a DF laser supplied simultaneously from separate solid propellant gas generators.

As is described in detail in Section V, lasing demonstrations were conducted using four different chemical lasers. The pioneering lasing demonstration using a solid propellant hydrogen generator was conducted at AFWL on a low power, subsonic flow laser operating in the HF chemical laser mode. The first lasing demonstrations using solid propellant deuterium and nitrogen generators were conducted at AFRPL on a low power chemical laser with a single nozzle which had cavity fuel injection orifices at the throat. This laser was operated in both the DF-CO<sub>2</sub> transfer chemical laser mode and the DF chemical laser mode using the deuterium and nitrogen generators. Subsequent deuterium generator tests and the first lasing demonstrations using a solid propellant gas generator to supply the nitrogen trifluoride plus fluorine oxidizer were conducted on a second low power DF laser at AFRPL. This second design used a more conventional DF laser nozzle configuration with separate oxidizer and cavity fuel nozzles. The final lasing demonstrations using scaled-up deuterium generators were conducted on a kilowatt power range, supersonic flow DF laser at AFWL.

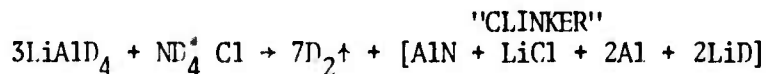
## SECTION II

### DEUTERIUM AND HYDROGEN GENERATORS

#### II.A. DEUTERIUM AND HYDROGEN GENERATOR FORMULATIONS

Formulations which generate high purity deuterium or hydrogen were developed. These formulations generate hydrogen or deuterium from the reaction between ammonium chloride and lithium aluminum hydride or the deuterated analogs of the two compounds. Essentially all of the reaction products except the deuterium or hydrogen gas are retained in the gas generator as a cohesive, sintered "clinker". The AFRPL deuterium and hydrogen generating formulations are derived from hydrogen generating formulations which were developed for inflating rescue marker balloons by the Naval Surface Weapons Center (NSWC), Indian Head, MD (References 3, 4). However, the original NSWC hydrogen generator formulations contained a stoichiometric mixture of sodium aluminum hydride and ammonium chloride plus an excess of lithium aluminum hydride. Because sodium aluminum deuteride is much less readily available and significantly more expensive than lithium aluminum deuteride, the AFRPL deuterium generating formulations used only lithium aluminum deuteride.

with the deuteroammonium chloride. The basic reaction for the deuterium generating formulation is given below.



For the actual gas generator formulations, the combustion products are more complex because iron oxide is added to increase the burning rate and a hydrocarbon polymer binder is added to increase the cohesiveness of larger gas generator grains.

In order to define the theoretical combustion properties of the hydrogen and deuterium generating formulations, extensive equilibrium thermochemistry calculations were performed using the AFRPL thermochemistry computer program (Reference 5). Both the ratio of  $\text{LiAlH}_4$  to  $\text{NH}_4\text{Cl}$  and the  $\text{Fe}_2\text{O}_3$  content strongly affect the reaction temperature. As is illustrated in Figure 2, the reaction temperature peaks near the stoichiometric ratio of one mole  $\text{LiAlH}_4$  per mole of  $\text{NH}_4\text{Cl}$  and decreases as excess  $\text{LiAlH}_4$  is added. The weight yield of hydrogen gas which is also plotted in Figure 2 is a weaker function of the  $\text{LiAlH}_4$  to  $\text{NH}_4\text{Cl}$  ratio. All of the data shown in Figure 2 were calculated for an  $\text{Fe}_2\text{O}_3$  content of 3.94 mole percent. The calculations were performed at a pressure of 344.8 kPa (50 psia), but both the theoretical and experimental combustion properties of these "clinker" type formulations are quite insensitive to pressure. As is illustrated in Figure 3, at a

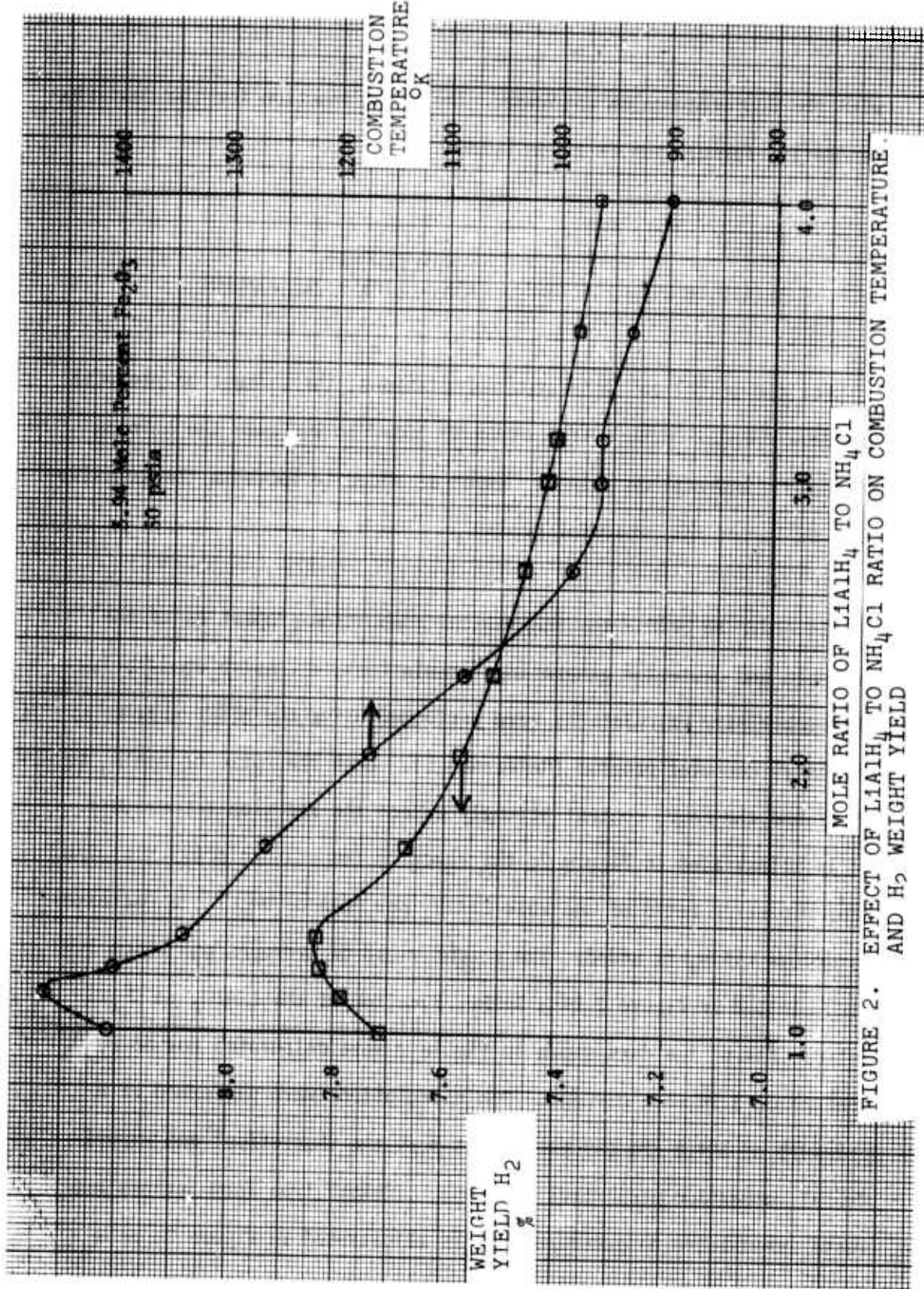


FIGURE 2. EFFECT OF LiAlH<sub>4</sub> TO NH<sub>4</sub>Cl RATIO ON COMBUSTION TEMPERATURE AND H<sub>2</sub> WEIGHT YIELD

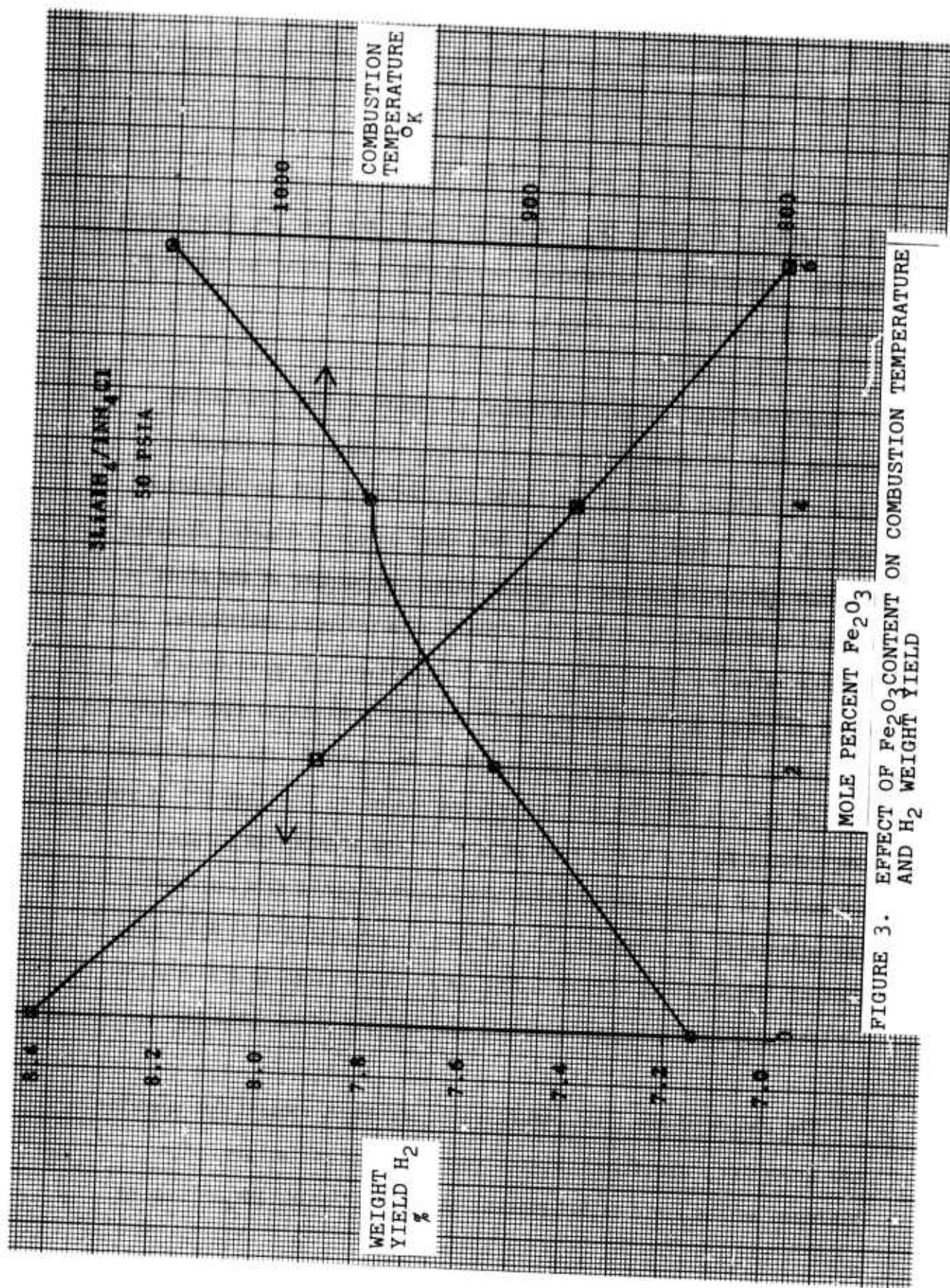
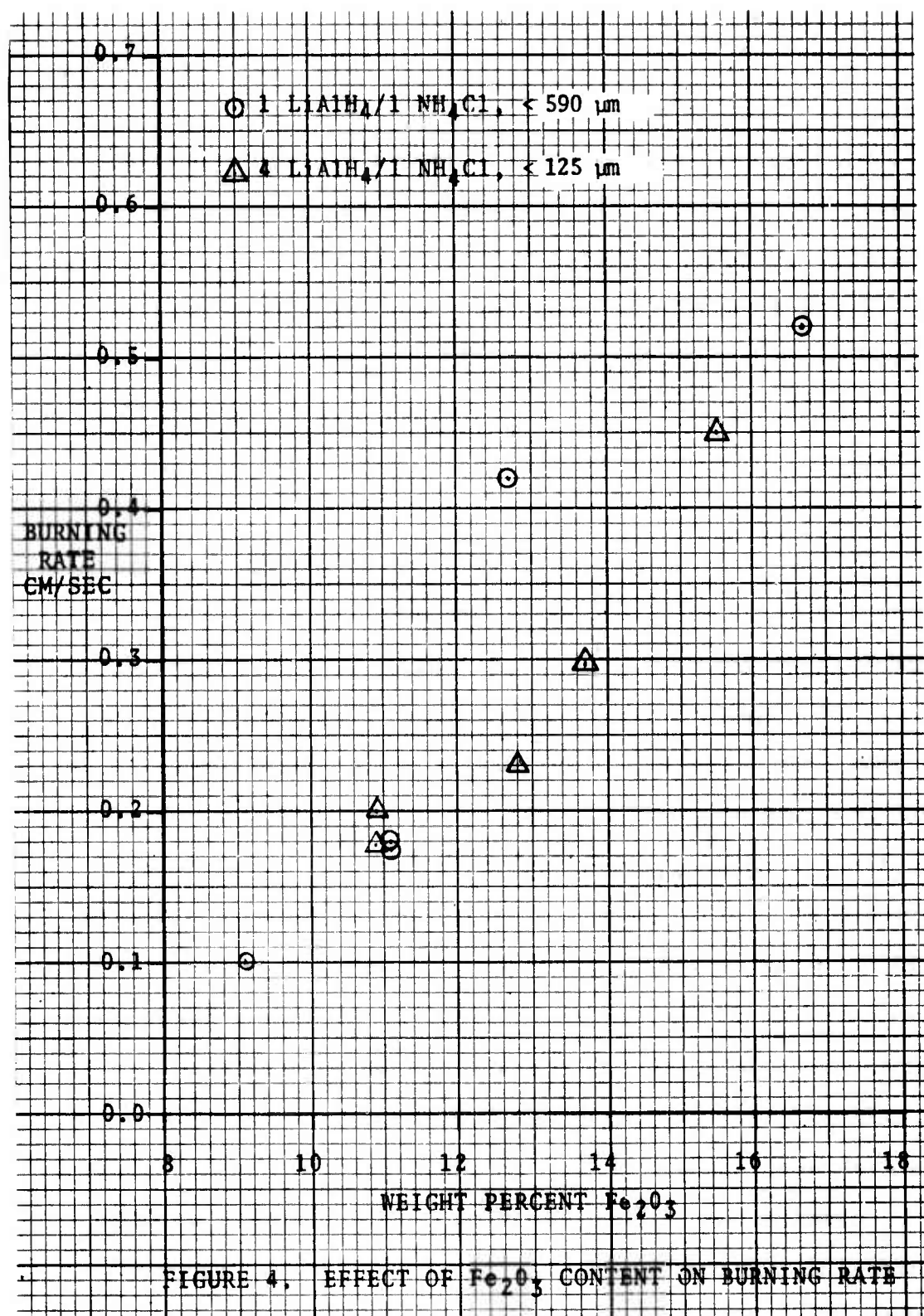


FIGURE 3. EFFECT OF  $Fe_2O_3$  CONTENT ON COMBUSTION TEMPERATURE AND  $H_2$  WEIGHT YIELD

fixed ratio of  $\text{LiAlH}_4$  to  $\text{NH}_4\text{Cl}$  equal to three, the reaction temperature increases rapidly and the hydrogen weight yield decreases as the  $\text{Fe}_2\text{O}_3$  content is increased from zero to six mole percent.

Experimentally, as is illustrated in Figure 4, the formulation burning rate increases rapidly as the  $\text{Fe}_2\text{O}_3$  content is increased. Figure 4 includes data for two  $\text{LiAlH}_4:\text{NH}_4\text{Cl}$  ratios and two ingredient particle size ranges. All of the data are for one centimeter diameter end burning samples pressed in glass tubes and burning at the AFRPL ambient pressure of 91.7 kPa (13.3 psia) in a nitrogen atmosphere. The burning rates for the  $4\text{LiAlH}_4:1\text{NH}_4\text{Cl}$  formulations are approximately equal to those for the  $1\text{LiAlH}_4:1\text{NH}_4\text{Cl}$  formulations at the same weight percent  $\text{Fe}_2\text{O}_3$ . For the data points shown in Figure 4, the finer particle size of the 4:1 formulations (ground and sieved to less than 125 micrometers) compensates for the higher heat release of the  $1\text{LiAlH}_4:1\text{NH}_4\text{Cl}$  stoichiometry of the 1:1 formulations which were prepared from coarser ingredients (< 590 micrometers). At the same particle size and  $\text{Fe}_2\text{O}_3$  content, formulations with an  $\text{LiAlH}_4:\text{NH}_4\text{Cl}$  ratio close to 1:1 characteristically have a higher burning rate than 3:1 or 4:1 formulations.

The choice of the  $\text{LiAlH}_4:\text{NH}_4\text{Cl}$  ratio and  $\text{Fe}_2\text{O}_3$  content for specific gas generator formulations depends upon a number of factors. The hydrogen weight yield is 3.9 percent higher at  $1\text{LiAlH}_4:1\text{NH}_4\text{Cl}$  than at



$3\text{LiAlH}_4:\text{1NH}_4\text{Cl}$  (7.71 percent and 7.42 percent hydrogen weight yield, respectively). However, the cohesiveness of the residue "clinker" is significantly better at  $\text{LiAlH}_4:\text{NH}_4\text{Cl}$  ratios of 3:1 or 4:1. Furthermore, as will be discussed below, mass spectrometer analysis of the gases generated by  $1\text{LiAlH}_4:\text{1NH}_4\text{Cl}$  formulations detected significant ammonia contamination of the hydrogen which does not occur for  $3\text{LiAlH}_4:\text{1NH}_4\text{Cl}$  or  $4\text{LiAlH}_4:\text{1NH}_4\text{Cl}$  formulations.

The theoretical combustion products for two hydrogen generating formulations are given in Table 1. The molar ratios of  $\text{LiAlH}_4$  to  $\text{NH}_4\text{Cl}$  and  $\text{Fe}_2\text{O}_3$  are identical in both formulations, but 0.57 mole percent of hydrocarbon binder is present in the second formulation. The hydrocarbon binder increases the cohesiveness of the pressed formulation for use in larger gas generator grains. The binder is "Kraton - Type 1107", a styrene-isprenene copolymer (nominal "molar" unit  $\text{C}_{20}\text{H}_{20}$ ) which is produced by Shell Oil Company. The non-gaseous combustion residue or "clinker" is a mixture of liquid and solid combustion products which are designated by (L) and (C), respectively. This mixture of liquid and solid combustion products is essential for the formation of a cohesive clinker which will completely retain the non-gaseous combustion products and yet remain sufficiently porous to allow the hydrogen gas produced in the combustion zone to flow readily through the previously combusted zone of the gas generator grain. An excessively molten clinker will slump and splatter liquid residue because of excessive pressure buildup

TABLE 1  
THEORETICAL COMBUSTION PRODUCTS OF HYDROGEN GENERATING  
FORMULATIONS WITH AND WITHOUT HYDROCARBON BINDER

<u>FORMULATION</u> (Mole %)	<u>NO BINDER</u>	<u>WITH BINDER</u>
LiAlH <sub>4</sub>	71.99	71.58
NH <sub>4</sub> Cl	24.07	23.93
Fe <sub>2</sub> O <sub>3</sub>	3.94	3.92
C <sub>20</sub> H <sub>20</sub> (Binder)	0.00	0.57
LiAlH <sub>4</sub> :NH <sub>4</sub> Cl	2.991	2.991
COMBUSTION TEMPERATURE, °K	961°	986°
<u>COMBUSTION PRODUCTS</u> (Mole %)		
<u>GASEOUS</u>		
H <sub>2</sub>	53.97	56.75
CH <sub>4</sub>	0.00	0.02
<u>"CLINKER"</u>		
Al(L)	13.25	8.63
LiH(L)	5.56	13.49
LiH(C)	7.69	0.00
LiCl(L)	7.59	7.72
AlN(C)	7.59	7.73
Fe(C)	2.49	2.53
LiAlO <sub>2</sub> (C)	1.86	1.90
Al <sub>4</sub> C <sub>3</sub> (C)	0.00	1.22

(L) - Liquid

(C) - Crystalline

within the grain. Formulations with insufficient concentrations of liquid constituents in the combustion products will "dust"-eject substantial quantities of solid particulates from the residue. For the formulations without binder, both liquid and solid lithium hydride are present in the clinker at the 961°K combustion temperature, which is the melting point of LiH. However, in the formulation with binder which has a combustion temperature 25°K higher, all of the LiH is molten. In Figure 2, the plateau in the combustion temperature curve near an  $\text{LiAlH}_4:\text{NH}_4\text{Cl}$  ratio of 3:1 corresponds to this 961°K melting point of LiH.

The equilibrium thermochemistry calculations predict that these hydrogen generating formulations, both with and without hydrocarbon binder, will produce very high purity hydrogen. For the formulation without binder, equilibrium thermochemistry predicts no gaseous contaminants with concentrations greater than 0.01 mole percent. For the formulation with binder, a trace of methane (less than 0.04 mole percent of the gaseous products) is predicted to be the only gaseous contaminant of the hydrogen evolved from the formulation.

Experimentally, very high purity hydrogen is indeed produced by the AFRPL hydrogen generating formulations which have  $\text{LiAlH}_4:\text{NH}_4\text{Cl}$  ratios of 3:1 to 4:1. Gas purity was determined by capturing samples of the gas

generator effluent in standard gas sample cylinders and then analyzing the samples with a mass spectrometer. This sampling technique accurately determines the gas composition generated by the AFRPL gas generator formulations which have combustion temperatures in the 800-1000°K range, and, therefore, do not produce any highly condensable gaseous species. However, for hotter formulations for which the equilibrium thermochemistry calculations predict that gaseous LiCl monomer and dimer plus LiH will appear in percent concentrations, this sampling technique is invalid because of contaminant condensation on the walls of the sampling apparatus.

An example of the hydrogen purity obtained from a  $4\text{LiAlH}_4:1\text{NH}_4\text{Cl}$  formulation is given in Table 2A. The gas sample was 99.5 mole percent  $\text{H}_2$ , with fractions of a percent  $\text{N}_2$ , CO, and  $\text{CH}_4$ . Residual traces of the ether solvent in which the  $\text{LiAlH}_4$  is synthesized are believed to have contributed to the slight contamination by CO and  $\text{CH}_4$ . The equilibrium thermochemistry calculation for this 4:1 formulation predicts no gaseous contaminants with concentrations greater than 0.0005 percent.

In contrast to the high purity hydrogen generated by the  $4\text{LiAlH}_4:1\text{NH}_4\text{Cl}$  formulation, the  $1\text{LiAlH}_4:1\text{NH}_4\text{Cl}$  formulation given in Table 2B generates hydrogen significantly contaminated by ammonia. The 6.8-7.0 mole percent  $\text{NH}_3$  in the 1:1 formulation gas samples is a concentration which is over three orders of magnitude higher than the 0.001 percent

TABLE 2

MASS SPECTROMETER ANALYSIS OF HYDROGEN  
GENERATOR GAS SAMPLES

FORMULATION	COMBUSTION PRODUCTS	
	SPECIES	CONCENTRATION (MOLE %)
A. $4\text{LiAlH}_4 : 1\text{NH}_4\text{Cl}$		
77.6 Mole % $\text{LiAlH}_4$	$\text{H}_2$	99.5
19.4 Mole % $\text{NH}_4\text{Cl}$	$\text{N}_2$	0.2
3.0 Mole % $\text{Fe}_2\text{O}_3$	CO	0.2
	$\text{CH}_4$	0.1
B. $1\text{LiAlH}_4 : 1\text{NH}_4\text{Cl}$	Test 4/12/72-1	Test 4/12/72-2
47.3 Mole % $\text{LiAlH}_4$	$\text{H}_2$	93.2
47.3 Mole % $\text{NH}_4\text{Cl}$		93.0
5.4 Mole % $\text{Fe}_2\text{O}_3$	$\text{NH}_3$	6.8
		7.0

$\text{NH}_3$  predicted by equilibrium thermochemistry. All of the gas sampling data in Table 2 were obtained from four gram samples of the formulations which were combusted at 13.3 psia. Because of this ammonia contamination problem for formulations with  $\text{LiAlH}_4:\text{NH}_4\text{Cl}$  ratios near 1:1, the AFRPL  $\text{H}_2$  and  $\text{D}_2$  generator formulation development effort concentrated on formulations with ratios of 3:1 or 4:1.

For the deuterium generator formulations, two additional factors affect the purity of the deuterium gas produced from the solid grain. The first factor is the isotopic purity of the  $\text{LiAlD}_4$  and  $\text{ND}_4\text{Cl}$ . These deuterated compounds are most readily commercially available at 98 percent isotopic purity (the deuterium isotope ( $\text{H}^2$ ) comprises 98 percent of all the hydrogen isotopes in the compound, and hydrogen ( $\text{H}^1$ ) comprises the remaining 2 percent). The "technical grade" compressed gaseous deuterium which is normally used for DF laser testing is also of 98 percent isotopic purity. Periodically, gas samples from the thermal decomposition of neat  $\text{LiAlD}_4$  were analyzed to verify that the batches of  $\text{LiAlD}_4$  supplied to AFRPL indeed met the 98 percent isotopic purity specification.

For the formulations containing binder, the second factor affecting gas purity is the additional hydrogen contamination from the hydrocarbon polymer. Deuterated binder polymers are not currently commercially

available and therefore the standard Kraton hydrocarbon polymer was used for the deuterium generating formulations. Table 3 illustrates the deuterium purity which can be achieved with formulations containing hydrocarbon binder. The mean isotopic composition of the gas generator effluent is 94.71 percent deuterium and 5.29 percent hydrogen. The majority of the hydrogen appears in the isotopically mixed molecule HD (9.72 percent), and only 0.43 percent appears as H<sub>2</sub>. This isotopic composition agrees very well with the theoretical composition of 95.08 percent deuterium and 4.92 percent hydrogen which is calculated assuming that the LiAlD<sub>4</sub> and ND<sub>4</sub>Cl are of 98 percent isotopic purity. The isotope exchange reactions which result in the hydrogen appearing principally as HD occur as the hydrogen from the binder pyrolysis and the deuterium from the LiAlD<sub>4</sub> and ND<sub>4</sub>Cl mix and flow out from the combustion zone through the hot (934°K), porous clinker. Sampling results from all three tests are very consistent. The gas samples were obtained at the outlet of a gas generator containing 16.16 gram, end-burning grains, 4.45 cm (1.75 in) in diameter, which were burned at 344.8-448.2 kPa (50-65 psia). The 3.1 weight percent Kraton binder in this 4LiAlD<sub>4</sub>:1ND<sub>4</sub>Cl formulation is sufficient to provide highly cohesive pressed grains.

Experimentally, the weight yield of deuterium gas is in close agreement with the yield predicted by equilibrium thermochemistry. The

TABLE 3  
DEUTERIUM GENERATOR GAS SAMPLING DATA

		<u>FORMULATION</u> (mole percent)	
$\text{LiAlD}_4^*$	76.40		
			$\text{LiAlD}_4:\text{ND}_4\text{Cl} = 4.0:1$
$\text{ND}_4\text{Cl}^*$	19.10		
$\text{Fe}_2\text{O}_3$	3.91		$T_{\text{comb}} = 934^\circ\text{K}$
$\text{C}_{20}\text{H}_{20}$ (Binder)	0.59		
		<u>GAS SAMPLE ANALYSIS</u> (mole percent)	
TEST NO.	483	484	485
$\text{D}_2$	89.38	90.17	90.00
$\text{HD}$	10.20	9.40	9.56
$\text{H}_2$	0.42	0.43	0.44
<u>ISOTOPIC PURITY</u>			
	THEORETICAL*	EXPERIMENTAL (MEAN)	
$\text{D}$	95.08	94.71	
$\text{H}$	4.92	5.29	

\* $\text{LiAlD}_4$  and  $\text{ND}_4\text{Cl}$  Nominally 98% Isotopic Purity

weight yield was determined by combusting formulation samples and capturing all of the deuterium evolved in a calibrated volume which was coupled to the gas generator. The deuterium yield was calculated from the pressure change and temperature in the calibrated volume. A set of seven combustion tests of a  $4\text{LiAlD}_4:1\text{ND}_4\text{Cl}$  formulation produced very consistent deuterium yield data. The formulation in mole percent was: 76.97  $\text{LiAlD}_4$ , 19.17  $\text{ND}_4\text{Cl}$ , and 3.85  $\text{Fe}_2\text{O}_3$ . The combustion sample weights ranged from 9.3 to 9.7 grams, and the observed deuterium weight yields were between 13.11 and 13.35 percent. For these seven tests, the mean weight yield was  $13.24 \pm 0.09$  percent which is 97.72 percent of the theoretical weight yield of 13.55 percent for this formulation. The formulation samples were pressed into 3.30 cm (1.3-in) diameter discs at packing pressures ranging from 3.45 to 20.7 MPa (500 to 3000 psi) and were combusted at pressures ranging from 414 to 1379 kPa (60 to 200 psia). The particle size distributions for the formulations were < 147 micrometers for one sample and 43-147 micrometers for the other six samples. The close agreement in deuterium weight yield between these seven samples demonstrates that the packing pressure, combustion pressure, and ingredient particle size have little influence on the deuterium weight yield.

However, the packing pressure and particle size do have a significant influence on the burning rate of the formulations and a weaker

influence on the average density of the pressed grains. The effect of particle size and packing pressure on the average density of 4.45 cm (1.75 in) diameter grains is shown in Figure 5. For the nine grains with the ingredients ground and sieved to less than 147 micrometers, the grain density increases by 7.7 percent for a 67 percent increase in packing pressure from 10.34 to 17.24 MPa (1500 to 2500 psi). The experimental scatter in density among the five nominally identical grains (< 147 micrometer particle size) packed at 13.79 MPa (2000 psi) is 2 percent. At 10.34 MPa (1500 psi), the two grains with mixtures of < 147 micrometer and < 43 micrometer ingredients packed to the highest density. All of the grain density data in Figure 5 is for the formulation designated 3LAD2 which was used in the deuterium generator scaleup tests. The composition of the 3LAD2 deuterium generator formulation and the analogous hydrogen generator formulation designated 3LAH2 are given in Table 4.

The burning rate of the 3LAD2 formulation is shown in Figure 6. The burning rate is a function of the ingredient particle size and the grain pressing pressure as well as the combustion pressure. A comparison of the three data points for the grains packed at 10.34 MPa (1500 psi) with the ingredients ground and sieved to less than 74 micrometers and the three data points for grains packed at the same pressure but with the ingredients ground and sieved to less than 105 micrometers illustrates the increase in burning rate and burning rate exponent with

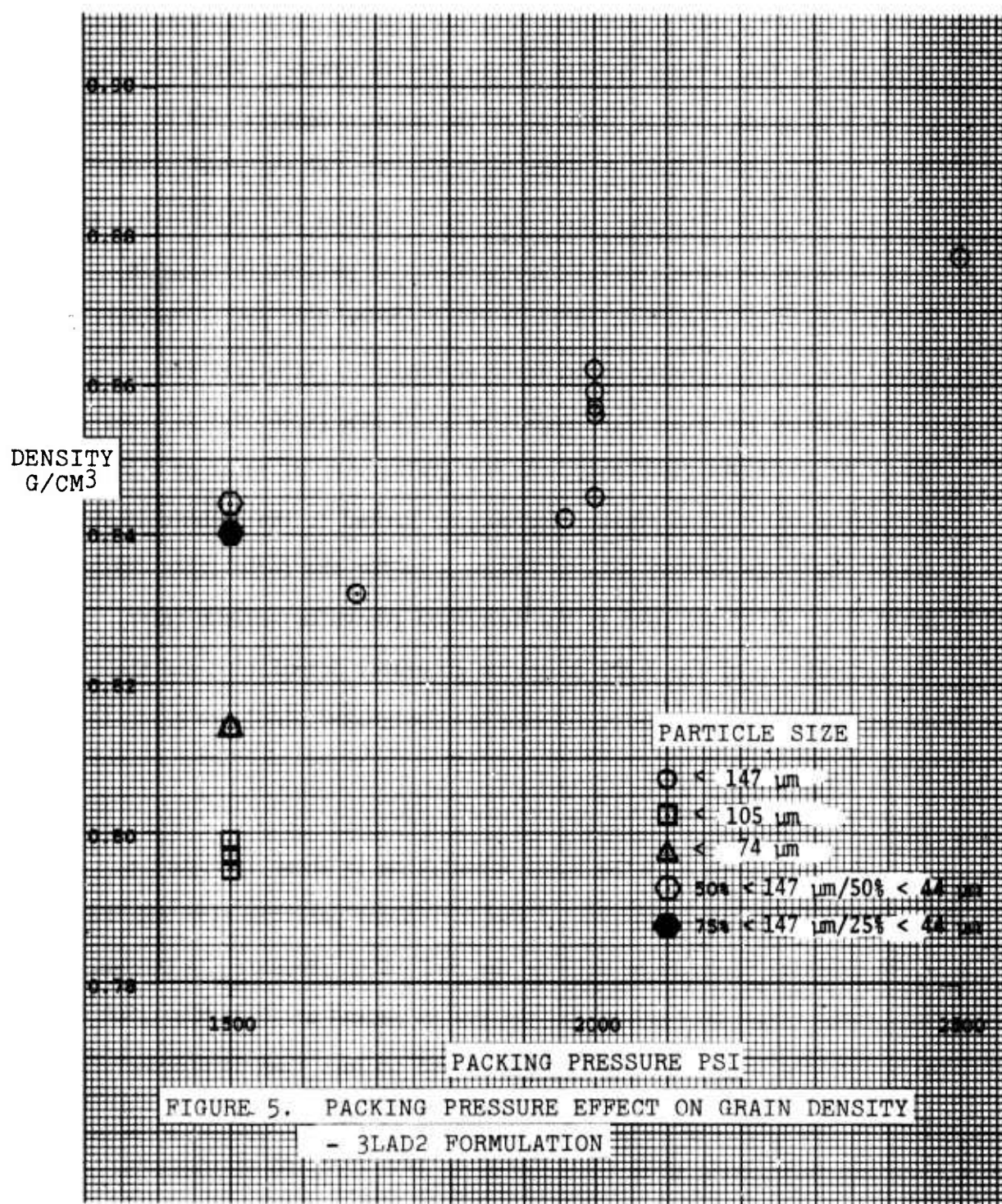


TABLE 4

AFRPL DEUTERIUM AND HYDROGEN GENERATOR  
SCALEUP FORMULATIONS 3LAD2 ( $D_2$ ) and 3LAH2 ( $H_2$ )

## 3LAD2 FORMULATION

$LiAlD_4$	58.0 Weight %
$ND_4Cl$	26.6 Weight %
$Fe_2O_3$	12.0 Weight %
Kraton <sub>(1)</sub>	3.4 Weight %

## 3LAH2 FORMULATION

$LiAlH_4$	56.8 Weight %
$NH_4Cl$	26.8 Weight %
$Fe_2O_3$	13.0 Weight %
Kraton <sub>(1)</sub>	3.4 Weight %

(1) Shell Oil Company "Kraton Type 1107" Styrene-isoprene Co-polymer

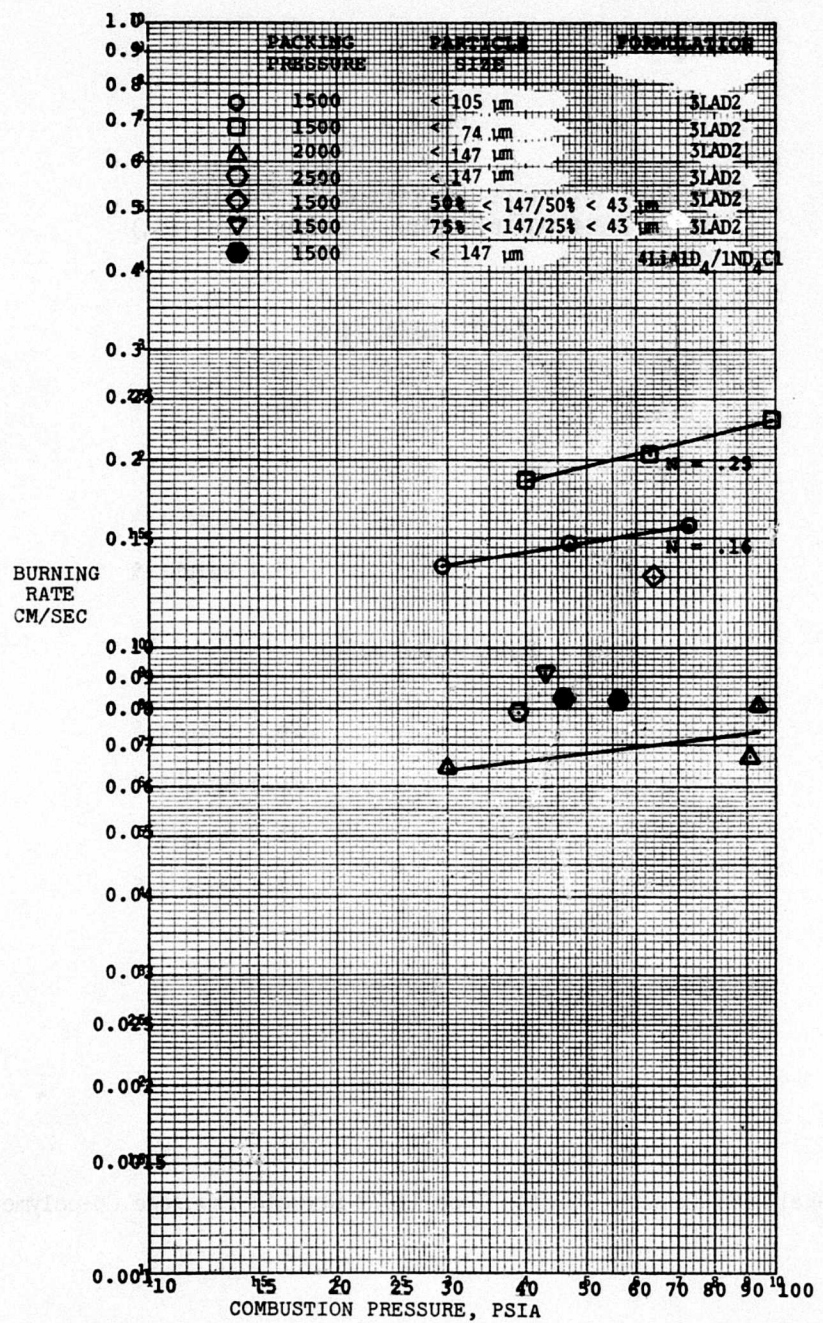


FIGURE 6. BURNING RATE VERSUS PRESSURE,  $\text{D}_2$  GENERATOR FORMULATIONS

the more finely ground ingredients. The burning rate of the grains with the ingredient particle size less than 74 micrometers is approximately 33 percent higher at 379.2 kPa (55 psia), and the pressure exponent of the burning rate,  $n$ , is 0.25 for the < 74 micrometer grains compared to  $n = 0.16$  for the < 105 micrometer grains. The three data points for grains with the coarsest particle size (< 147 micrometers, 13.79 MPa (2000 psi) packing pressure) are more than a factor of two lower in burning rate than the grains with < 105 micrometer ingredient particle size. Adding very finely ground (< 43 micrometer) ingredients to the coarse (< 147 micrometer) ingredients significantly increased the burning rate as is shown by the two burn rate data points for grains containing 50 percent and 25 percent by weight of the < 43 micrometer ingredients. However, the formulation batches with ingredients ground to < 43 micrometers were quite sensitive to ignition by friction during processing, a problem which did not occur with the less finely ground ingredients. Two burning rate data points for a formulation with an  $\text{LiAlD}_4:\text{ND}_4\text{Cl}$  molar ratio of 4:1 instead of the 3:1 ratio of the 3LAD2 formulation are also included in Figure 6. All of the burning rate data points in Figure 6 were obtained from 4.445 cm (1.75 in) diameter end-burning grains which were combusted in the Mod 1 high flow rate  $\text{D}_2$  gas generator hardware which is described in Section II.C. As is also discussed in Section II.C., the grains formulated with the coarsest ingredients (< 147 micrometers) frequently exhibited very low frequency (2-5

Hz) oscillations in gas generator pressure with amplitudes of from 5 to 20 percent of the average chamber pressure.

## II.B. DEUTERIUM AND HYDROGEN GENERATOR FORMULATION PROCESSING SCALEUP AND HAZARDS TESTING

The initial deuterium and hydrogen generator formulations were processed by hand inside benchtop-scale nitrogen atmosphere dryboxes. Because lithium aluminum hydride and deuteride react with atmospheric moisture, the entire formulation and grain preparation sequence was conducted inside the drybox. Separate dryboxes were used for the deuterated ingredients and the normal hydrogen containing ingredients in order to avoid isotopic cross-contamination. The dryboxes were equipped with continuous recirculation drying trains which used a bed of synthetic zeolite material (Linde 'Molecular Sieve') to remove water contamination from the nitrogen atmosphere. Moisture levels in the dryboxes were monitored with aluminum oxide thin-film type humidity sensors. The moisture level in the dryboxes was very low, and the frost point was typically between -70°C and -100°C. The formulation ingredients were ground separately by hand in a mortar and pestle and then sieved to the required particle size range. The initial formulations were then mixed by hand and pressed into gas generator grains using a hand-operated mechanical press.

In preparation for the high flow rate deuterium generator tests in the spring and summer of 1975, the formulation processing was scaled up to 200 gram batches of the deuterium generating formulation 3LAD2 and the hydrogen generating formulation 3LAH2 which are detailed in Table 4. The  $\text{LiAlD}_4$  or  $\text{LiAlH}_4$ ,  $\text{ND}_4\text{Cl}$  or  $\text{NH}_4\text{Cl}$ , and  $\text{Fe}_2\text{O}_3$  for these scaleup batches were still ground and sieved by hand in the small dryboxes. The quantity of each of these three ingredients required for the formulations was then placed in an appropriate size polyethylene bottle and mixed for thirty minutes to one hour by attaching the bottle to a rotating mixer operating at approximately sixty revolutions per minute. The binder solution for the 3LAD2 and 3LAH2 formulations was prepared separately from the inorganic ingredients. The binder solution was prepared by dissolving 32 grams of the Shell Kraton binder in 400 milliliters of toluene which had been previously dried with calcium hydride and distilled.

For the 100 and 200 gram scaleup batches, the final mixing of the dry ingredients with the binder solution was conducted in the large "walk-in" nitrogen atmosphere drybox shown in Figure 7. Formulation ingredients, gas generator components, and tools were passed into the drybox through the two airlocks at the right and left center of the photo. Items within the drybox could be handled directly through the glove ports in the drybox windows or remotely using mechanical manipulator arms which penetrated the shield wall on the far side of the

drybox. For equipment installation or maintenance, this drybox could be entered through a large "walk-in" door which is located to the right of the area shown in Figure 7. The water content of the nitrogen atmosphere in this drybox was kept at very low levels by dual continuous recirculation drying trains using synthetic zeolite beds for moisture absorption. The volume of this "walk-in" drybox was sufficient to prevent a hazardous pressure buildup in the event of an accidental ignition of a 200 gram formulation batch and the subsequent generation of large volumes of warm deuterium or hydrogen gas. Batch mixing and grain pressing were conducted remotely from behind the blast wall at the far side of the drybox.

The propellant mixer and hydraulic press which are visible in the upper left window of the drybox in Figure 7 are shown in closeup in Figure 8. The hydraulic press assembly is on the right, the Baker-Perkins Vertical Planetary Mixer is on the left, and the scale which was used to weigh the ingredients and finished grains is visible in the lower center of the photo.

Processing of the 200 gram formulation batches required approximately two hours per batch. The premixed dry ingredients were placed in the bowl of the planetary mixer and the binder solution was then added. The formulation was then mixed at ambient temperature and pressure at

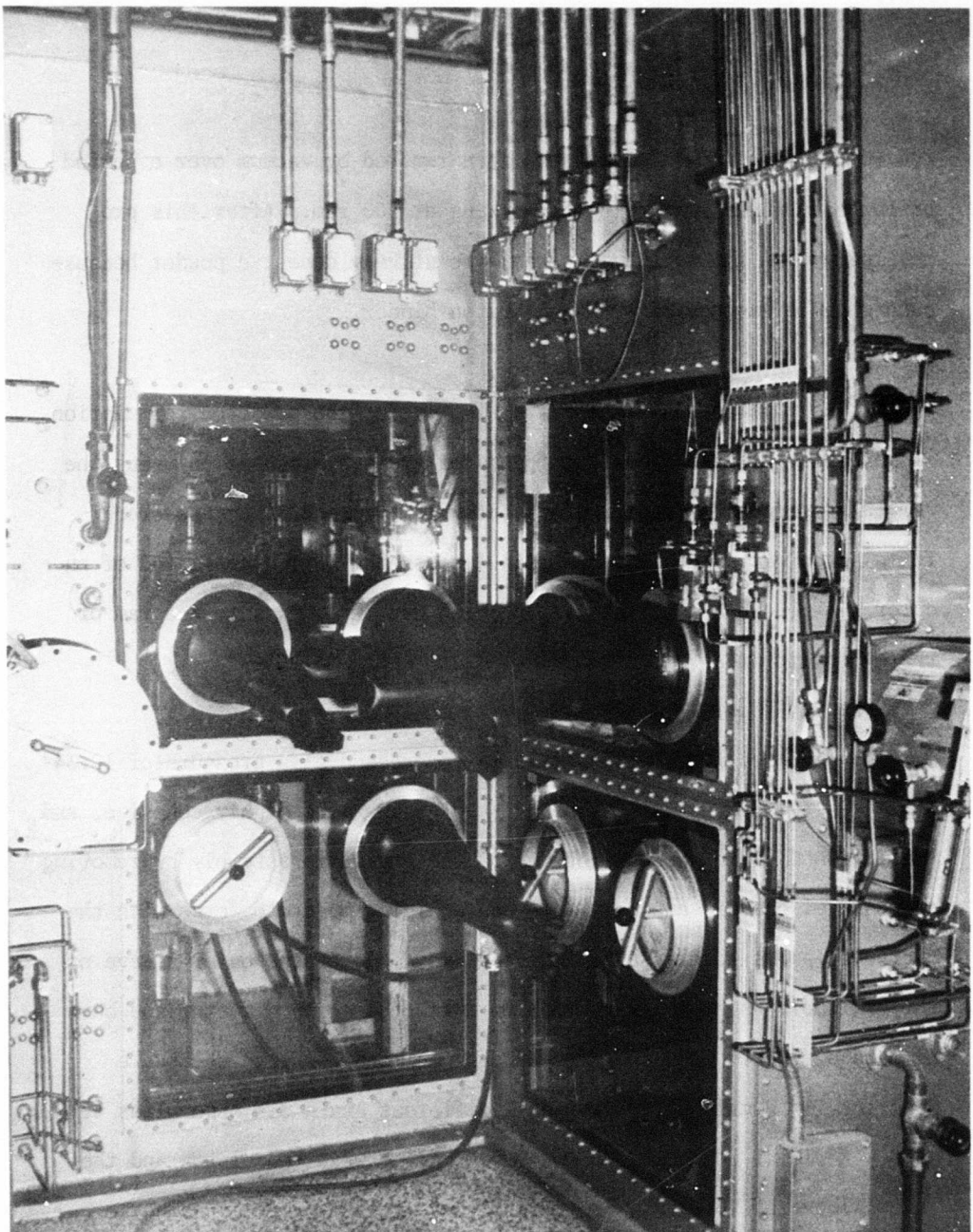


Figure 7. "Walk-in" Drybox for Processing Scaleup Batches of Deuterium and Hydrogen Generator Formulations.

300 rpm. The toluene solvent was then removed by vacuum over a period of one hour while continuing the mixing at 300 rpm. After this processing cycle, the formulation was a relatively cohesive powder because each granule was coated with the Kraton binder.

As the final step in the processing cycle, the powdered formulation was pressed into the final gas generator grain configuration using the remotely operated hydraulic press shown in Figure 8. The powdered formulation was placed into a grain die assembly which consisted of an outer sleeve and a matching piston which was threaded into the ram of the hydraulic press.

The powdered formulation was then compressed at a pressure of 10.34-17.24 MPa (1500-2500 psi). The pressed grains were highly cohesive, and the finished grains were removed from the grain die assembly by removing the base of the die assembly and then applying moderate force with the hydraulic press to press the finished grain out of the outer sleeve of the grain die assembly. In order to match the grain diameter and burn time requirements of the different gas generator designs which are described in Section II.C., several different grain die assemblies were used. A radial gap of 0.178 mm (0.007 in) between the piston and the outer sleeve of the grain die assembly was found to be a reasonable compromise between formulation "extrusion" through larger gaps and

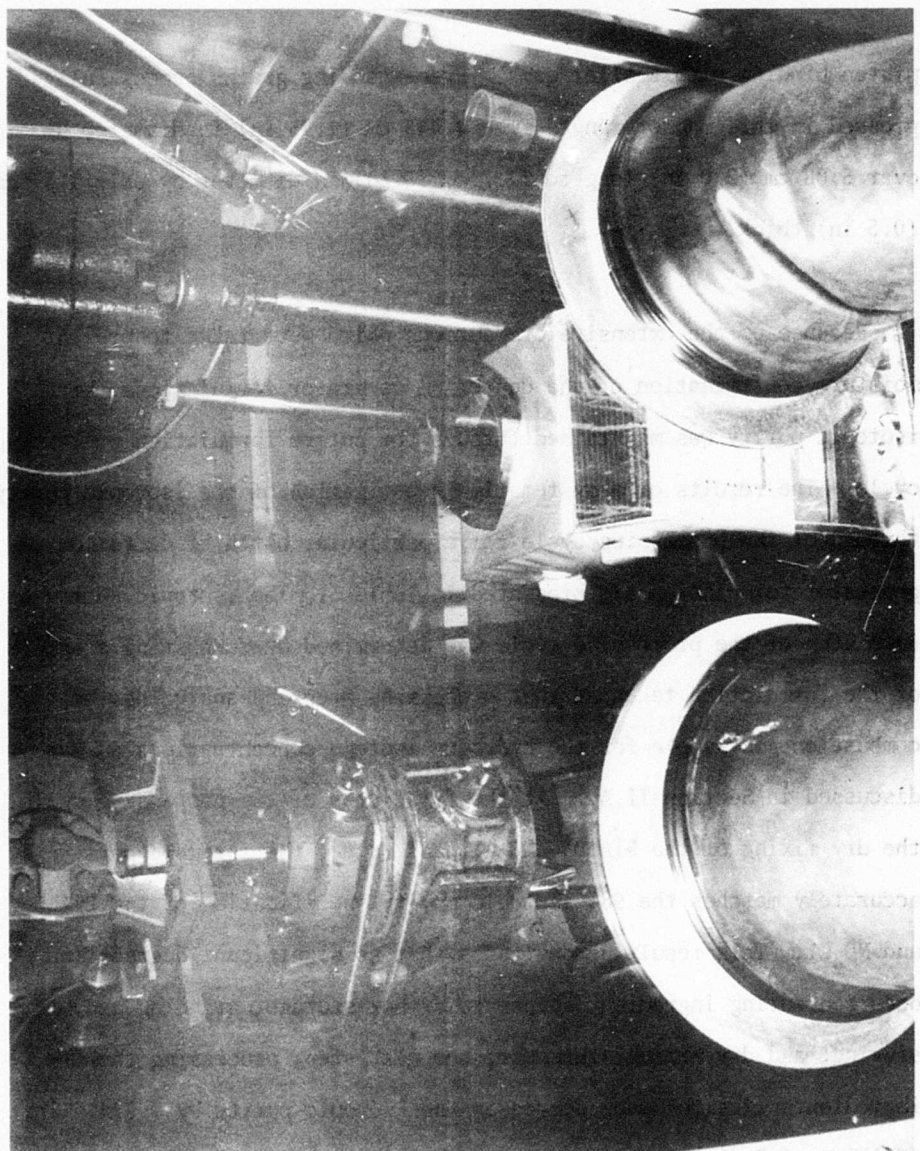


Figure 8. Formulation Mixer and Hydraulic Grain Press Inside Drybox

piston binding with smaller gaps. Free-standing grains successfully pressed in this manner ranged from 4.445 cm (1.75 in) in diameter by over 5.08 cm (2.0 in) long to 12.7 cm (5 in) in diameter by only 1.27 cm (0.5 in) thick.

Because of the extensive precautions which were taken to prevent moisture contamination of the deuterium generator formulations, high isotopic purity was maintained through the entire formulation processing cycle. The results of a systematic investigation of the isotopic purity throughout the processing cycle for a particular batch of deuterium generator formulation are presented in Table 5. The isotopic purity at each step of the processing cycle was determined by combusting a sample of the formulation taken at that processing step and analyzing the combustion gas sample for the hydrogen isotope concentrations as was discussed in Section II.A.. At the first step of the processing cycle, the dry mixing of the LiAlD<sub>4</sub>, ND<sub>4</sub>Cl, and Fe<sub>2</sub>O<sub>3</sub>, the isotopic purity accurately matches the 98% isotopic purity specification of the LiAlD<sub>4</sub> and ND<sub>4</sub>Cl. This result demonstrates that no significant degradation occurred during ingredient shipment, drybox storage, grinding and sieving, and dry mixing. However, the next step, processing the dry ingredients with toluene, decreases the isotopic purity by 0.92%. The addition of 3.41 weight percent Kraton hydrocarbon binder to the toluene in the wet mix processing step of the cycle decreases the deuterium

TABLE 5

DEUTERIUM GENERATOR FORMULATION ISOTOPIC PURITY  
THROUGHOUT THE PROCESSING CYCLE

<u>Processing Cycle Step</u>	<u>Isotopic Purity</u>	
	D, Atom %	H
3 LiAlD <sub>4</sub> + ND <sub>4</sub> Cl + Fe <sub>2</sub> O <sub>3</sub> Formulation		
Ingredients Dry Mixed Only	97.92	2.08
Ingredients Processed With Toluene	97.00	3.00
Processed with Toluene Containing 3.41 wt% Kraton Hydrocarbon Binder	95.34	4.66
Processed with Toluene Containing Kraton Binder and 0.85 wt% "Conco Oil" Hydrocarbon Oil	92.04	7.96

isotopic purity to 95.34% as is expected for this substantial introduction of normal hydrogen. The final entry in Table 5 illustrates the effect of adding 0.85 weight percent "Conco Oil", a hydrocarbon oil produced by Continental Oil Company. The addition of Conco Oil to the processing cycle degrades the deuterium isotopic purity by over three percent and did not improve the processing characteristics of the formulation to any discernable extent. Therefore, the Conco Oil was deleted from all subsequent formulations.

In preparation for large scale deuterium generator tests at AFRPL and AFWL, a test series was conducted to quantify the hazards associated with the AFRPL 3LAH2 and 3LAD2 H<sub>2</sub> and D<sub>2</sub> gas generator formulations. The hazards test series included mechanical impact tests, thermal stability tests, unconfined burning tests, and detonation tests using explosive booster charges. No detonations of the H<sub>2</sub> and D<sub>2</sub> generator grains occurred in any of the tests. After reviewing this hazards test data, the Aerospace Safety Division, Office of the Inspector General, Headquarters Air Force Systems Command issued an interim hazards classification of "Flammable Solids" for the AFRPL 3LAD2 and 3LAH2 formulations.

The hazards tests for the two gas generator formulations were conducted in accordance with the procedures specified in Chapter 3, 'Minimum

Test Criteria for Bulk Explosive Compositions," of TO 11A-1-47 which is entitled "Explosives Hazard Classification Procedures". A complete test matrix was conducted with the 3LAH2 hydrogen generating formulation. Because of the cost of conducting a full test matrix with the more expensive deuterated 3LAD2 formulation, the tests with the deuterated formulation were limited to one detonation test, one card gap test, and the complete matrix of impact sensitivity tests. As expected, the results of the tests with the deuterated formulation were identical to the results with the normal hydrogen formulation.

The detonation tests (in which a blasting cap is used to attempt to initiate a detonation of an unconfined cylindrical sample of the formulation) showed no evidence of detonation of the gas generator formulations. The ten samples of the 3LAH2 formulation (five were used in the thermal stability and unconfined burning tests) were  $4.445 \pm .025$  cm ( $1.75 \pm 0.01$  in) in diameter by  $5.182 \pm 0.051$  cm ( $2.04 \pm 0.02$  in) long. These grains contained  $63.10 \pm 0.40$  grams of 3LAH2 formulation at an average density of  $0.786 \text{ g/cm}^3$ . The single detonation test grain of the 3LAD2 formulation was  $4.445$  cm ( $1.75$  in) in diameter by  $5.486$  cm ( $2.16$  in) long and contained  $67.88$  grams of the formulation at an average density of  $0.796 \text{ g/cm}^3$ . There was no evidence of detonation of the formulation samples in any of the five 3LAH2 formulation tests or the single 3LAD2 formulation test. The fragments of the grains which were shattered by the blasting cap burned slowly in the air following the initiation attempts.

Four "card gap" tests were conducted in which a pentolite booster charge was used in an attempt to initiate a detonation of a formulation sample confined in a heavy-walled steel tube. The formulation samples were pressed into 3.632 cm (1.43 in) inside diameter steel tubes 13.970 cm (5.5 in) long with 0.559 cm (0.22 in) thick walls. The three grains of the 3LAH2 formulation contained  $119.0 \pm 3.0$  grams at an average density of  $0.811 \text{ g/cm}^3$ , and the single sample of the 3LAD2 formulation contained 123 grams of the deuterated formulation at an average density of  $0.838 \text{ g/cm}^3$ . All of the "card gap" tests were conducted without any blast attenuating cards between the booster charge and the formulation sample ("zero cards"). No detonations were observed. The coupling of the detonations of the pentolite booster charges to the witness plates through the 3LAH2 and 3LAD2 formulation samples appeared to be slightly greater than the coupling through the reference inert composite propellant sample because the indentations in the witness plates were slightly greater with the gas generator samples.

The ignition, unconfined burning, and mechanical impact tests provided additional data to substantiate the conclusion drawn from the detonation and card gap tests that the 3LAH2 and 3LAD2 formulations are non-detonable. The mechanical impact tests on 10 mg samples showed no evidence of detonation, reaction, smoke, or noise up to the 200 kg-cm limit of the impact tester (4 kg weight dropped 50 cm). In the ignition

and unconfined burning tests, the five 63 gram grains of 3LAH2 formulation burned vigorously but smoothly.

The thermal stability test samples showed no evidence of ignition or decomposition after 24 or 48 hours at 75°C (166°F) in air. In Figure 9, the 63 gram grain of 3LAH2 formulation which had been held at 75°C (166°F) in air for 24 hours is shown alongside a matching grain which had not been heated. The 48 hour thermal stability test grain showed no significant change from the discoloration which is visible on the surface of the 24 hour test grain in Figure 9. There was no weight loss from either the 24 or 48 hour thermal test samples. However, the structural integrity of the edges of the thermal test samples was degraded, and, therefore, the edges of the thermal test grains were more easily chipped during handling as is evident in the photo of the thermal test grain on the left in Figure 9. From differential scanning calorimeter tests, the ignition temperature for the 3LAD2 formulation was determined to be 160°C (319°F).

As is typical for alkali metal hydrides, the  $\text{LiAlH}_4$  or  $\text{LiAlD}_4$  in the 3LAH2 or 3LAD2 formulations reacts vigorously with water, liberating hydrogen which may ignite. The Kraton binder on the hydride particles in the processed formulations significantly reduces the reactivity of the grains. As was demonstrated by the thermal stability tests plus the extensive test experience with the grains, these formulations will not

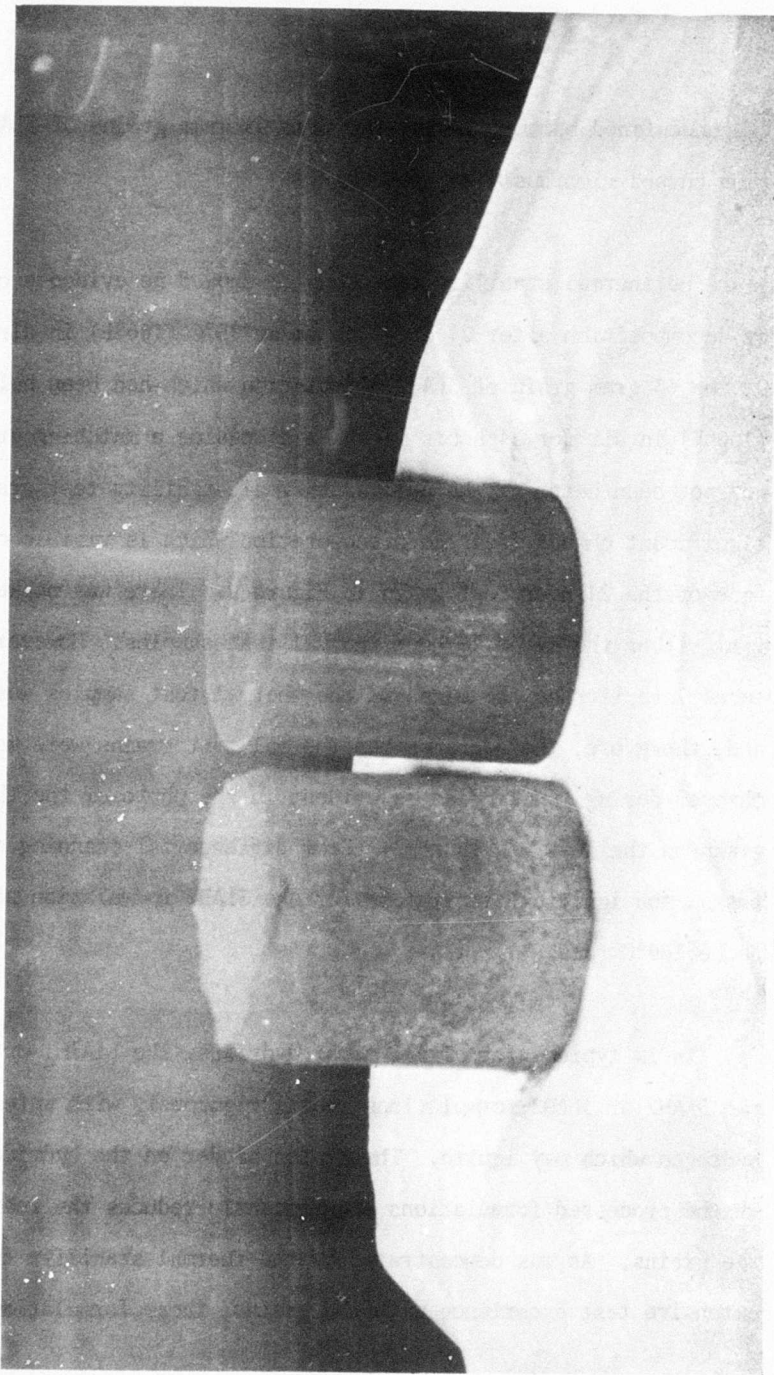


Figure 9. Thermal Stability Test Grain of 3LAH2 Formulation  
After 24 Hours at 75°C in Air Beside Baseline Grain.

ignite when exposed to atmospheric moisture, even at elevated temperatures. However, wetting the grains with liquid water will result in ignition.

After reviewing this hazards test data for the 3LAH2 and 3LAD2 formulations, the Aerospace Safety Division granted the following interim hazards classification for these formulations: quantity distance class-2; storage compatibility group-A; DOT class-flammable solid; DOT markings-flammable solid N.O.S.

During the processing scaleup effort, approximately three kilograms (6.6 lb) of deuterated formulation were processed. Except for the 200 grams of 3LAD2 formulation used in the hazards tests, the three kilograms of deuterated formulation were expended in the extensive series of deuterium gas generator scaleup tests described in the next section. In addition, 1.2 kilograms of the 3LAH2 hydrogen generator formulation were processed for use in the hazards tests and lasing demonstrations.

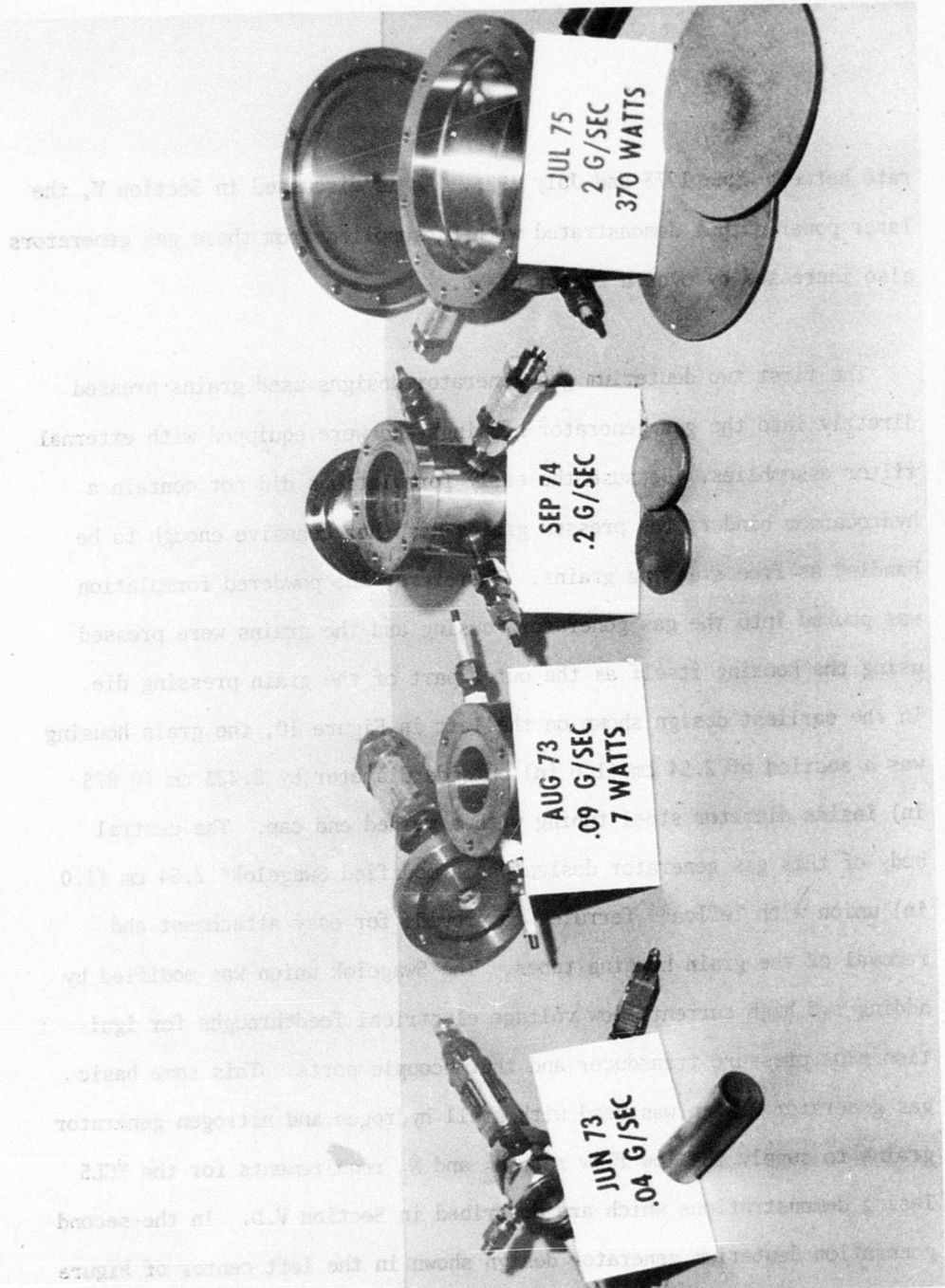
Because the LiAlD<sub>4</sub> and ND<sub>4</sub>Cl used in the deuterium generator formulations were purchased in relatively small quantities from commercial specialty chemical supply houses, the cost was relatively high. The price paid for the LiAlD<sub>4</sub> procured for this program ranged from \$5.00 per gram in 100 gram quantities to \$4.00 per gram for one kilogram lots.

The prices for  $\text{ND}_4\text{Cl}$  were similar. Because  $\text{LiAlD}_4$  contains 19.21 percent deuterium by weight, the price of \$4.00 per gram of  $\text{LiAlD}_4$  corresponds to \$20.82 per gram of deuterium obtainable from the  $\text{LiAlD}_4$ . However, the price of deuterium gas itself in similar quantities from the same commercial sources was approximately \$6.00 per gram. Therefore, the price per gram of deuterium from  $\text{LiAlD}_4$  was approximately 3.5 times the price of gaseous  $\text{D}_2$  from the same commercial sources. In contrast to the high price of commercial deuterium, the price for bulk gaseous deuterium procured for AFWL laser testing by the Air Force Logistics Command from the Energy Research and Development Administration (ERDA) is currently \$0.358 per gram, a factor of 16.7 times lower. The synthesis of  $\text{LiAlD}_4$  is simple and readily scalable (Reference 6), and the primary cost element is the cost of the deuterium itself. Therefore, if  $\text{LiAlD}_4$  were produced on pilot plant scale (as  $\text{LiAlH}_4$  currently is) using low cost deuterium produced by ERDA, the price of  $\text{LiAlD}_4$  could be expected to drop by over an order of magnitude.

### II.C. DEUTERIUM AND HYDROGEN GAS GENERATORS

The evolution of the deuterium gas generator designs developed under this program is depicted in Figure 10. The earliest gas generator design which is on the left in Figure 10 delivered 0.04 g/sec of  $\text{D}_2$ . The final deuterium gas generator design, which is on the right in Figure 10, delivered 2 g/sec of  $\text{D}_2$ , a factor of 50 scaleup in  $\text{D}_2$  flow.

Figure 10. Evolution of deuterium gas generators



rate between June 1973 and July 1975. As is discussed in Section V, the laser power output demonstrated with  $D_2$  supplied from these gas generators also increased by over a factor of 50.

The first two deuterium gas generator designs used grains pressed directly into the gas generator housings and were equipped with external filter assemblies. Because the early formulations did not contain a hydrocarbon binder, the pressed grains were not cohesive enough to be handled as free standing grains. Therefore, the powdered formulation was poured into the gas generator housing and the grains were pressed using the housing itself as the outer part of the grain pressing die. In the earliest design shown on the left in Figure 10, the grain housing was a section of 2.54 cm (1.0 in) outside diameter by 2.223 cm (0.875 in) inside diameter steel tubing with a welded end cap. The central body of this gas generator design was a modified Swagelok\* 2.54 cm (1.0 in) union with Teflon\*\* ferrules to provide for easy attachment and removal of the grain housing tubes. The Swagelok union was modified by adding two high current, low voltage electrical feedthroughs for ignition plus pressure transducer and thermocouple ports. This same basic gas generator design was used with small hydrogen and nitrogen generator grains to supply the low flow rate  $H_2$  and  $N_2$  requirements for the XCL5 lasing demonstrations which are described in Section V.D. In the second generation deuterium generator design shown in the left center of Figure

10, the ignition current feedthroughs were threaded directly into the grain housing and the bolt-on cover was sealed with an O-ring. Three versions of this basic design were fabricated with different internal diameters to provide a range of  $D_2$  flow rates for lasing tests. The seven deuterium weight yield tests which were described in Section II.B. were conducted using the 3.302 cm (1.3 in) inside diameter version of this gas generator design. Both the first and second generation designs used external filter assemblies (shown attached to the tops of the gas generators in Figure 10) to filter out fine particulates ejected from the gas generator formulations. In both of these designs, the grain was ignited by a Nichrome wire which was placed in contact with the top surface of the grain during assembly of the gas generator. The high current required to heat the Nichrome wire to the ignition temperature of the formulation was supplied through the copper or brass cores of the ignition feedthroughs which project from the sides of the gas generators in Figure 10.

The third generation deuterium generator assembly which is in the center right of Figure 10 is depicted schematically in Figure 11. In this design which was designated the 'Mod 1" high flow rate deuterium generator, the particulate filter is inside the gas generator. This Mod 1 design was used with free-standing grains of the deuterium or hydrogen generator formulations which contained Kraton binder to improve the cohesiveness of the grains. As is depicted schematically in Figure 11,

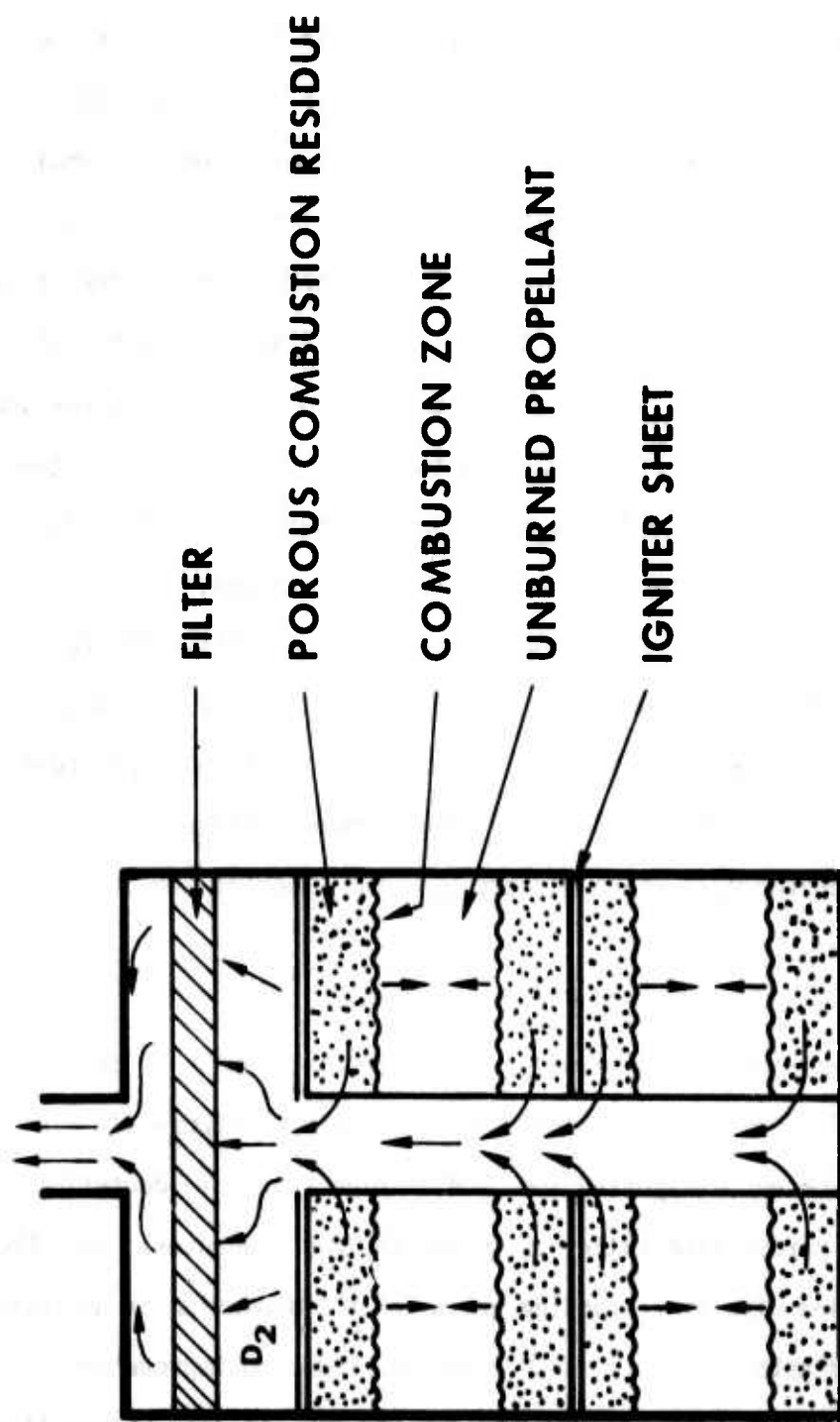


Figure 11. Mod 1 Deuterium Generator - Schematic

the original configuration for the Mod 1 gas generators used multiple grain discs with 1.245 cm (0.490 in) diameter central holes. The multiple grain discs were ignited simultaneously on both the top and bottom surfaces to provide high burning surface area within a small diameter gas generator. As is shown schematically in Figure 11, the  $D_2$  gas generated in the multiple combustion zones flows inward through the porous residue in the grain discs. This grain configuration was very similar to the configuration used in the hydrogen generators developed by the Naval Surface Weapons Center, Indian Head, MD, for inflating rescue marker balloons. However, for laser applications the variation in total burning surface area (and therefore  $D_2$  flow rate) during the burn was too great with multiple centrally perforated grain discs. Therefore, the majority of tests with the Mod 1 gas generator used a single end burning grain disc without a central perforation.

To ignite the larger surface areas of the 4.445 cm (1.75 in) diameter Mod 1 deuterium generator grains, a sheet igniter material was used which produced no gaseous combustion products to contaminate the deuterium. This sheet igniter material or "heat paper" resembled blotter paper and was produced by KDI Score, Inc.\*. The igniter material consisted of zirconium, barium chromate, and asbestos fibers processed into a cohesive sheet approximately 1 mm (0.039 in) thick. The material was supplied wet and, while wet, could be readily cut with a knife into

a disc matching the grain surface. The igniter material was not impact sensitive in either the wet or dry state and, while wet, was not readily ignitable. Once the igniter sheets had been cut to shape, they were oven dried for at least 10 hours at  $180 \pm 10^{\circ}\text{F}$ . The nominal specifications for this material were as follows: burning rate -  $17.78 \text{ cm/sec}$  ( $7.0 \text{ in/sec}$ ); heat release per unit area -  $37.12 \text{ cal/cm}^2$ ; heat release per unit weight -  $385.0 \text{ cal/g}$ . From differential scanning calorimeter tests, the ignition temperature for this sheet igniter material was determined to be approximately  $245^{\circ}\text{C}$  ( $472^{\circ}\text{F}$ ).

Details of the construction of the Mod 1 high flow rate deuterium gas generator are shown in Figure 12. The inside diameter of the gas generator was selected to provide approximately  $0.25 \text{ mm}$  ( $0.010 \text{ in}$ ) radial clearance for the free-standing grains which were pressed to a  $4.445 \text{ cm}$  ( $1.75 \text{ in}$ ) nominal outside diameter. Four stubs of  $0.9525 \text{ cm}$  ( $0.375 \text{ in}$ ) outside diameter by  $0.8103 \text{ cm}$  ( $0.319 \text{ in}$ ) inside diameter tubing were provided at  $90^{\circ}$  increments around the gas generator housing. Two of the tubing stubs were used for ignition feedthroughs, and the other two were used for pressure transducers, pressure relief valves, or thermocouples as required for a particular test. The ignition feedthrough consisted of a  $0.4801 \text{ cm}$  ( $0.189 \text{ in}$ ) diameter copper rod press-fitted into a center bore in a nylon rod which was then turned down to  $0.762 \text{ cm}$  ( $0.300 \text{ in}$ ) outside diameter at one end to slip through the tubing stubs and to  $0.635 \text{ cm}$  ( $0.250 \text{ in}$ ) outside diameter at the other

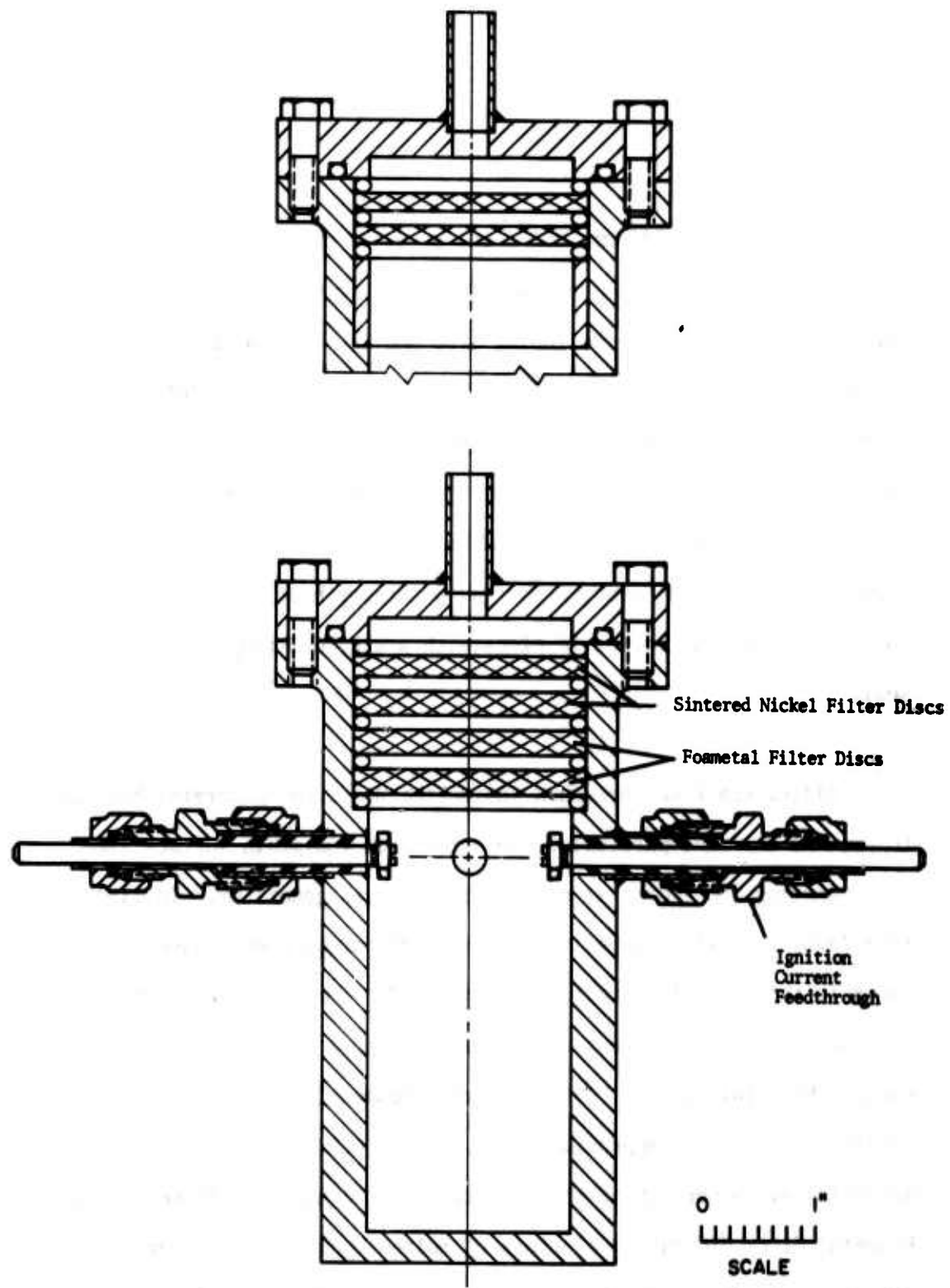


Figure 12. Mod 1 Deuterium Gas Generator - Detailed Cross Section

end. A Swagelok 0.9525 cm (0.375 in) by 0.635 cm (0.250 in) reducing union with nylon or Teflon ferrules was used to make a seal against both the outside diameter of the tubing stub and the outside diameter of the nylon insulator. The inner ends of the copper rods were slotted and threaded so that the ends of the Nichrome ignition wire could be clamped in the slot with a nut. With these clamping nuts removed, the entire ignition feedthrough assembly could be readily inserted into or withdrawn from the tubing stub on the gas generator housing. The gas generator cover was bolted in place with a single O-ring as the gas seal.

A filter stack was provided inside the Mod 1 gas generator housing to prevent any fine particulates ejected from the grain surface from contaminating the deuterium output from the gas generator. Initially, four layers of filter material of graduated porosity were used as is shown in the main illustration in Figure 12. The first two filter discs for the original configuration were an open pore nickel foam material called "Foametal"\*. The "45 pore" grade Foametal filter discs had a maximum pore size of approximately 0.056 cm (0.022 in) and a density of approximately 5 percent of the density of solid nickel. These coarse Foametal discs did catch splatters of molten igniter residue or occasional larger fragments of formulation residue. However, the 3LAD2 and

3LAH2 formulations (and the related 4LiAlH<sub>4</sub>:1NH<sub>4</sub>Cl formulations) produced such highly cohesive clinkers that these initial two coarse filtration discs of Foametal were deleted from later tests. The final two filter discs were of sintered nickel 0.478 cm (0.188 in) thick. The first sintered nickel filter disc had a nominal pore size of 50  $\mu\text{m}$  and the final disc had a nominal pore size of 10  $\mu\text{m}$ . O-ring seals were used at the outer edge of all of the filter discs. For the later tests with the Mod 1 gas generator, a spacer was used in place of the two Foametal discs as is shown in the second cross section in Figure 12. The total pressure differential across the two sintered nickel filter discs ranged from 6.9 to 13.8 kPa (1 PSID to 2 PSID) depending on the burning rate of the deuterium generator grain. For a typical 19.2 second test of a 17.48 gram grain of 3LAD2 formulation, the pressure differential across the filters remained less than 6.9 kPa (1 PSID) throughout the deuterium flow test. The nitrogen flow pressure differential across the individual filter discs was checked both before and after this test at a constant flow rate of 49 liters/min of nitrogen. The nitrogen flow pressure differential across the 50  $\mu\text{m}$  filter disc rose from 10.5 Torr pre-test to 11.2 Torr post-test, an increase of 6.7 percent. The pressure differential across the 10  $\mu\text{m}$  filter disc rose from 60.5 Torr to 63.8 Torr, an increase of 5.5 percent. Thus, only a slight amount of filter clogging occurred during the test. Normally, the filter discs were thoroughly cleaned with acetone and water and then dried before being re-used.

To prevent gas generator overpressurization, Nupro\* type 6C check valves were used as resealable pressure relief valves. One of these relief valves is shown attached to the nearest tubing stub on the housing of the Mod 1 gas generator in the right center of Figure 10. For most of the deuterium generator tests, the replaceable springs installed in these valves were designed for a cracking pressure of 690 kPa (100 PSIA). These valves provided tight vacuum seals, high flow area to rapidly vent overpressure transients, and reliable resealing after venting.

For the definitive deuterium flow rate tests with both the Mod 1 and the subsequent Mod 2 gas generators, the metering nozzle assembly shown in cross section in Figure 13 was coupled to the outlet of the gas generator. The detailed design and calibration of the interchangeable metering nozzles themselves is discussed in detail in Appendix B of Reference 7. Modified 2.54 cm (1.0 in) Swagelok unions provided pressure transducer and thermocouple ports both upstream and downstream of the metering nozzle. The inlet and outlet tubing for the metering nozzle assembly was the same 0.9525 cm (0.375 in) outside diameter by 0.8103 cm (0.319 in) inside diameter tubing used for the gas generator outlet tubes and the deuterium supply lines to the lasers.

During tests with the 3LAD2 formulation in the Mod 1 gas generators, the measured deuterium gas temperatures inside the gas generator were

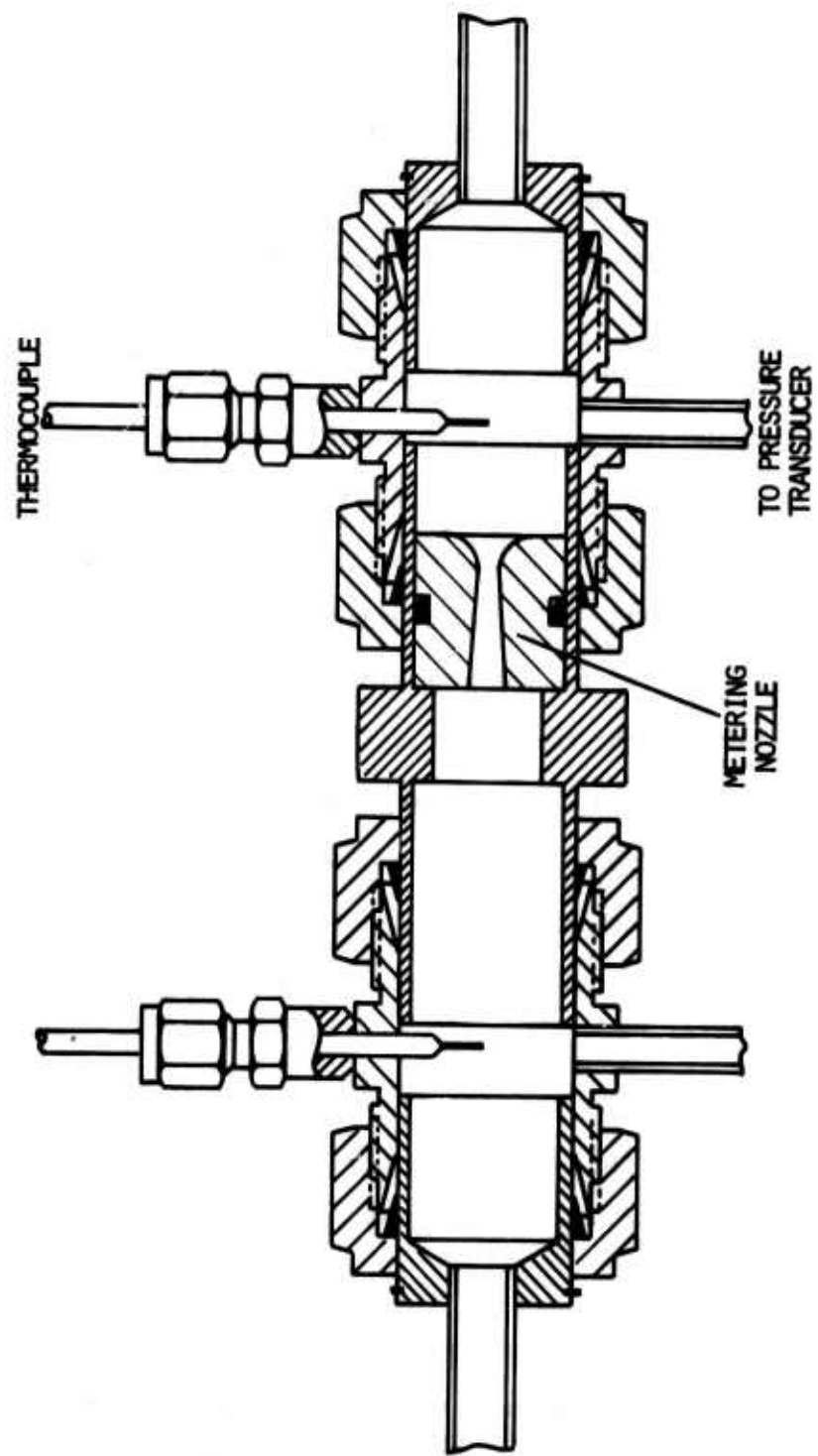


Figure 13. Deuterium Metering Nozzle Assembly

approximately 370 to 470 °K below the 986°K combustion temperature predicted by the equilibrium thermochemistry calculations for this formulation which were discussed in Section II.A. The high heat losses from the relatively small grains to the relatively massive gas generator hardware definitely contributed to the low measured gas temperatures. The highest deuterium temperatures were measured for the tests with the highest D<sub>2</sub> flow rates and the largest total quantities of formulation loaded into the gas generator. The temperatures were measured with a fine tip (0.794 mm (0.0313 in) diameter) thermocouple inserted through one of the tubing stubs on the gas generator housing into the center of the free volume between the top of the grain and the bottom of the filter stack. The peak deuterium gas temperatures for high flow rate tests ranged from 583°K for a test with two 16.16 gram center-perforated grains ignited on all four end surfaces to 618°K for a longer duration test with a single 32.32 gram center-perforated grain ignited on both end surfaces. In a lower flow rate test of a single 22 gram grain ignited on only one end, the peak gas temperature was 523°K. For the tests with the smallest (16.16 gram nominal) grains ignited on one end, the peak gas temperatures ranged from 498°K to 513°K.

In the Mod 1 deuterium generator tests, the temperature of the deuterium delivered to the plenum of the metering orifice assembly (Figure 13) never rose significantly above ambient temperature. The low

temperature of the output deuterium (25-35°C) was due to the large heat losses from the gas to the filter stack, the gas generator cover, and the tubing connecting the gas generator to the metering orifice assembly.

The pressure and temperature data traces which were recorded on an oscilloscope for two tests of the 3LAD2 formulation ground to two different particle sizes are shown in Figures 14a and 14b. The data traces in Figure 14a are for a grain with the ingredients ground and sieved to  $< 74 \mu\text{m}$  (Test 532) which was packed at 10.34 MPa (1500 PSI). The upper trace is the pressure at the inlet plenum for the metering nozzle, the matching middle trace is the pressure inside the gas generator, and the slowly rising lowest trace is the temperature at the metering nozzle inlet plenum. Early in the test, the pressure differential across the filters (the difference between the gas generator pressure and the metering orifice pressure) is approximately 6.9 kPa (1 PSID), and by the end of the test the filter pressure drop increased to approximately 13.8 kPa (2 PSID). The metering nozzle throat diameter for this test was 1.361 mm (0.0536 in). The pressure at the metering orifice at mid-burn (4.4 seconds after ignition) was 275.8 kPa (40 PSIA), the temperature was 28°C, and the corresponding  $\text{D}_2$  flow rate was 0.349 g/sec. The data traces shown in Figure 14b were for a 17.55 gram grain with the ingredients ground and sieved to  $< 105 \mu\text{m}$  (Test 533). The grain packing pressure and the metering nozzle were the same as for Test 532. The

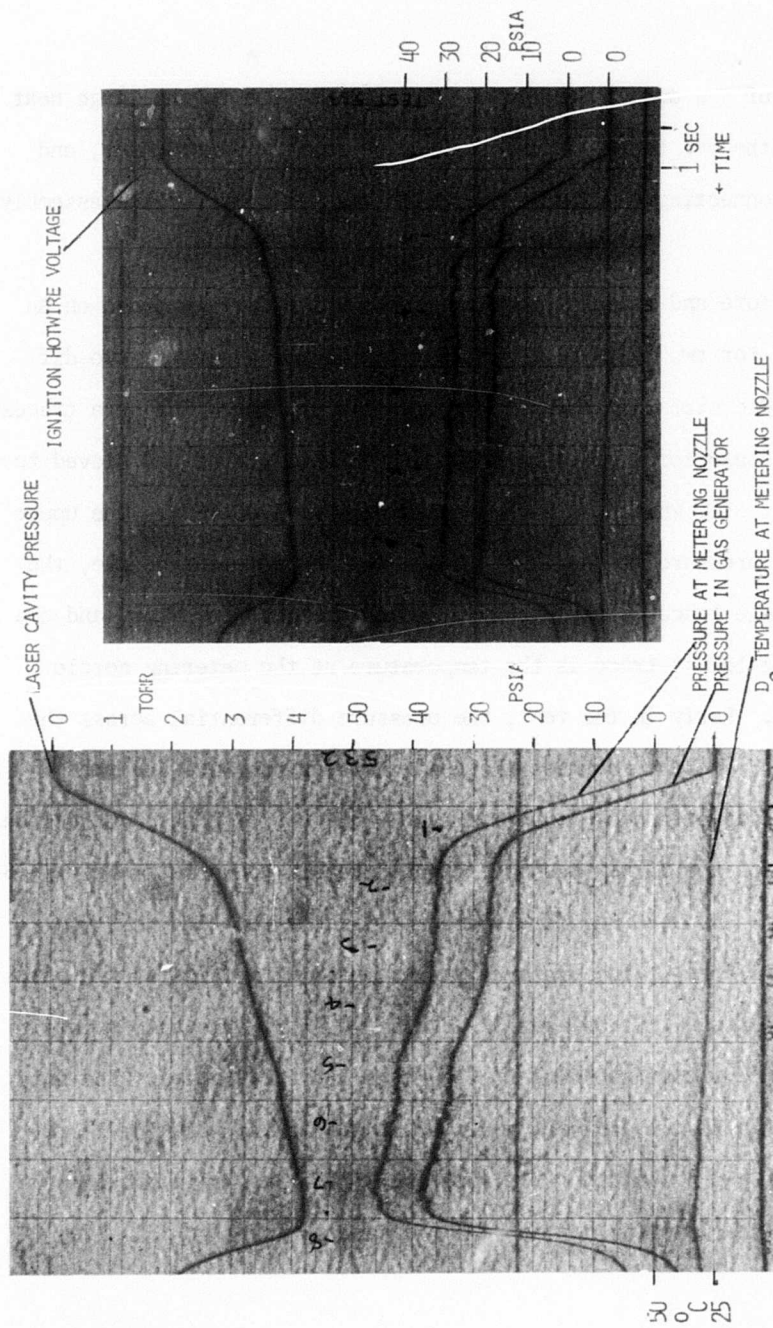


FIGURE 14. OSCILLOGRAPH DATA TRACES FOR TWO TESTS OF GRAINS OF 3LADD FORMULATION WITH DIFFERENT INGREDIENT PARTICLE SIZES IN MOD 1 DEUTERIUM GENERATOR

grain formulated with the coarser ingredients (Test 533) burned more slowly (as was discussed in Section II.B.) and, therefore, at mid-burn, the pressure at the metering orifice was 193.1 kPa (28 PSIA), the temperature was 25°C, and the corresponding  $D_2$  flow rate was 0.245 g/sec which is 29.7 percent lower than in Test 532 with the finer ingredient particle size. The moderate amplitude irregularities or "blips" which are visible in the pressure trace of Test 533 between 1.5 and 3.5 seconds after ignition occurred frequently in grains formulated with the coarser ( $< 105 \mu\text{m}$ ) ingredients.

The characteristic difference in the amplitude of the combustion pressure oscillations or "noise" between grains formulated with  $< 74 \mu\text{m}$  ingredients and those formulated with  $< 105 \mu\text{m}$  ingredients is illustrated in Figure 15. Different metering nozzles were used for the tests of the two grains which are shown in Figure 15 in order to compensate for the slower burning rate of the coarser formulation and keep the combustion pressures comparable. The data traces shown in Figure 15a are for a grain with the ingredient particle size  $< 74 \mu\text{m}$  which was tested using a metering nozzle with a 1.120 mm (0.0441 in) throat diameter (Test 531). The mean combustion pressure is progressive during the burn, but the amplitude of the combustion noise is low (approximately  $\pm 13.8 \text{ kPa}$  (2 PSI) maximum,  $\pm 3.4 \text{ kPa}$  (0.5 PSI) typical). The pressure at mid-burn (4 sec) was 424 kPa (61.5 PSIA), the temperature at the metering orifice was 26°C, and the corresponding  $D_2$  flow rate was

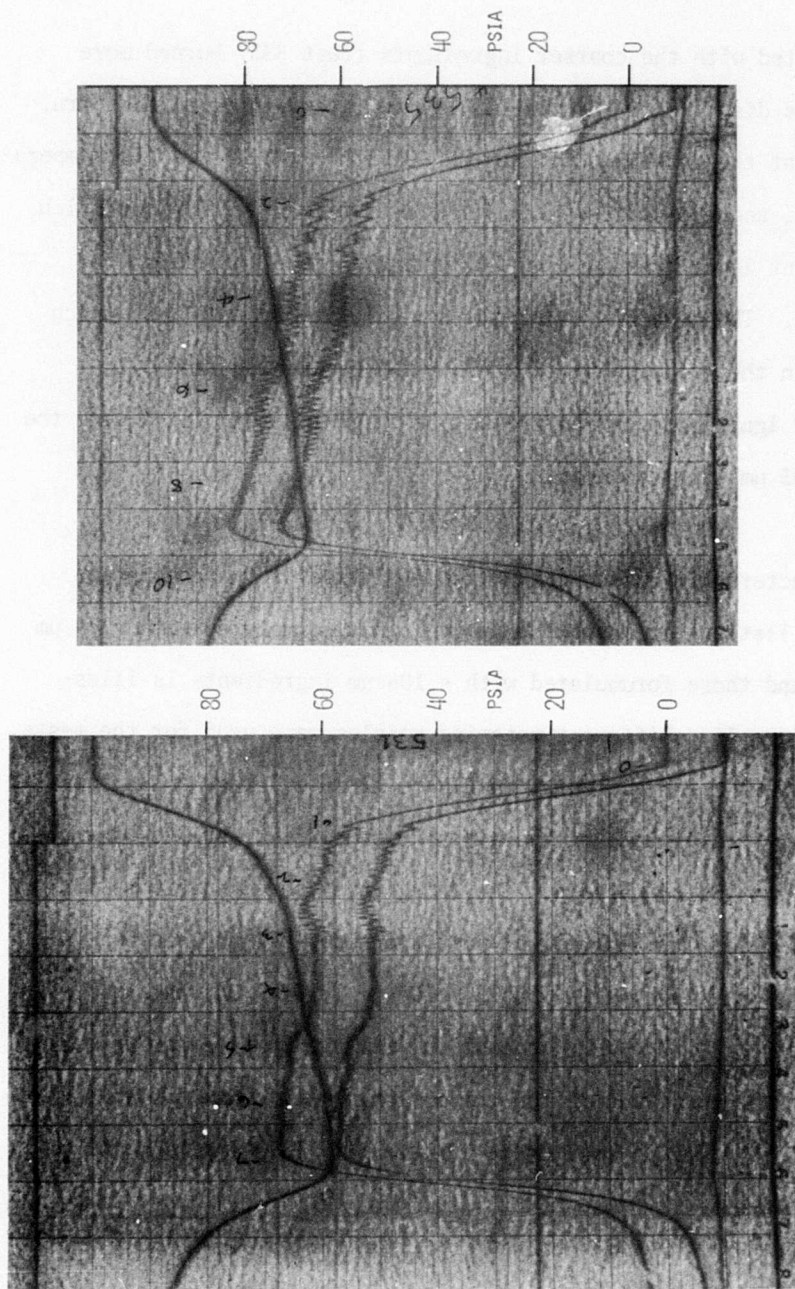


FIG 15A, TEST 531, PARTICLE SIZE  $< 74 \mu\text{m}$

FIG 15B, TEST 535, PARTICLE SIZE  $< 105 \mu\text{m}$

FIGURE 15. COMBUSTION NOISE COMPARISON BETWEEN GRAINS OF 3LA02 FORMULATION WITH INGREDIENT PARTICLE SIZES  $< 74 \mu\text{m}$  AND  $< 105 \mu\text{m}$

0.365 g/sec. For comparison, the data traces shown in Figure 15b are for a 17.58 gram grain with the ingredient particle size < 105  $\mu\text{m}$  which was tested using a metering nozzle with a 0.9093 mm (0.0358 in) throat diameter (Test 535). The amplitude of the combustion pressure oscillations in this test with the coarser ingredients was significantly higher (approximately  $\pm 20.7$  kPa (3 PSI) maximum,  $\pm 10.3$ -6.9 kPa (1.5-1.0 PSI) typical) than in Test 531 with the more finely ground ingredients. The mean pressure for this test was also progressive during the burn. At mid-burn (5.5 sec), the pressure and temperature at the metering orifice were 517 kPa (75 PSIA) and 26°C, and the corresponding  $\text{D}_2$  mass flow rate was 0.289 g/sec.

Fifty tests were conducted with the two Mod 1 deuterium gas generators. This gas generator design was the standard test configuration during the formulation refinement effort which led to the 3LAH2 and 3LAD2 "standard" formulations. All of the formulation burning rate data which was presented in Figure 6 of Section II.A. was acquired from grains tested in this gas generator configuration. Approximately 840 grams (1.9 lb) of deuterated formulations were tested in the Mod 1 gas generators.

The final deuterium gas generator design developed under this program was designated the Mod 2 high flow rate configuration. The Mod

2 gas generator is shown on the far right in Figure 10. The design deuterium flow rate range of 2.0 to 2.5 gD<sub>2</sub>/sec for the Mod 2 gas generator was selected to match the D<sub>2</sub> flow rate requirements for the high power lasing demonstrations at AFWL which are described in Section V. The two sintered nickel internal filter discs are shown in front of the date, flow rate and laser power placard. As shown in the photo, two of the Nupro type 6C pressure relief valves were used for this Mod 2 design because of the higher deuterium flow rates. This gas generator was designed for end-burning grain discs with a nominal diameter of 12.7 cm (5.0 in).

A detailed cross section of the Mod 2 deuterium generator design is shown in Figure 16. The ignition current feedthroughs were of the same design used successfully with the Mod 1 gas generators. The high burning rate of the "heat paper" non-gassing igniter sheet provided rapid ignition of the entire grain surface once the igniter sheet itself had been locally ignited by the Nichrome hotwire. Two sintered nickel filter discs were used. In addition to the 0.475 cm (0.187 in) thick sheets of sintered nickel in 50  $\mu$ m and 10  $\mu$ m nominal pore sizes\* which had been used for filter discs in the Mod 1 gas generators, 0.229 cm (0.090 in) thick sheets of screen-supported sintered nickel in 35  $\mu$ m nominal pore size\*\* were used for the first stage filter discs for some of the tests.

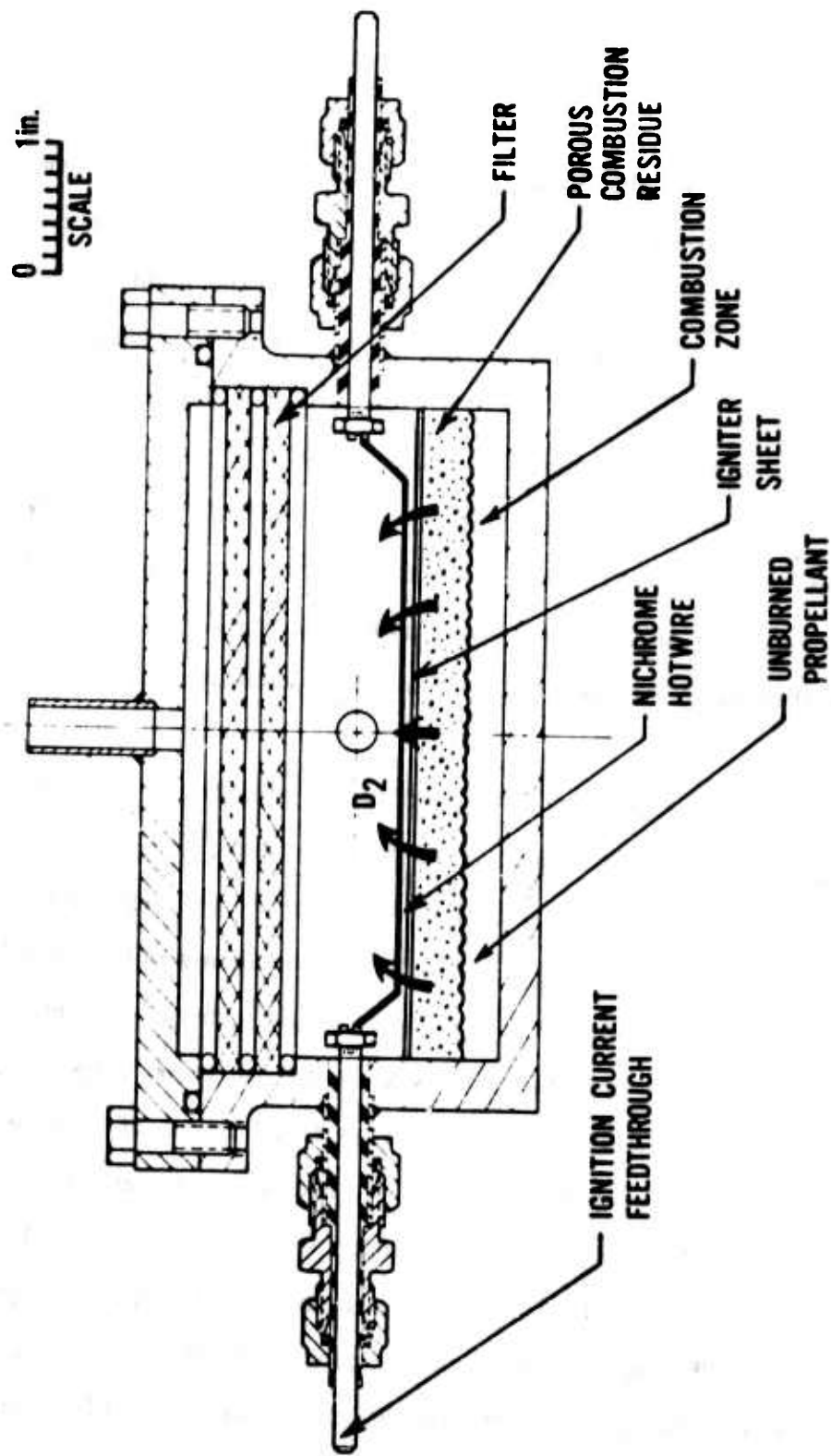


Figure 16. Cross Section of Mod 2 High Flow Rate Deuterium Generator

A close-up photograph of one of the three Mod 2 gas generators fabricated under this program is shown in Figure 17. The two sintered nickel filter discs (50  $\mu\text{m}$  and 10  $\mu\text{m}$ ) are in the right foreground of the photo, and a standard 144 gram grain of the 3LAD2 formulation is in the foreground inside a plastic bag. The diameter:thickness ratio for these 12.70 cm (5.00 in) diameter by 1.27 cm (0.50 in) thick grains was 10:1, but the 3LAH2 and 3LAD2 formulations are sufficiently cohesive to permit routine handling of these thin grain discs. Four similar grains were successfully shipped by normal commercial truck from Edwards AFB in California to Kirtland AFB in New Mexico without damage to the grains.

During the post-test disassembly and cleaning of the Mod 2 gas generator hardware following the initial tests, light films of clear, oily material were found on the inside of the gas generator cover, in the outlet tubing, and in the metering nozzle assembly. Samples of the oily contaminant from the inside of the gas generator cover and from a liquid nitrogen cold trap inserted in the deuterium output line for one test were analyzed. The analysis found traces of toluene, substituted as well as deuterated aromatic hydrocarbons, and cyclic paraffins with various degrees of deuteration. These trace condensable contaminants in the deuterium stream were apparently decomposition products from the "Kraton" styrene-isoprene copolymer binder which had been thermally cracked and partially deuterated as they evolved through the

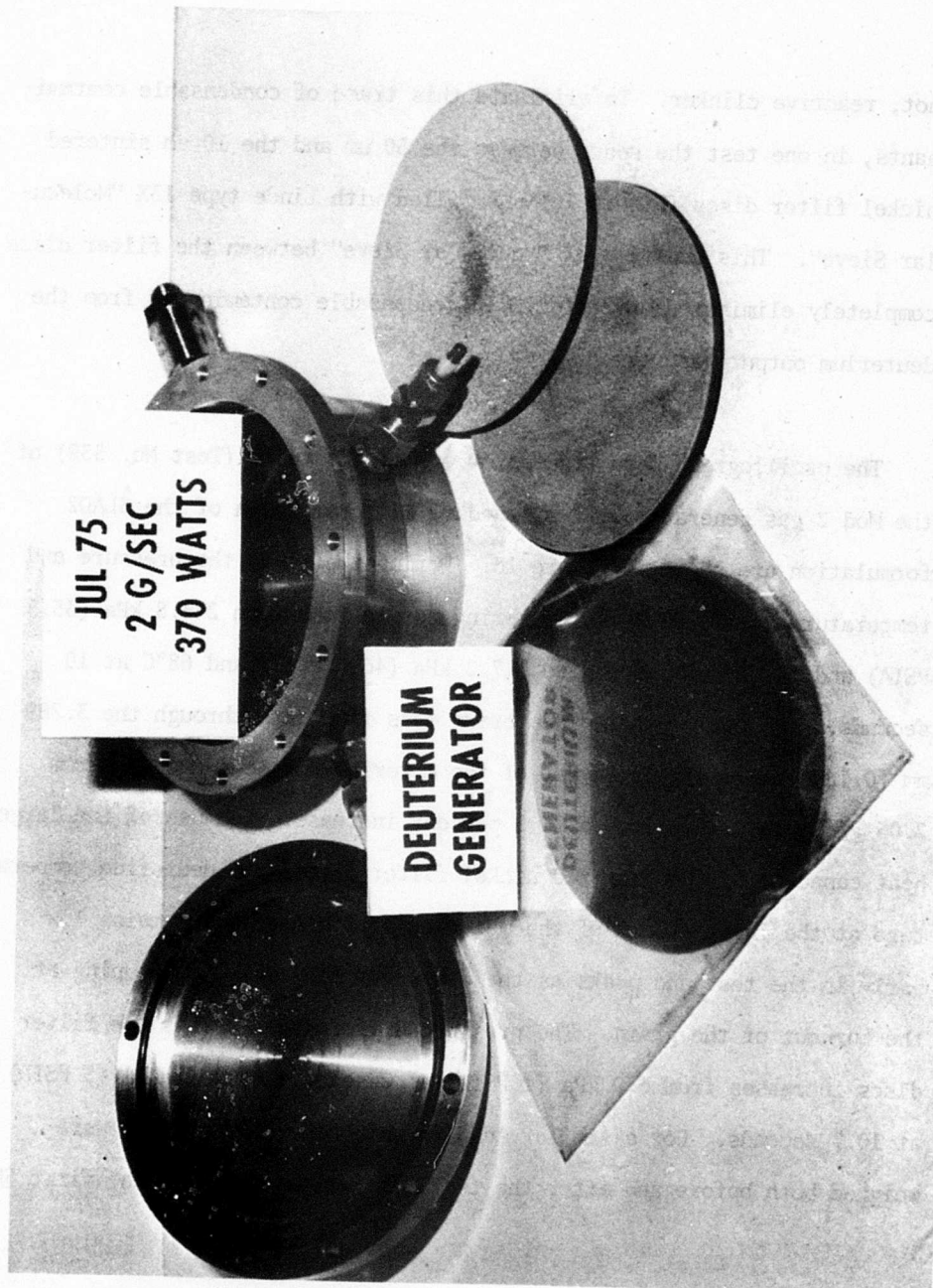


Figure 17. Mod 2 High Flow Rate Deuterium Generator with Grain of 3LAD2 formulation.

hot, reactive clinker. To eliminate this trace of condensable contaminants, in one test the space between the 50  $\mu\text{m}$  and the 10  $\mu\text{m}$  sintered nickel filter discs (Figure 16) was filled with Linde type 13X 'Molecular Sieve'. This addition of 'Molecular Sieve' between the filter discs completely eliminated any detectable condensable contaminants from the deuterium output gas stream.

The oscillograph data traces for one of the tests (Test No. 539) of the Mod 2 gas generator with a standard 144 gram grain of the 3LAD2 formulation are shown in Figure 18. During the test, the pressure and temperature at the deuterium metering nozzle rose from 244.8 kPa (35.5 PSIA) and 26°C at 2 seconds to 317.2 kPa (46.0 PSIA) and 68°C at 10 seconds. The corresponding deuterium mass flow rate through the 3.289 mm (0.1295 in) diameter throat of the metering nozzle increased from 2.05 g/sec to 2.49 g/sec, a 21.5 percent increase. Because of the large heat capacity of the sintered nickel filter discs, the deuterium temperature at the inlet plenum of the metering nozzle assembly remains low early in the test and peaks as the deuterium flow rate is dropping at the burnout of the grain. The pressure differential across the filter discs increases from 6.9 kPa (1 PSID) at 2 seconds to 20.7 kPa (3 PSID) at 10.7 seconds. For a similar test in which the filter discs were weighed both before and after the test, the weight gain for the first 50

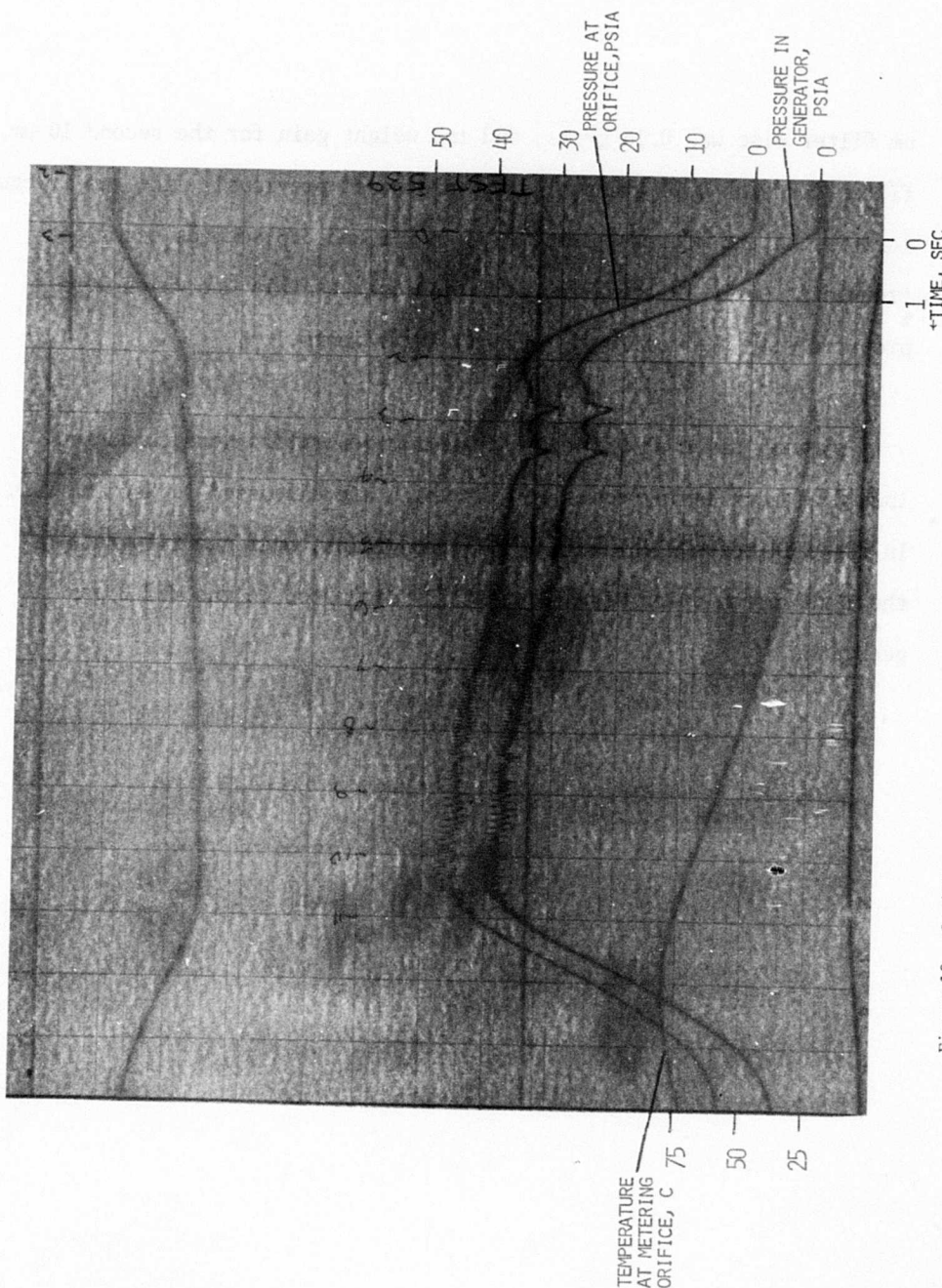


Figure 18. Oscillograph Data Traces for Mod 2 Deuterium Generator Test with 3LAD2 Grain

$\mu\text{m}$  filter disc was 0.26 grams, and the weight gain for the second 10  $\mu\text{m}$  filter disc was 0.21 grams. As was discussed previously, the two irregularities in the pressure trace between 2.5 and 3.5 seconds occurred frequently early in the burns of grains such as this one which were prepared with the coarser ( $< 105 \mu\text{m}$ ) ingredients.

Fourteen tests of the Mod 2 deuterium generators were conducted including four lasing tests at AFWL which are discussed in Section V.D. In these 14 tests with nominal 144 gram grains, over two kilograms of the 3LAD2 formulation were successfully combusted in the Mod 2 gas generator.

## SECTION III

### FLUORINE GAS GENERATORS

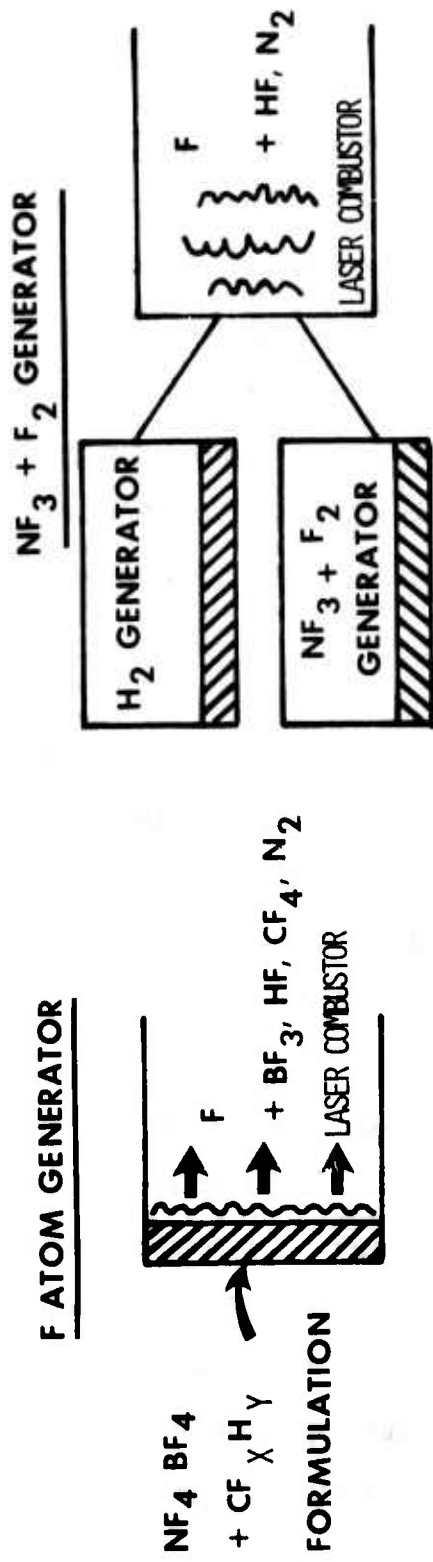
#### III.A. FLUORINE GENERATOR FORMULATIONS

Because fluorine compounds are characteristically either extremely reactive or extremely stable, developing a solid formulation which could supply fluorine for a laser combustor was the most difficult of the laser gas generator development tasks. As is illustrated schematically in Figure 19, there are two fundamentally different approaches toward supplying the fluorine for a DF chemical laser combustor.

The first approach which is depicted on the left in Figure 19 is designated the "F atom generator" or "totally consumable formulation" approach. In this approach, a fluorinated oxidizer which produces entirely gaseous decomposition products is formulated with a fluorocarbon or hydrocarbon polymer binder. By adjusting the oxidizer-rich stoichiometry of the formulation, the combustion temperature can be brought into the temperature range (1500-2000°K) where the free fluorine liberated by the decomposition of the excess oxidizer is partially or totally dissociated into atomic fluorine. Ducting these hot combustion

products containing atomic fluorine from a separate gas generator to the laser combustor would be impractical. Therefore, these "F atom generator" or "totally consumable" formulations would be burned in the main laser combustor so that the fluorine atoms could flow directly into the laser's fluorine nozzles and on into the lasing cavity as depicted in Figure 1.

This first approach to a fluorine generator has the advantage of simplicity because a single formulation directly produces the fluorine atoms required by the laser. However, this approach also has a major disadvantage because all of the combustion products from the formulation appear in the laser combustor flow. As is depicted in Figure 19, for a typical "totally consumable" formulation containing the oxidizer  $\text{NF}_4\text{BF}_4$  and a fluorohydrocarbon polymer binder (represented as CHF), large concentrations of  $\text{BF}_3$  and  $\text{CF}_4$  are present in the combustion products. The large concentrations of these heavy polyatomic species in the combustion products from the solid formulation significantly increase the average molecular weight,  $\bar{M}$ , and decrease the average specific heat ratio,  $\gamma$ , of the laser combustor gas mixture compared to a standard laser combustor gas mixture generated by combusting gaseous  $\text{NF}_3$  with a hydrocarbon fuel such as ethylene,  $\text{C}_2\text{H}_4$ . With current DF chemical laser nozzle designs, an increase in  $\bar{M}$  and a decrease in  $\gamma$  of the combustor gases significantly degrades the laser performance as will be discussed in Section V. Therefore, the first approach to a fluorine generator, the "F atom generator" or "totally consumable" formulation, would



**COMBUSTION PRODUCTS:**  
— COOL NF<sub>3</sub> + F<sub>2</sub> GAS EVOLVED  
— SOLID "CLINKER" RETAINS OTHER PRODUCTS

**ADVANTAGES:**  
— "NORMAL" COMBUSTOR  
— COMPOSITION (HIGH  $\delta$ , LOW  $\bar{M}$ )  
— LASER PERFORMANCE UNCHANGED

**DISADVANTAGES:**  
— UNDESIRABLE COMBUSTOR COMPOSITION (LOW  $\delta$ , HIGH  $\bar{M}$ )

**DISADVANTAGE:**  
— TWO GAS GENERATORS REQUIRED

Figure 19. Comparison of fluorine generator approaches

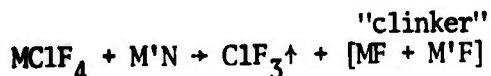
significantly degrade the performance of current DF laser nozzle designs. However, at the time this fluorine generator development effort began, only limited experimental data was available to quantify the effects on DF laser performance of significant increases in  $M$  and decreases in  $\gamma$  (Reference 8). The first definitive data on the deleterious effects of large changes in these combustor gas properties was obtained during the formulation development effort from tests on the small XCL5 DF laser at AFRPL which are discussed in Section V.C. and from other AFWL-funded laser tests.

The second approach to a fluorine generator is to develop a solid formulation which generates a relatively cool gas stream containing a high concentration of an undissociated fluorinated oxidizer which is suitable for use in the laser combustor. This cool gas stream containing the fluorinated oxidizer can then be ducted from the gas generator to the laser combustor. In the laser combustor, part of the fluorinated oxidizer is burned with hydrogen or a hydrocarbon fuel, and the excess of the fluorinated oxidizer is thermally dissociated to liberate the fluorine atoms required by the laser. A successful example of this second approach to a fluorine generator, the " $\text{NF}_3 + \text{F}_2$  generator", is schematically illustrated on the right side of Figure 19. The solid formulation generates a relatively cool stream of gaseous  $\text{NF}_3$  and  $\text{F}_2$ , and all of the other combustion products are retained in the gas generator as a sintered "clinker".

This second approach of using a "clinker" to trap the undesirable combustion products in the gas generator as a cohesive solid residue is similar in principle to the approach which was successfully used for the deuterium and hydrogen generator formulations which were described in Section II. The primary advantage of this second approach to a fluorine generator is that the laser performance is undegraded because no heavy polyatomic contaminant species are introduced into the laser combustor. Therefore, the laser performance is the same as if the laser were fed a mixture of the standard oxidizers,  $\text{NF}_3$  and  $\text{F}_2$ , from a conventional gaseous reactant supply system. However, to achieve an "all-solids" reactant supply system with this second approach to a fluorine generator, an additional gas generator to supply the hydrogen fuel for the combustor is required. Formally, gas generators based on this second approach are not necessarily fluorine ( $\text{F}_2$ ) generators because the primary gaseous product from the formulations may be a fluorinated oxidizer such as  $\text{NF}_3$  or  $\text{ClF}_3$  rather than elemental fluorine.

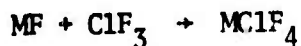
Both approaches to a fluorine generator were investigated under this program, and several different types of formulations were examined for each approach. In the subsequent paragraphs, the fluorine generator formulations which were investigated will be discussed in approximately the order in which they were examined.

The first type of fluorine generator formulation to be evaluated was based on the "clinker" approach to the fluorine generator problem. This initial type of formulation used the reaction of a tetrafluorochlorate salt with a metal nitride to generate chlorine trifluoride ( $\text{ClF}_3$ ) and nitrogen plus the residual "clinker". The approximate combustion reaction is:



where M is either potassium or cesium and M' is aluminum, magnesium or lithium.

The major advantage of the tetrafluorochlorate salts is the relative ease of synthesis. The salts are prepared by the reaction of the corresponding metal fluoride with chlorine trifluoride according to the following reaction:

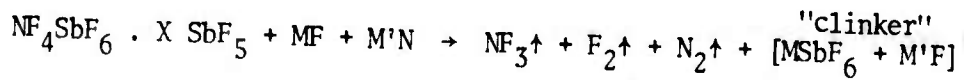


The reaction is incomplete resulting in an excess of the metal fluoride. After reaction for three days at room temperature, the potassium tetrafluorochlorate analysis was  $\text{KClF}_4 \cdot 0.61\text{KF}$ . The analysis of the cesium

tetrafluorochlorate, synthesized under identical conditions, was  $\text{CsClF}_4$  0.18 CsF.

Investigation of this type of formulation was terminated at the second step in the formulation development process due to the poor burning characteristics observed for all of the formulations tested. The formulations either would not sustain combustion or would burn too rapidly to be useful as a fluorine source for chemical laser applications. Other properties of the tetrafluorochlorate salts which caused work with these compounds to be discontinued were: (1) the corrosivity of the tetrafluorochlorate salts and chlorine trifluoride; (2) the low weight yield of available fluorine; (3) the presence of  $\text{ClF}_3$  vapor in equilibrium with the tetrafluorochlorate salts even at room temperature.

The second type of fluorine generator system which was evaluated was a "clinker" formulation based on the oxidizer tetrafluoroammonium hexafluoroantimonate,  $\text{NF}_4\text{SbF}_6$ . In this type of formulation, the exothermicity required to decompose the  $\text{NF}_4\text{SbF}_6$  and sustain the combustion reaction is obtained from the fluorination of a metal nitride fuel and from the formation of a metal hexafluoroantimonate by the  $\text{SbF}_5$  liberated from the  $\text{NF}_4\text{SbF}_6$  and an alkali metal fluoride component of the formulation. The approximate combustion reaction is given below.

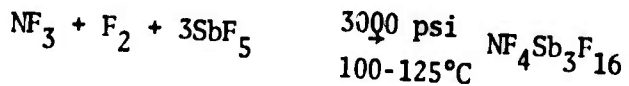


where M is either potassium or cesium and M' is aluminum, magnesium or lithium. The  $\text{NF}_4\text{SbF}_6$  cannot be readily obtained in a pure state. It exists in combination with antimony pentafluoride,  $\text{SbF}_5$ , where X usually varies from 0.6 to 0.8 depending on the conditions used for the synthesis and the degree of purification. The metal fluoride is added in excess to trap the volatile  $\text{SbF}_5$  as the solid metal hexafluoroantimonate.

The relatively cool  $\text{NF}_3$  produced by this reaction made this system very attractive because all of the baseline operating conditions for the AFRPL test laser were established using gaseous  $\text{NF}_3$ . Thus, a convenient comparison could be drawn between the performance of the laser device operating on bottled  $\text{NF}_3$  or on the  $\text{NF}_3 + \text{F}_2$  generated by this fluorine generator system. Other significant advantages of this system are: (1) the  $\text{NF}_4\text{SbF}_6 \cdot X \text{SbF}_5$  is mildly corrosive; (2) the  $\text{NF}_3$  produced by the reaction is non-corrosive, mildly toxic with well established toxicology, and non-detonable; (3) the  $\text{NF}_4\text{SbF}_6 \cdot X \text{SbF}_5$  is non-detonable; and (4) the  $\text{NF}_4\text{SbF}_6 \cdot X \text{SbF}_5$  has no vapor pressure at room temperature.

Although this system has the distinct advantage of producing cool  $\text{NF}_3$ , it also has several intrinsic disadvantages. First, it is low in available fluorine. Second, because the exothermicity and burn rate are controlled by the type and quantity of metal nitride employed, it was not possible to totally eliminate the corrosive fluorine produced by the reaction through combustion with the metal nitride and still maintain

suitable burning characteristics. Third, the  $\text{NF}_4\text{SbF}_6 \cdot X \text{SbF}_5$  is not commercially available and is difficult to synthesize. The synthesis is accomplished by the reaction of  $\text{NF}_3$ ,  $\text{F}_2$ , and  $\text{SbF}_5$  at high temperature and pressure. As is discussed in References 8 and 9, the conditions for the synthesis yielding the purest final product of  $\text{NF}_4\text{SbF}_6$  are as follows:



Two Days



2-3 days

The formulations investigated during this evaluation were composed of a mixture of from 53 to 92 weight percent of  $\text{NF}_4\text{SbF}_6 \cdot X \text{SbF}_5$ , from 0.5 to 2 weight percent of aluminum, magnesium or lithium nitride, and from 7 to 46 weight percent of potassium or cesium fluoride. Aluminum oxide was also successfully used as the fuel constituent instead of the nitrides. The weight yield of available fluorine from these clinker formulations is strongly dependent on the molecular weight of the alkali metal fluoride used to trap the  $\text{SbF}_5$  and on the amount of additional  $\text{SbF}_5$  (complexed with the  $\text{NF}_4\text{SbF}_6$ ) which must be trapped. The use of the

lighter alkali metal fluorides such as NaF and KF would increase the fluorine weight yields. However, the heavier alkali metal fluorides form more thermally stable hexafluoroantimonates which continue to trap the SbF<sub>5</sub> at higher grain combustion temperatures. The theoretical weight yields of available fluorine from these formulations range from 22.58 percent for an NF<sub>4</sub>SbF<sub>6</sub> + KF formulation to 14.59 percent for an NF<sub>4</sub>SbF<sub>6</sub> . 0.8 SbF<sub>5</sub> + 1.8 CsF formulation.

Extensive gram-scale characterization tests were conducted with formulations containing NF<sub>4</sub>SbF<sub>6</sub> . 0.8 SbF<sub>5</sub> oxidizer with CsF as the trapping agent and AlN as the fuel. Ingredient compatibility tests of mixtures of powdered potassium fluoride, lithium nitride, and NF<sub>4</sub>SbF<sub>6</sub> . X SbF<sub>5</sub> were also conducted. Small samples of the pressed powder mixtures were ignited with a Nichrome wire heated by an electrical current resulting in a steady, stable combustion of the sample. Impact sensitivity tests were conducted on all formulations examined utilizing a standard drop weight tester. The results were negative at 250 kilogram-centimeters (5 kilogram weight dropped 50 centimeters). The properties of the grain that are essential for the formation of a cohesive clinker, the importance of clinker cohesiveness in preventing particulate ejection, and the effect that the composition of the formulation has on the properties of the clinker have been discussed in Section II. Considering these criteria, the optimum burn rate range for

this type of fluorine generator formulation was determined to be approximately 0.1 cm/sec at 13.3 psia.

The combustion product composition was experimentally determined for the gas generating formulation consisting of 66.3 weight percent  $\text{NF}_4\text{SbF}_6$  . 0.6  $\text{SbF}_5$ , 33.1 weight percent cesium fluoride, and 0.6 weight percent aluminum nitride. This analysis was conducted using the molecular beam time-of-flight mass spectrometer described in Reference 2. A helium purge around the combustion sample eliminated atmospheric contamination. The experimental results are given below:

Mole Percent - Gases	Experimental	Theoretical
$\text{NF}_3$	71.0	52.6
$\text{F}_2$	14.0	44.7
$\text{N}_2$	10.0	2.6
HF	3.0	
NO	1.0	

The presence of hydrogen fluoride and the lower-than-predicted concentration of fluorine were attributed to the passivation of the hardware by fluorine. The presence of NO was attributed to known NO contamination of the  $\text{NF}_4\text{SbF}_6 \cdot X \text{ SbF}_5$ .

The actual weight yield of free fluorine from this type of formulation is considerably lower than the theoretical fluorine yield from the oxidizer itself. Counting all five moles of fluorine atoms (5F from  $\text{F}_2$  +  $\text{NF}_3$ ) per mole of  $\text{NF}_4\text{SbF}_6$ , the theoretical fluorine weight yield of  $\text{NF}_4\text{SbF}_6$  itself is 29.16%. For typical formulations, the fluorination of the metal nitride fuel consumes approximately ten percent of the theoretically available fluorine. The addition of the KF or CsF to trap the volatile  $\text{SbF}_5$  sharply decreases the net fluorine weight yield. For the actual formulation which was used for the lasing demonstrations which are described in Section V, the net yield of free fluorine was 10.60 percent. The molar composition for this formulation is  $\text{NF}_4\text{SbF}_6 \cdot 0.8 \text{ SbF}_5 + 1.98 \text{ CsF} + 0.167 \text{ AlN}$ , and the theoretical molar composition of the gaseous products is  $1.0 \text{ NF}_3 + 0.75 \text{ F}_2 + 0.08\text{N}_2$ . By weight, this formulation is 61.87 percent  $\text{NF}_4\text{SbF}_6 \cdot 0.8 \text{ SbF}_5$ , 37.28 percent CsF, and 0.85 percent AlN. Experimentally, the density of a typical pressed grain of this formulation was  $2.43 \text{ g/cm}^3$ , and the burning rate was 0.113

cm/sec at 151.7 kPa (22 PSIA). Burning rate data from tests of 2.54 cm (1.0 in) diameter grains of this formulation are presented in Section III.C. (Figure 22).

The first type of "totally consumable" or "F atom generator" formulation which was investigated used xenon tetrafluoride oxidizer with polytetrafluoroethylene fuel. This type of formulation produces atomic fluorine as the major combustion product, and both of the secondary constituents, xenon and carbon tetrafluoride, are known to be very slow vibrational deactivators of DF. The approximate combustion reaction is:



where N = number of moles. For the range of ingredient mole ratios of interest for chemical lasers, the flame temperatures are high enough to dissociate most of the free fluorine.

Extensive theoretical equilibrium thermochemistry calculations were carried out for this class of formulations for values of N from 1 to 2. The calculations were performed with the computer program described in Reference 5 using standard thermodynamic data with heats of formation of -51.5 Kcal/mole and -195.0 Kcal/mole for  $XeF_4$  and  $(CF_2)_2$ , respectively. These calculations at 6 psia total pressure indicated that only free

fluorine, carbon tetrafluoride, and xenon are produced over the temperature range of interest for chemical lasers. The predicted mole percentage compositions of the gaseous combustion products for five values of N are given below.

<u>Gases</u>	<u>Mole Percent</u>				
	<u>N=2.0</u>	<u>N=1.9</u>	<u>N=1.8</u>	<u>N=1.7</u>	<u>N=1.6</u>
F	45.6	46.5	45.4	43.0	40.0
F <sub>2</sub>	2.9	1.0	0.2	0.1	0.0
Xe	25.8	25.6	25.8	26.2	26.7
CF <sub>4</sub>	25.7	26.9	28.6	30.8	33.3
T, °K	1396	1518	1699	1916	2152
Weight % F + F <sub>2</sub>	14.7	13.9	12.8	11.8	10.6

The composition of combustion products was experimentally determined for several ratios of xenon tetrafluoride to polytetrafluoroethylene. The analysis was conducted using the molecular beam type time-of-flight mass spectrometer which is described in Reference 2. A helium purge

around the combustion sample eliminated atmospheric contamination. However, the helium purge mixed with the combustion products which reduced the gas temperature and thus increased the ratio of molecular to atomic fluorine through fluorine atom recombination. Because of this purge quenching effect, the comparison of theoretical and experimental results given below includes the parameter "F Total" which is the total free fluorine plus the fluorine combined as HF, expressed entirely as atomic fluorine. Losses of fluorine due to reaction with the Nichrome ignition wire and the walls of the sampling apparatus are believed to have contributed to the lower observed fluorine concentrations.

Mole Percent - Gases (N=2)	<u>Theoretical</u>	<u>Experimental</u>
"F Total"	50.0	38.8
F	45.6	19.2
F <sub>2</sub>	2.9	8.0
Xe	25.7	35.2
CF <sub>4</sub>	25.7	30.9
HF	0.0	6.7

Although the "totally consumable" xenon tetrafluoride/polytetrafluoroethylene formulations have some attractive features, the safety hazards of all formulations containing  $\text{XeF}_4$  oxidizer led to the termination of experiments with these formulations prior to a lasing demonstration. The  $\text{XeF}_4/\text{C}_2\text{F}_4$  formulations do produce moderate (14.7-10.6 percent) fluorine weight yields, and the secondary constituents Xe and  $\text{CF}_4$  are kinetically innocuous in DF chemical lasers. However, the overriding disadvantage of all formulations containing  $\text{XeF}_4$  is the possibility of forming the extremely sensitive explosive hydrolysis product  $\text{XeO}_3$  if the  $\text{XeF}_4$  is exposed to moisture (Reference 11). In addition, the  $\text{XeF}_4$  has a vapor pressure of 2.5 Torr at 25°C (Reference 12) which results in oxidizer migration and loss from formulation samples.

As an alternative to  $\text{XeF}_4$  oxidizer for "totally consumable" formulations,  $\text{XeF}_2$ , which does not hydrolyze to the hazardous  $\text{XeO}_3$  (References 9 and 10), was investigated. The vapor pressure of  $\text{XeF}_2$  is 4.6 Torr at 25°C (Reference 12). Formulations using  $\text{XeF}_2$  oxidizer with polytetrafluoroethylene, polyethylene, or mixtures of the two polymers as fuel combusted cleanly. However, the fluorine weight yield for all of the formulations with  $\text{XeF}_2$  oxidizer is low, and the average molecular weight of the combustion products is high. The substitution of polyethylene for some or all of the polytetrafluoroethylene in  $\text{XeF}_2$  formulations increased the exothermicity of the binder combustion and decreased the

average molecular weight of the combustion products. However, the addition of polyethylene also introduced substantial quantities of HF into the combustion products which is undesirable because HF rapidly deactivates vibrationally excited DF.

One of the "F atom generator" formulations with  $\text{XeF}_2$  oxidizer which was studied both analytically and experimentally had the following molar composition: 75.67 percent  $\text{XeF}_2$ , 16.22 percent  $\text{CH}_2$ , and 8.11 percent  $\text{C}_2\text{F}_4$ . By weight, this formulation contained 92.50 percent  $\text{XeF}_2$ , 1.64 percent  $\text{CH}_2$ , and 5.86 percent  $\text{C}_2\text{F}_4$ . The theoretical flame temperature for this formulation at 91.70 kPa (13.3 PSIA) is 2577°K. In reality, heat losses to combustor hardware and the quenching effect of added diluent would reduce the combustor temperature by approximately 40 percent to near 1550°K. In calculating the fluorine yield from these "F atom generator" formulations, it is important to take into account these heat loss and diluent quenching effects which would reduce the temperature in an actual laser combustor. At the full theoretical flame temperature of the solid formulation itself, the major combustion product  $\text{CF}_4$  is significantly dissociated into  $\text{CF}_3$ ,  $\text{CF}_2$ , CF, and F. This  $\text{CF}_4$  dissociation can result in unrealistically high apparent yields of free fluorine in equilibrium thermochemistry calculations which do not take the heat loss and diluent quenching effects into account. At a reduced temperature of 1553°K and a pressure of 91.70 kPa (13.3 PSIA), the formulation given above has a theoretical free fluorine weight yield of

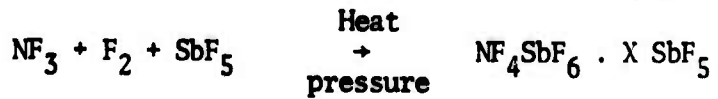
2.966 percent. Under these conditions, the molar composition of the combustion products is 13.10 percent F, 0.13 percent  $F_2$ , 20.02 percent HF, 20.02 percent  $CF_4$ , and 46.73 percent Xe. The corresponding average molecular weight is 85.52, and the specific heat ratio is 1.264.

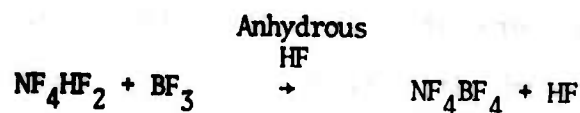
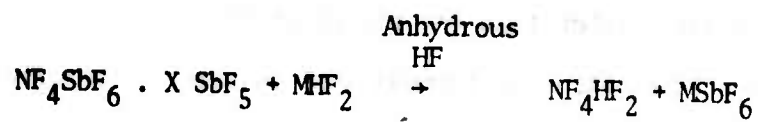
Experimentally, the formulation described in the previous paragraph had a burning rate of 0.085 cm/sec (0.0335 in/sec) at 91.70 kPa (13.3 PSIA) and a density of 3.44 g/cm<sup>3</sup>. A similar formulation without the polyethylene had a density of 3.27 g/cm<sup>3</sup> and a burning rate of 0.082 cm/sec (0.032 in/sec) at the same pressure. The molar composition of this second formulation was 71.78 percent  $XeF_2$  and 28.22 percent  $C_2F_4$ . The corresponding composition by weight was 81.15 percent  $XeF_2$  and 18.85 percent  $C_2F_4$ . For these combustion samples, the particle sizes for the ingredients were as follows:  $XeF_2$   $\leq$  163  $\mu m$ ,  $CH_2$   $\leq$  149  $\mu m$ , and  $C_2F_4$  (Fluoropak 80)  $\leq$  250  $\mu m$ .

As will be discussed in Section V, tests with the AFRPL small scale XCL5 laser and other AFWL-funded tests with much larger chemical lasers demonstrated that the laser performance (with current technology nozzles) is severely degraded by combustor gas flows with high average molecular weights and low specific heat ratios. Therefore, formulation development work on the  $XeF_2$ -oxidized "totally consumable" formulations was terminated.

The quest for "totally consumable" formulations with weight yields of free fluorine higher than the yields attainable with  $XeF_2$  oxidizer led to the investigation of formulations containing the oxidizer tetrafluoroammonium tetrafluoroborate,  $NF_4BF_4$ . This oxidizer has a high theoretical fluorine yield of 53.72 percent by weight (5 moles of F from  $NF_3 + F_2$  per mole of  $NF_4BF_4$ ). Furthermore, the  $NF_4BF_4$  has no vapor pressure at room temperature (it is thermally stable to 280°C), and the  $BF_3$  liberated by the decomposition of  $NF_4BF_4$  has only a moderate deactivation rate for the vibrationally excited DF in the laser cavity.

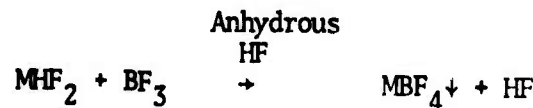
"Totally consumable" formulations using the oxidizers  $NF_4SbF_6$  or  $NF_4AsF_6$  had previously been tested in gram quantities by Rocketdyne (Reference 9), and similar formulations using  $NF_4BF_4$  as the oxidizer had also been examined theoretically under the same program. However, at the time that this AFRPL formulation development effort was being conducted, high purity  $NF_4BF_4$  was not available in experimental quantities. At that time, the only synthetic route known that was capable of producing usable quantities of  $NF_4BF_4$  relied on the metathetical reaction employing  $NF_4SbF_6$  (Reference 10). The synthetic route is given below:

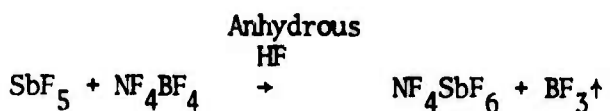
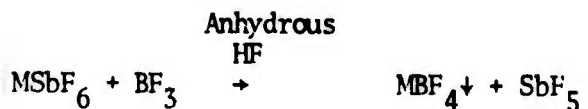




M = Ag or Tl

The following co-reactions significantly reduce the purity of the  $\text{NF}_4\text{BF}_4$  produced by this procedure.





The highest purity achieved using this technique was 85-90 percent before purification and 93 percent after purification. The experimental work was performed on this system prior to the attainment of maximum purity. Thus, the Rocketdyne-synthesized  $\text{NF}_4\text{BF}_4$  used in this early phase of the fluorine generator development effort was only 76 percent pure. The major impurities were 20 percent  $\text{NF}_4\text{SbF}_6$  and 4 percent  $\text{AgBF}_4$ .

In Figure 20, the theoretical combustion properties of  $\text{NF}_4\text{BF}_4$ /polytetrafluoroethylene formulations are plotted for formulations containing from 54 to 60 mole percent  $\text{NF}_4\text{BF}_4$  with the balance of the formulation  $\text{C}_2\text{F}_4$ . The weight yield of free fluorine, the adiabatic combustion temperature, and the molar concentrations of the combustion products are shown.

THIS REPORT HAS BEEN DELIMITED  
AND CLEARED FOR PUBLIC RELEASE  
UNDER DOD DIRECTIVE 5200.20 AND  
NO RESTRICTIONS ARE IMPOSED UPON  
ITS USE AND DISCLOSURE.

DISTRIBUTION STATEMENT A

APPROVED FOR PUBLIC RELEASE,  
DISTRIBUTION UNLIMITED.

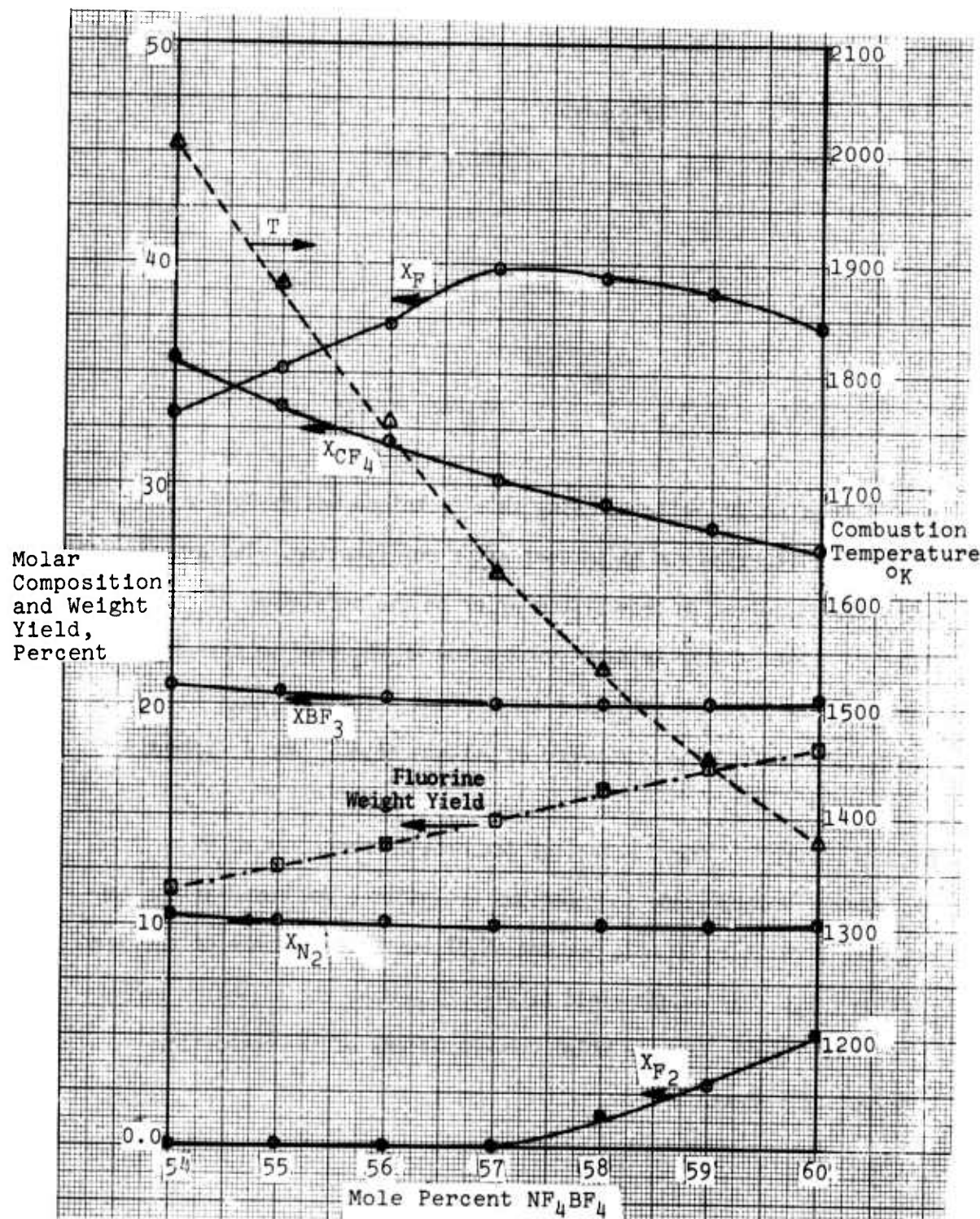


Figure 20. Theoretical Combustion Properties of  $NF_4BF_4$ /Polytetrafluoroethylene Formulations

The composition of the combustion products was experimentally determined for several ratios of  $\text{NF}_4\text{BF}_4$  to Teflon. The analysis was conducted using the molecular beam time-of-flight mass spectrometer which is described in Reference 2. A helium purge around the combustion sample was also employed to eliminate atmospheric contamination as described previously. A comparison between the theoretical and experimental results for two formulation compositions is given in Table 6. Losses of fluorine due to reaction with the Nichrome ignition wire and the walls of the sampling apparatus are believed to have contributed to the lower observed fluorine concentrations. The theoretical weight yields of free fluorine for these two formulations are 11.5 and 7.19 percent for the formulations containing 54 and 50 percent  $\text{NF}_4\text{BF}_4$ , respectively. For  $\text{NF}_4\text{BF}_4$  itself, the full theoretically available fluorine yield (5F from  $\text{NF}_3 + \text{F}_2$  per mole of  $\text{NF}_4\text{BF}_4$ ) is 53.72 weight percent. The theoretical average molecular weights and specific heat ratios are 53.24 and 1.151 for the 54 percent  $\text{NF}_4\text{BF}_4$  formulation and 60.89 and 1.128 for the 50 percent  $\text{NF}_4\text{BF}_4$  formulation.

Burning rate data for these  $\text{NF}_4\text{BF}_4$  formulations were obtained by combusting (in a nitrogen atmosphere) 1.270 cm (0.5 in) long grains pressed into 0.953 cm (0.375 in) diameter bores in nickel combustion sample holder rods. For the 54 percent  $\text{NF}_4\text{BF}_4$  formulation, the burning rate for four grains combusted at 89.7-96.5 kPa (13-14 PSIA) was  $0.081 \pm$

TABLE 6

Comparison of Experimental and Theoretical Combustion Products from  $\text{NF}_4\text{BF}_4$ /Polytetrafluoroethylene Formulations

Formulation Composition (Mole % $\text{NF}_4\text{BF}_4$ /Mole % Teflon)	A <u>50/50</u>	A <u>54/46</u>	B <u>50/50</u>	B <u>54/46</u>
<b>Combustion Products:</b>				
Products in Mole %	<u>Experimental</u>		<u>Theoretical</u>	
F-Atom	4.9	8.6	22.7	33.1
$\text{F}_2$	7.5	9.5	0.0	0.0
$\text{BF}_3$	12.3	15.6	22.1	20.9
$\text{CF}_4$	64.6	60.6	43.8	35.5
$\text{N}_2$	10.7	5.7	11.0	10.4
F-Total as F-Atom	18.5	25.2	22.7	33.1
Temp, °K	-	-	2494	2008

A - 76%  $\text{NF}_4\text{BF}_4$ , 20%  $\text{NF}_4\text{SbF}_6$ , 4%  $\text{AgBF}_4$

B - 100% Pure  $\text{NF}_4\text{BF}_4$

0.005 cm/sec (0.032 in/sec). For three grains of the same formulation which were combusted at 179.3-186.2 kPa (26-27 PSIA), the burning rate was  $0.108 \pm 0.005$  cm/sec. From these data, the pressure exponent for this formulation is 0.43. For a similar grain of the 50 percent  $\text{NF}_4\text{BF}_4$  formulation, the burning rate at 103.4 kPa (15 PSIA) was 0.079 cm/sec. For these formulations, the impact sensitivity test results were negative up to the 250 kg-cm impact energy limit of the standard drop weight tester.

Formulations with polyethylene substituted for some or all of the polytetrafluoroethylene were also investigated with  $\text{NF}_4\text{BF}_4$  oxidizer. As was the case with the  $\text{XeF}_2$ -oxidized formulations, for the same theoretical combustion temperature, the substitution of  $\text{CH}_2$  for  $\text{C}_2\text{F}_4$  lowered the average molecular weight and increased the specific heat ratio of the combustion products. Experimentally, the substitution of  $\text{CH}_2$  for  $\text{C}_2\text{F}_4$  also increased the burning rate. A sample of a formulation with the molar composition of 0.6  $\text{NF}_4\text{BF}_4$ /0.3  $\text{CH}_2$ /0.15  $\text{C}_2\text{F}_4$  had a burning rate of 0.106 cm/sec at 69.0-96.5 kPa (10-14 PSIA) and a density of  $1.99 \text{ g/cm}^3$ . An all-polyethylene formulation composed of 0.6 moles of  $\text{NF}_4\text{BF}_4$  and 0.4 moles of  $\text{CH}_2$  exhibited very good burning characteristics and had a burning rate of 0.148 cm/sec at 62.1 kPa (9 PSIA) and a density of  $1.93 \text{ g/cm}^3$ . Impact sensitivity tests with this latter formulation were positive at an impact level of 60 kg-cm (2 kg x 30 cm). The autoignition temperature for the  $\text{NF}_4\text{BF}_4$  formulations containing polyethylene was

113-115°C (235-239°F) compared to the autoignition temperature of 300°C (572°F) observed for the formulations containing only polytetrafluoroethylene. The  $\text{NF}_4\text{BF}_4$  itself is thermally stable to 280°C (536°F).

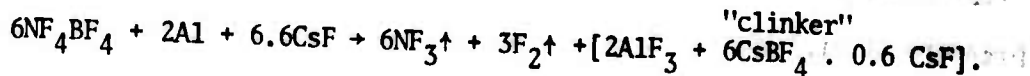
As is discussed in Section V, lasing tests on the AFRPL small-scale XCL5 DF laser using mixtures of bottled gases to simulate the extremely low specific heat ratios and high molecular weights of the combustion products from  $\text{NF}_4\text{BF}_4$ -oxidized "F atom generator" formulations demonstrated that reasonable laser performance could not be obtained with those combustor gas properties. Therefore, development work on these "totally consumable"  $\text{NF}_4\text{BF}_4$ -oxidized formulations was terminated.

At that point in the fluorine generator development effort, it became apparent that the "clinker" type " $\text{NF}_3 + \text{F}_2$  generator" formulations using  $\text{NF}_4\text{SbF}_6$  had the greatest potential for a successful lasing demonstration on the AFRPL XCL5 laser. Although the weight yields from the  $\text{NF}_4\text{SbF}_6$  clinker formulations were low, the fact that the primary gaseous product of the formulations was relatively cool  $\text{NF}_3$  made the task of matching the oxidizer flow rate required for the XCL5 laser (which normally operated on bottled gaseous  $\text{NF}_3$ ) relatively straightforward. Chronologically, some of the characterization tests of the  $\text{NF}_4\text{SbF}_6$  clinker formulations which were described earlier in this section were actually carried out at this stage of the fluorine generator

development effort. The processing of the larger  $\text{NF}_3 + \text{F}_2$  generator grains used in the lasing tests is discussed in Section III.B, and the design of the  $\text{NF}_3 + \text{F}_2$  gas generator hardware and some of the test results are presented in Section III.C.

After the first successful lasing demonstration with the  $\text{NF}_3 + \text{F}_2$  gas generator, the formulation development effort was concentrated on formulations which offered higher weight yields of available fluorine. By June 1975, very high purity  $\text{NF}_4\text{BF}_4$  finally became available in gram quantities from a synthesis contract with Rocketdyne which was jointly funded by AFRPL, AFWL, and the Naval Surface Weapons Center (Reference 10). This very high purity  $\text{NF}_4\text{BF}_4$  was synthesized by an ultraviolet photolysis technique. A clinker formulation was investigated because the previous phases of this development effort had demonstrated that only the clinker formulations could generate combustor gas compositions which were compatible with current technology DF laser nozzle designs.

The  $\text{NF}_4\text{BF}_4$  clinker formulation which demonstrated the best combustion characteristics used MDX 65 aluminum powder as the fuel and used cesium fluoride to trap the volatile boron trifluoride as the solid cesium tetrafluoroborate. The combustion reaction is given below.



At this stoichiometry, the fluorination of the aluminum fuel consumes 50 percent of the  $F_2$  liberated by the decomposition of the  $NF_4BF_4$ . This generates sufficient exothermicity to sustain the reaction with a burning rate of 0.1 cm/sec at a pressure of 91.7 kPa (13.3 psia). A 10 percent excess of cesium fluoride is added to assure complete retention of the boron trifluoride. For this formulation, the theoretical weight yield of available fluorine is 21.53 percent. The formulation was also tested for impact sensitivity. The results were negative below 150 kilogram-centimeters (3 kilogram weight dropped 50 centimeters). Above this impact energy level, a flash and small report with incomplete reaction was observed.

### III.B. FLUORINE GENERATOR FORMULATION PROCESSING

The approach to the preparation of the fluorine generator formulations was straightforward. The crystalline ingredients were first ground separately to a fine powder in a dry nitrogen atmosphere. All of the formulations are very reactive with moisture and thus must be handled in a moisture-free atmosphere at all times. Therefore, all formulation preparations were conducted in a nitrogen atmosphere dry box equipped with a drying train and operated at a very low humidity level (typically a -100°C frost point). The typical dry box nitrogen atmosphere conditions were a pressure of 91.7 kPa (13.3 psia), and a temperature of 15 to 20°C. All

formulation ingredients were sieved separately to a particle size of less than 162  $\mu\text{m}$ . The quantity of each ingredient for the selected formulation was then weighed out separately. All of the ingredients were placed in an appropriate size Teflon beaker in preparation for mixing. The ingredients were thoroughly mixed in the Teflon beaker by stirring with a Teflon coated spatula. For the smaller combustion samples, the thoroughly mixed formulation was pressed into a cohesive solid grain employing a packing pressure of 12.4 MPa (1800 psi) delivered by a hand-operated mechanical press. The packing pressure was measured with an electronic force transducer (load cell). For the larger  $\text{NF}_3 + \text{F}_2$  generator grains, a small hydraulic press installed within the drybox was used to apply the 10.3 MPa (1500 psi) packing pressure used for those 2.54 cm (1.0 in) diameter grains. Fluorine-compatible "Kel-F" oil was used in the press hydraulic circuit.

Various fluorine generator grain sizes were used depending on the type of formulation and the burning rate. For the fluorine generator formulations, nickel rods with grain cavities of various diameters and lengths bored in one end were used as the grain containers. For the gram-scale combustion samples used during the formulation characterization tests, 1.27 cm (0.5 in) outside diameter nickel rods with grain cavities of 0.953 cm (0.375 in) or 0.635 cm (0.25 in) diameter by 1.27 cm (0.5 in) or 0.635 cm (0.25 in) in depth were used. For the smaller grains, a definite "heat sink" effect due to heat losses from the small

combustion samples to the relatively massive, high thermal conductivity nickel walls of the grain containers was noted. The smaller grains typically exhibited lower burning rates and more frequently extinguished before complete combustion of the grain. For the clinker formulations, the clinkers from the larger grains were significantly more molten. This grain size effect on the combustion properties of the  $\text{NF}_3 + \text{F}_2$  generator formulation used in the lasing tests is discussed in greater detail in the following section.

Ignition of fluorine generator samples was readily achieved using a Nichrome hot wire technique in which an electrical current of sufficient magnitude to heat the Nichrome wire to the ignition temperature of the sample was passed through the wire which was in physical contact with the sample surface.

### III.C. $\text{NF}_3 + \text{F}_2$ GAS GENERATOR

A cross section of the  $\text{NF}_3 + \text{F}_2$  gas generator design which was used for the lasing tests with the  $\text{NF}_4\text{SbF}_6$ -oxidized clinker formulation is shown in Figure 21. Many of the details of this gas generator design are similar to the Mod 1 and Mod 2  $\text{D}_2$  gas generator designs. However, the entire  $\text{NF}_3 + \text{F}_2$  gas generator was fabricated from nickel 200 instead of the 300 series stainless steels used in the  $\text{D}_2$  generators. Nickel

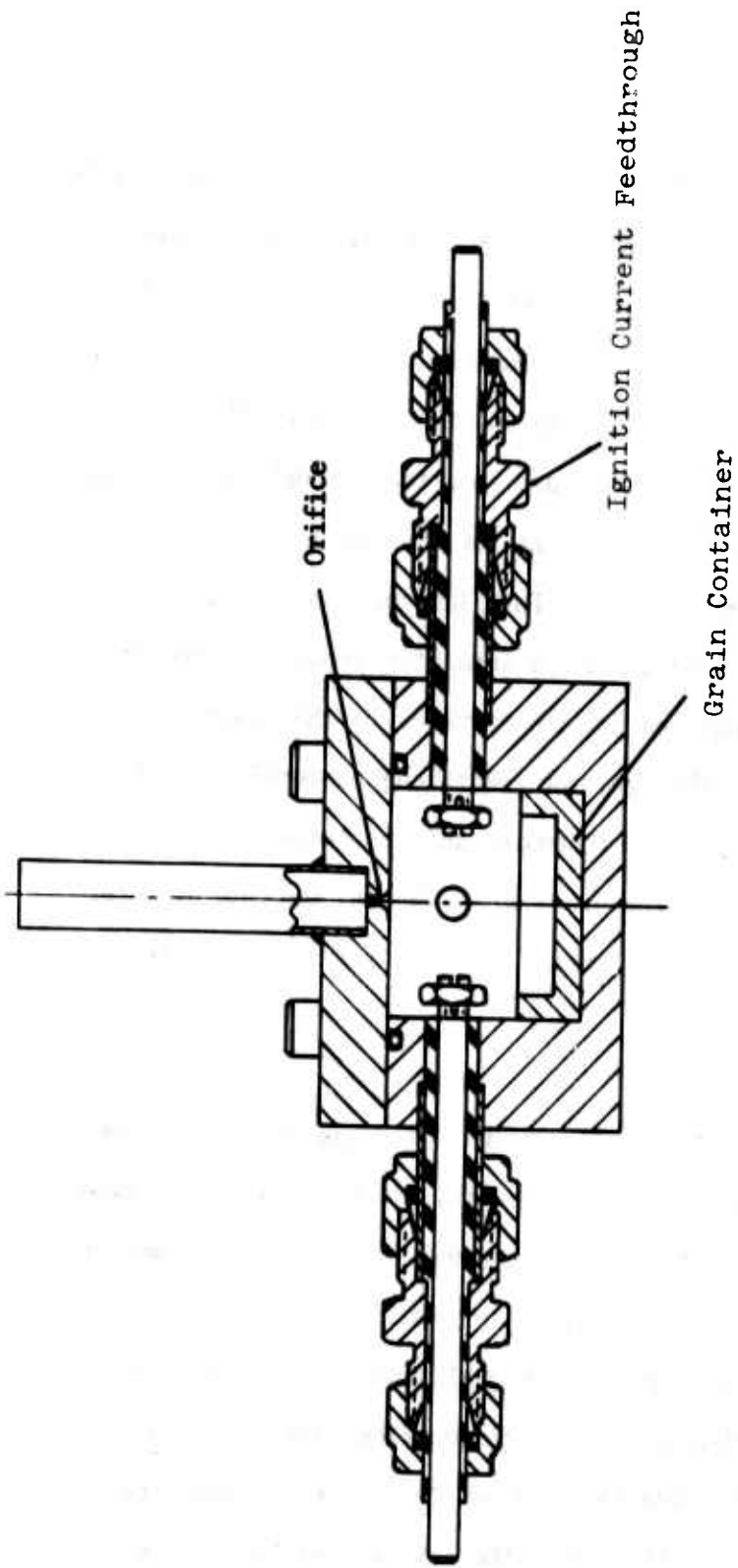


Figure 21.  $\text{NF}_3 + \text{F}_2$  Gas Generator

was selected to maximize the  $\text{NF}_3 + \text{F}_2$  gas generator survivability due to the excellent fluorine compatibility of nickel at high temperatures (Reference 13). The mechanical designs of the three 0.953 cm (0.375 in) outside diameter tubing stubs which are spaced at  $90^\circ$  increments around the outside of the gas generator housing and the design of the two ignition feedthrough assemblies which are inserted through two opposing tubing stubs are identical to the designs for the Mod 1  $\text{D}_2$  generator which were described in Section II.C. For fluorine compatibility, polytetrafluoroethylene was used for the insulator around the copper ignition current feedthrough and for the ferrules in the Swagelok reducing unions which seal the ignition feedthrough assemblies. The O-ring seal between the gas generator housing and the cover was also polytetrafluoroethylene. The one 0.635 cm (0.250 in) outside diameter tubing stub on the gas generator housing was used for the pressure transducer.

The  $\text{NF}_3 + \text{F}_2$  gas generator design includes a sonic orifice in the gas generator cover. This 0.838 mm (0.033 in) diameter orifice between the interior of the gas generator and the 0.953 cm (0.375 in) diameter outlet tubing was included in the design to permit the  $\text{NF}_3 + \text{F}_2$  generator grains to burn at pressures several times higher than the pressure in the laser combustor. With this orifice, the  $\text{NF}_3 + \text{F}_2$  generator operated at 234.4 kPa (34 PSIA) while the laser combustor pressure was 37.9 kPa (5.5 PSIA) during the lasing Test No. 501 which

is described in Section V.C. Furthermore, by flowing the  $N_2$  diluent for the laser combustor into the  $NF_3 + F_2$  generator and then out through the orifice into the laser combustor, the pressure in the gas generator at the time of the  $NF_3 + F_2$  generator grain ignition could be increased from less than 6.9 kPa (1 psia) to 34.5-69.0 kPa (5-10 psia). This pressurization of the  $NF_3 + F_2$  gas generator using the  $N_2$  diluent eliminated the problem of difficult ignition of the  $NF_3 + F_2$  generator grains at very low pressures. A Swagelok tee fitting was used to couple both the  $N_2$  inlet line and the pressure relief line to the one remaining 0.953 cm (0.375 in) diameter tubing stub on the gas generator housing which was not used for an ignition feedthrough. A Nupro type 6C check valve set for a 69 kPa (10 psi) opening pressure differential was used in the  $N_2$  inlet line to prevent backflow from the  $NF_3 + F_2$  generator into the  $N_2$  supply system. A second Nupro type 6C valve with a spring set for an opening pressure of 440 kPa (63 psia) was used as a pressure relief valve. The vent line from the pressure relief valve was routed directly into the laser vacuum pumping system. Polytetrafluoroethylene O-rings were used successfully in both valves.

The pressurization of the  $NF_3 + F_2$  gas generator with the  $N_2$  diluent flow significantly reduced the incidence of orifice plugging by particulates ejected from the  $NF_3 + F_2$  generator grain during low pressure ignition. The orifice plugged in two out of three tests without  $N_2$

pressurization of the gas generator. In contrast, out of six tests with the gas generator initially pressurized with  $N_2$  to between 24.1 and 77.2 kPa (3.5 to 11.2 psia), the gas generator orifice plugged on only one test. In all three tests where the orifice plugged, the Nupro relief valve successfully vented the combustion products into the laser vacuum system until the grain burned out and then resealed.

The nitrogen flow into the gas generator also enhanced hardware survivability by diluting and cooling the mixture of  $NF_3$  and  $F_2$  generated by the grain. No damage to any of the metallic components of the gas generator was observed in any of the nine tests. However, some regression of the polytetrafluoroethylene insulators around the copper ignition current feedthrough rods was noted.

The  $NF_4SbF_6/CsF/A1N$  formulation for the laser tests was pressed into 2.54 cm (1.00 in) diameter by 0.508 cm (0.200 in) deep holes bored into 3.175 cm (1.25 in) outside diameter by 0.953 cm (0.375 in) thick nickel 200 discs. The 3.213 cm (1.265 in) inside diameter of the gas generator housing allowed clearance for insertion and removal of the grain discs when the ignition feedthroughs were withdrawn from the tubing stubs.

The eight tests of the 2.54 cm (1.0 in) diameter, 6.26 gram grains in this  $NF_3 + F_2$  gas generator hardware provided additional data on the

combustion properties of the  $\text{NF}_4\text{SbF}_6 \cdot 0.8 \text{ SbF}_5/1.98 \text{ CsF}/0.167\text{AlN}$  formulation. When the clinkers from these larger grains were examined after a test, it appeared that the clinker had been significantly more molten than had been the case with the smaller combustion samples. "Splatters" of clinker were found on the side walls of the gas generator housing and on the underside of the cover after several tests. Burning rate data calculated from the pressure traces of the best seven tests of these larger grains is plotted in Figure 22. From these data, the burning rate pressure exponent is approximately 0.4 although there is considerable scatter in the data. The differences in the average combustion pressures for these seven tests of nominally identical grains are due primarily to large changes in the  $\text{N}_2$  diluent flow rate into the  $\text{NF}_3 + \text{F}_2$  generator. Pressure traces from laser tests with the  $\text{NF}_3 + \text{F}_2$  gas generator coupled to the combustor of the AFRPL XCL5 DF laser are presented in Section V.C.

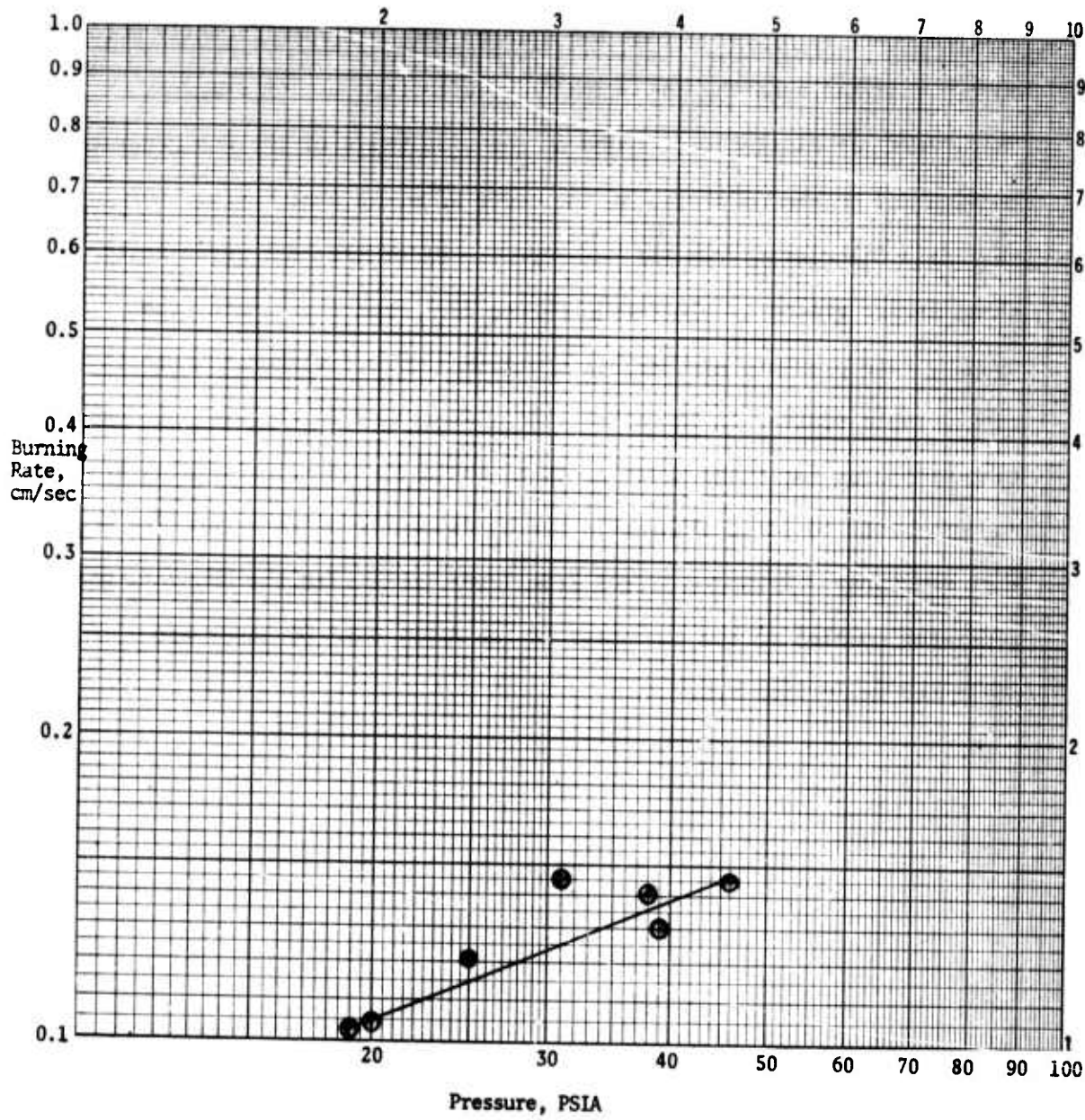


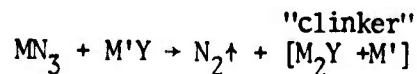
Figure 22. Burning Rate Data for  $\text{NF}_4\text{SbF}_6/\text{CsF}/\text{AlN}$  Formulation from Tests of 2.54 cm (1.0 in) Diameter Grains in  $\text{NF}_3 + \text{F}_2$  Gas Generator

## SECTION IV

### NITROGEN GAS GENERATORS

#### IV.A. NITROGEN GENERATOR FORMULATIONS

Formulations which generate high purity nitrogen or nitrogen plus carbon dioxide were developed. These formulations generate nitrogen from the reaction between an alkali metal azide and a metal oxide, nitrate, sulfide, perchlorate, and/or carbonate. Essentially all of the reaction products except the nitrogen gas are retained in the gas generator as a cohesive sintered "clinker". The AFRPL nitrogen generating formulations are similar in concept to compositions investigated by United Technology Center of Sunnyvale, California, for analogous applications (Reference 14). The basic thermite reaction is of the "Goldschmidt" type as given below:



where M is sodium, potassium or possibly lithium, and M'Y is sodium nitrate, ferrous sulfide, ferric oxide, sodium perchlorate, and/or ferrous carbonate.

The structural integrity of the residual "clinker" and the nitrogen gas purity were acutely dependent on the mixture of liquid and solid combustion products that remained to form the "clinker". The nitrogen generating formulations were the most sensitive of all the generators to this phenomenon. This residue must remain sufficiently porous to allow the nitrogen gas produced in the combustion zone to flow readily through the previously combusted area and yet contain an adequate concentration of liquid constituents to prevent the ejection of solid particles. An excessively molten clinker will slump and spatter liquid residue because of excessive pressure buildup within the grain. Particulate ejection and "dusting" were also strongly dependent on the nitrogen gas evolution rate, and a maximum practical burning rate existed for each particular formulation.

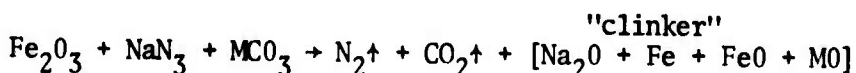
Numerous formulations were screened through the first step in the formulation process. However, the only binary nitrogen generator systems which consistently gave acceptable results throughout the second and third steps (combustion characterization and combustion product sampling) in the formulation development process were the compositions consisting of from 30 to 50 weight percent sodium azide and from 70 to 50 weight percent ferric oxide. Formulations with less than 30 weight percent

sodium azide would not sustain combustion. The formulations that were composed of more than 50 weight percent sodium azide produced a nitrogen gas evolution rate too great for the "clinker" to maintain adequate structural integrity and thus prevent particulate ejection and "dusting". This problem was due primarily to the increase in burn rate from 0.2 cm/sec for the 30 weight percent sodium azide formulation to 0.4 cm/sec for the 50 weight percent formulation and the accompanying decrease in structural integrity of the grain due to the increase in exothermicity which produces a more molten residue. All of the formulations within this range of composition produce essentially 100 percent pure nitrogen. The theoretical combustion temperatures for the formulations range from 600°K for the 30 weight percent sodium azide formulations to 1000°K for the 50 weight percent formulations. The corresponding experimental combustion temperatures were found to be approximately 200°K less than theoretical. Densities ranged from 1.6 to 1.8 g/cc depending on packing pressures. However, the gas evolution rate per unit area remained essentially constant for a particular formulation. The increase in density with increased packing pressure was offset by a decrease in linear burn rate resulting in the constant gas evolution rate. The formulation consisting of 65% by weight ferric oxide and 35% by weight sodium azide yielded 85 cm<sup>3</sup>/sec of nitrogen gas per square centimeter of grain with an overall weight yield of 22%. Lasing tests were conducted with three nitrogen gas generating formulations with the following compositions (by weight): 65 percent ferric oxide/35 percent sodium

azide; 67.5 percent ferric oxide/32.5 percent sodium azide; and 60 percent ferric oxide/40 percent sodium azide.

Formulations which could potentially have provided higher weight yields of nitrogen were also investigated. Formulations consisting of ferric oxide, sodium azide, and one or more compounds from the group consisting of ferrous carbonate, ferrous sulfide, sodium perchlorate, and sodium nitrate produced nitrogen weight yields of up to 30%. Unfortunately, the higher burning rate of these more exothermic formulations resulted in unacceptable "clinker" properties.

Nitrogen plus carbon dioxide generators for possible DF-CO<sub>2</sub> transfer chemical laser applications were also developed. These formulations were designed to employ the exothermicity of the thermite reaction to thermally decompose a metal carbonate into the metal oxide plus CO<sub>2</sub>. The approximate combustion reaction is as follows:



where M is iron, magnesium or calcium. In some instances, more energetic oxidizers such as sodium perchlorate were added to increase the exothermicity. One of the more promising formulations was composed of the

following ingredients on a mole basis: sodium azide 44.75%, sodium perchlorate 4.5%, ferric oxide 4.5%, ferrous carbonate 12.5%, and calcium magnesium carbonate 33.75%. This formulation produced 77.8% nitrogen and 22.2% carbon dioxide on a mole basis at a burn rate of 0.56 cm/sec. The total gas yield was 26.6 percent by weight.

All of the nitrogen and nitrogen plus carbon dioxide gas generator formulations exhibited no impact sensitivity and low burn rate pressure exponents. For some of the formulations, the burn rate decreased slightly with increased pressure, and some would not sustain combustion at pressures above about 1000 psi.

#### IV.B. NITROGEN GENERATOR FORMULATION PROCESSING

The preparation of the nitrogen and nitrogen plus carbon dioxide generators was similar and straightforward. The crystalline ingredients were first ground separately to a fine powder except for the ferric oxide which was used as supplied. All of the formulation ingredients except the ferric oxide were sieved separately to a particle size range of from 43 to 146  $\mu\text{m}$ . All of the ingredients were dried at a temperature of 140°C. The ingredients were stored in a desiccator in preparation for mixing. The quantity of each ingredient for the selected formulation was then weighed out separately. All of the ingredients

were placed in an appropriate size container in preparation for mixing. The ingredients were then thoroughly mixed by stirring with a spatula.

During the mixing step of the processing cycle, approximately 3 to 6 weight percent water was added in the form of a fine mist by employing an atomizing sprayer. The mixture was stirred continuously during the addition of the water to achieve uniformity. The addition of water during processing is essential for adequate structural integrity of the finished grains. The enhancement of grain cohesiveness by water addition during processing is attributed to intergranular bonding through the recrystallization during the grain drying cycle of the fraction of the sodium azide which was dissolved during the wet mixing.

Next, the thoroughly mixed formulation was pressed into a cohesive solid grain at a packing pressure of 10.34 MPa (1500 psi) delivered by a hydraulic or mechanical press. Grain sizes varied depending on the formulation and the desired gas flow rate. The grains were then dried overnight at a temperature of 140°C. Processing in this manner results in a brick-like grain of good structural integrity.

#### IV.C. NITROGEN GAS GENERATORS

To ignite the  $N_2$  or  $N_2 + CO_2$  gas generators, the same non-gassing sheet igniter material ("heat paper") which was used for the  $D_2$  and  $H_2$  gas generators and which is described in Section II.C. was employed.

The sheet igniter material itself was ignited with a Nichrome hotwire which was also used to hold the igniter sheet against the surface of the grain.

For the initial lasing tests with the  $N_2$  generators at AFRPL which are described in Section V.B., the  $N_2$  generator grain can was coupled directly to the laser combustor. Therefore, the grains burned at very low pressures ranging from 27.6 to 48.3 kPa (4-7 psia). To match the relatively high flow rate requirements of this initial test laser, a grain diameter of 6.033 cm (2.375 in) was required. The very low combustor pressure made ignition of the  $N_2$  generator grains difficult, and the low pressure coupled with the relatively large grain diameter made the problems of particulate ejection from the grain and grain breakup quite severe. The laser assembly with the  $N_2$  generator grain can is shown in Section V.B.

For the subsequent lasing tests with the AFRPL XCL5 DF laser which are described in Section V.C., a separate  $N_2$  gas generator assembly operating at higher pressure was employed. The use of a separate gas generator with a sonic metering orifice between the  $N_2$  generator and the low pressure in the laser combustor allowed the  $N_2$  generator grains to burn in the 345-690 kPa (50-100 psia) pressure range where the problems with particulate ejection and grain breakup were less severe. To meet

the lower flow rate requirements of the XCL5 laser, grain diameters ranging from 0.953 cm (0.375 in) to 1.270 cm (0.50 in) were used. Grain cavities of the required diameter and length were bored into one end of 2.54 cm (1.00 in) outside diameter stainless steel rods. These rods were then inserted into one end of a modified 2.54 cm (1.0 in) Swagelok union which formed the center of the gas generator assembly. This  $N_2$  gas generator design was an adaption of the first generation  $D_2$  generator design which is shown on the left in Figure 10. A Nupro type SS-4F-7 inline filter with a 7  $\mu\text{m}$  filter element was coupled to the outlet of the  $N_2$  gas generator to prevent any particulates ejected by the grain from clogging the micrometering valve which was used to set the  $N_2$  generator operating pressure.

The pressure trace from a test (No. 502) of one of these low flow rate  $N_2$  generators used with the XCL5 laser is shown in Figure 23. For this test, the grain diameter was 0.953 cm (0.375 in), the grain length was 3.175 cm (1.25 in), and the formulation was 60 weight percent ferric oxide and 40 weight percent sodium azide. The mid-burn pressure of 565.4 kPa (82 psia) corresponds to an  $N_2$  flow rate of 4.68 liters (S.T.P.) per minute for the particular setting of the  $N_2$  micrometering valve which was used for this test. The slightly regressive pressure trace was typical for these relatively long, small diameter grains. The slow pressure buildup after grain ignition and the long tailoff are due

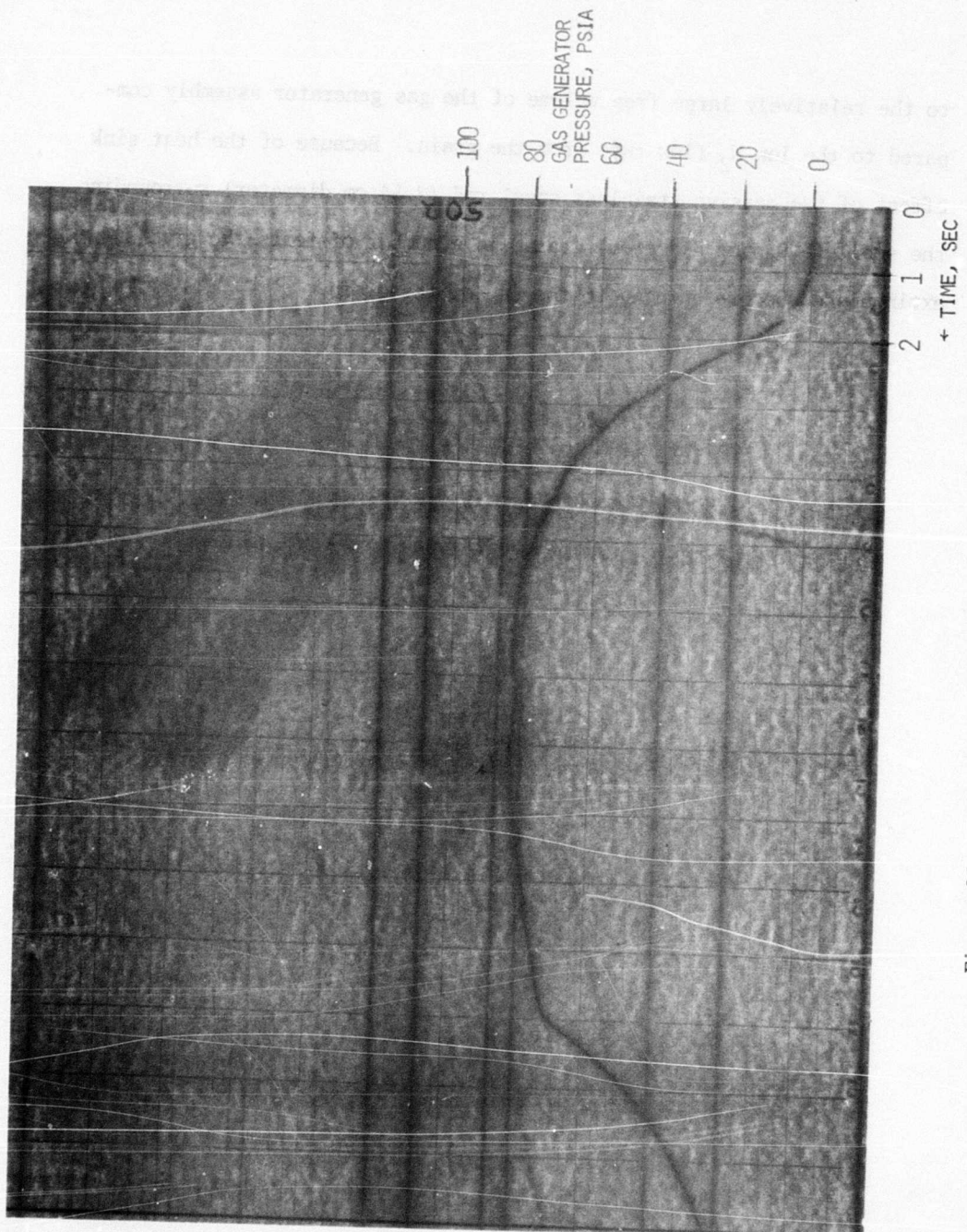


Figure 23. Pressure Trace for Nitrogen Generator Test (No 502)

to the relatively large free volume of the gas generator assembly compared to the low  $N_2$  flow rate from the grain. Because of the heat sink effect of the massive stainless steel rod (2.54 cm diameter) surrounding the small (0.953 cm diameter) grain, in a number of tests the grains extinguished before burning to the end of the grain.

## SECTION V

### LASING DEMONSTRATIONS WITH SOLID PROPELLANT GAS GENERATORS

The first successful lasing demonstrations using reactants supplied from solid propellant gas generators were conducted under this program. These lasing demonstrations were conducted using four different chemical lasers. The pioneering lasing demonstration using a solid propellant hydrogen generator was conducted at AFWL on a low power, subsonic flow laser operating in the HF chemical laser mode. The first lasing demonstrations using solid propellant deuterium and nitrogen generators were conducted at AFRPL on a low power chemical laser with a single nozzle which had cavity fuel injection orifices at the throat. This laser was operated in both the DF-CO<sub>2</sub> transfer chemical laser mode and the DF chemical laser mode using the deuterium and nitrogen generators. Subsequent deuterium generator tests and the first lasing demonstrations using a solid propellant gas generator to supply the nitrogen trifluoride plus fluorine oxidizer were conducted on a second low power DF laser at AFRPL. This second design used a more conventional DF laser nozzle configuration with separate oxidizer and cavity fuel nozzles. The final lasing demonstrations using scaled-up deuterium generators were conducted on a kilowatt power range, supersonic flow DF laser at AFWL. These lasing demonstrations are discussed in chronological order in the following sections.

#### V.A. HYDROGEN GENERATOR LASING DEMONSTRATIONS AT AFWL:

The first demonstrations that a chemical laser could indeed be operated with one of the laser's reactants supplied from a solid propellant gas generator were conducted at AFWL on 14 and 15 March 1973. For these tests, the first generation hydrogen generator developed by AFRPL was coupled to a low power HF laser at AFWL. This first generation hydrogen generator is shown on the left in Figure 10, and the design is discussed in Section II.C. The AFWL subsonic flow laser was a duplicate of the design developed by Falk (Reference 15). However, for these tests, the laser was operated in the HF chemical laser mode rather than in the DF-CO<sub>2</sub> transfer chemical laser mode. In this laser design, fluorine atoms are generated in the low temperature combustor by the reaction between nitric oxide (NO) and molecular fluorine. The hydrogen cavity fuel is injected into the subsonic flow through rows of injection holes in an array of spraybar tubes at the combustor exit. The laser system is shown in Figure 24 with the hydrogen gas generator in the left center. The broadband power meter which was used to measure the out-coupled power from the laser is in the lower right corner of the photograph.

For this test series, the fluorine and helium flow rates were held at nominally constant values, the hydrogen cavity fuel flow rate was

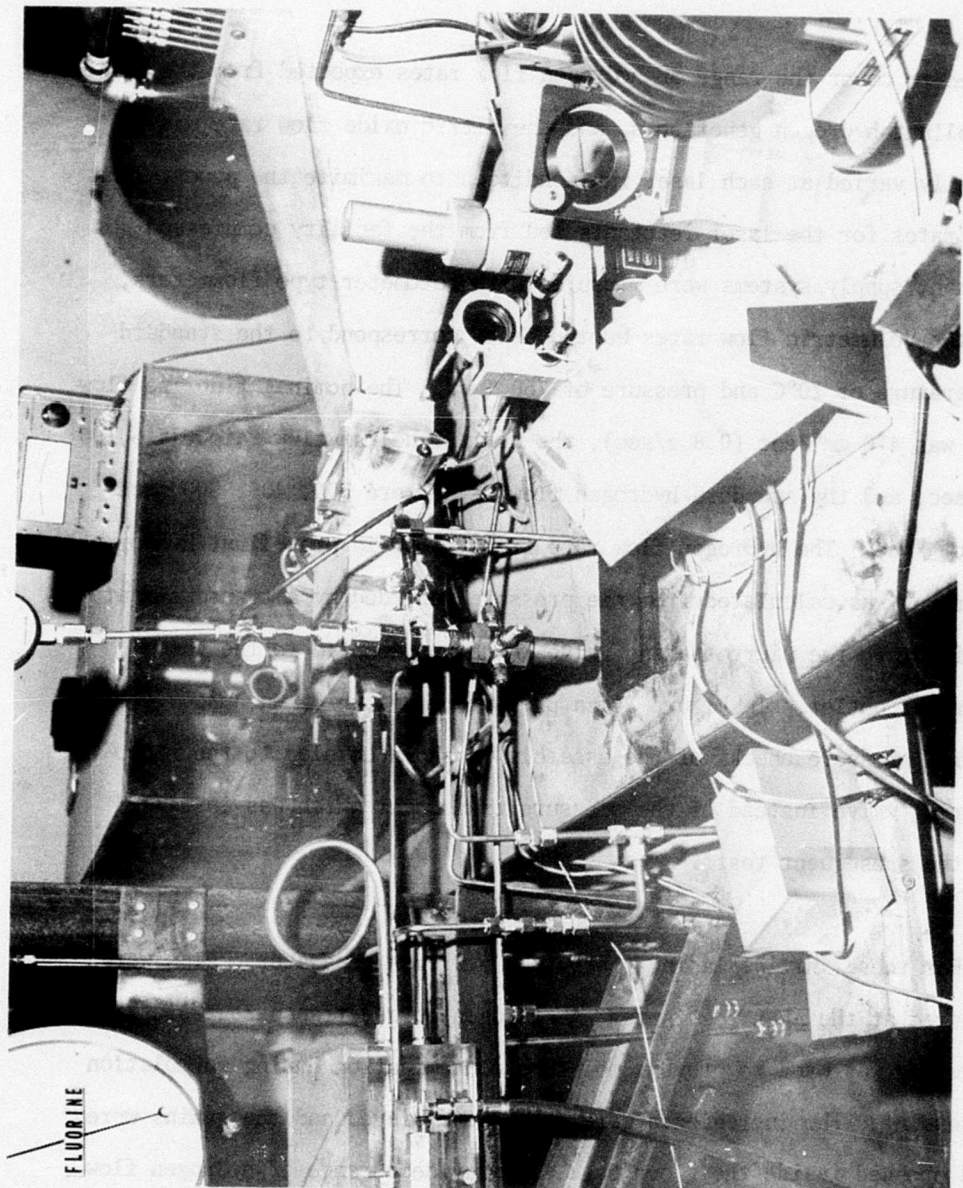


Figure 24. AFRPL First Generation Hydrogen Generator Coupled to AFWL Subsonic Flow HF Laser for the First Lasing Demonstration

varied to cover the range of hydrogen flow rates expected from the solid propellant hydrogen generators, and the nitric oxide flow rate was manually varied at each laser run condition to maximize the power. The flow rates for the laser reactants fed from the facility compressed gas reactant supply systems were measured with rotameter-type flowmeters, and the volumetric flow rates quoted below correspond to the standard temperature of 20°C and pressure of 760 Torr. The nominal fluorine flow rate was 470  $\text{cm}^3/\text{sec}$  (0.8 g/sec), the nominal helium flow rate was 5,100  $\text{cm}^3/\text{sec}$ , and the standard hydrogen flow rates were 300, 400, 500, and 600  $\text{cm}^3/\text{sec}$ . The hydrogen flow rate from the solid propellant hydrogen generator was calculated from the pressure recorded by a transducer at the inlet to the micrometering valve which was coupled to the gas generator outlet. In Figure 24, a pressure gauge which was used for the initial pressure checks of the assembly is shown coupled to the micrometering valve instead of the pressure transducer which was installed for the subsequent tests.

For these initial lasing tests, the hydrogen generator grains were prepared at the AFWL test site. A nitrogen-purged transparent plastic glove bag was used to prevent moisture contamination during formulation processing. The ingredients were ground and sieved and the grains were hand pressed inside the glove bag. To provide a range of hydrogen flow rates with a constant 2.22 cm (0.875 in) grain diameter, the grain

burning rates were altered by changing the  $\text{LiAlH}_4:\text{NH}_4\text{Cl}$  ratio and the ingredient particle size range of the formulation batches. Formulation batches with  $\text{LiAlH}_4:\text{NH}_4\text{Cl}$  ratios of both 3:1 and 4:1 were tested. The  $\text{LiAlH}_4$  was ground and sieved to  $< 147 \mu\text{m}$  for all of the formulations. For the higher burning rate batches, the  $\text{NH}_4\text{Cl}$  particle size was  $< 43 \mu\text{m}$  and for the lower burning rate batches the  $\text{NH}_4\text{Cl}$  particle size range was between  $43 \mu\text{m}$  and  $147 \mu\text{m}$ . Because of the hand processing in an improvised facility, there were variations in combustion pressure history from grain to grain. Nevertheless, the laser operated successfully in 15 out of 16 gas generator tests, and only the accidental misalignment of one of the laser cavity mirrors prevented lasing on the 16th gas generator test.

These lasing tests demonstrated that, within the accuracy limits of the data, the power output when the laser was operating on hydrogen supplied by the solid propellant gas generator was the same as the power output when the laser was operating on hydrogen supplied by the compressed gaseous hydrogen feed system. This result was anticipated because, as was discussed in Section II.A., the gas sampling tests had previously demonstrated that the hydrogen generator formulations produced very high purity hydrogen. In Figure 25, the laser power output is plotted as a function of hydrogen flow rate for both the tests with hydrogen supplied from the gas generator and the baseline tests with

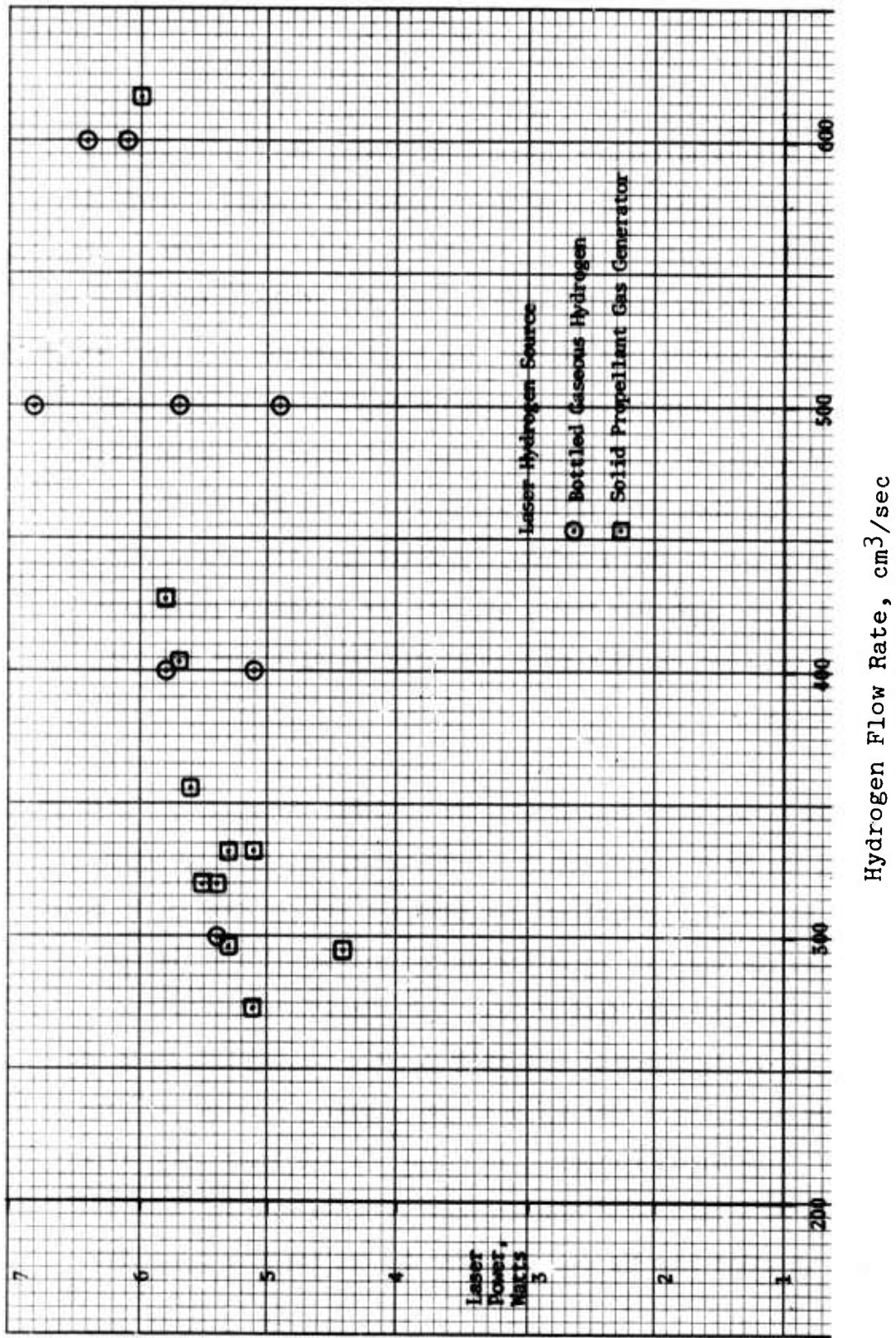


Figure 25. Comparison of Laser Output Power Using Hydrogen From Solid Propellant Gas Generators and From Compressed Gas Feed System

hydrogen from the standard facility hydrogen feed system. There is considerable scatter in both sets of output power data, but both sets lie within the same performance band. The considerable test-to-test variation in output power for this laser is due to changes in the NO flow rate, deviations from the nominal helium flow rate, and differences in optical cavity alignment.

V.B. DEUTERIUM AND NITROGEN GENERATOR LASING DEMONSTRATIONS USING  
AFRPL LASER WITH THROAT INJECTION NOZZLE

At AFRPL Test Area 1-14, a special test facility was installed for the low power lasing tests to demonstrate the feasibility of the solid propellant laser gas generators. The laser system was installed in an enclosed test bay which was separated from the adjacent control and instrumentation room by a blast wall with two blast doors. A dedicated analog data acquisition system provided up to 18 channels of data on a direct-write oscillograph record. This laser facility was designed for low power, short duration lasing tests to permit lasing feasibility demonstrations with minimum quantities of the solid gas generator formulations. Multiple compressed gas reactant supply systems were installed so that the baseline laser performance could be established using gases from these conventional reactant supply systems before substituting solid propellant gas generators to supply one or more of the reactant gases. Nitrogen trifluoride,  $NF_3$ , was the oxidizer for all of the laser

tests except the tests with the solid propellant  $\text{NF}_3 + \text{F}_2$  generators which are described in the next section.

To provide the vacuum pumping required to permit the laser to operate with cavity pressures of a few Torr, this laser facility included a unique liquid nitrogen cooled cryopump assembly rather than steam ejectors or mechanical vacuum pumps which are conventionally used with chemical lasers. The cryopump system maintains a low pressure in the laser cavity through the very rapid physical adsorption of the laser exhaust gases onto the extremely large effective surface area of canisters filled with pellets of synthetic zeolite material chilled to liquid nitrogen temperature. This cryopump assembly used six Varian Triple VacSorb\* pump canisters which were filled with Linde Type 5A Molecular Sieve pellets. As is shown in Figure 26, each cryopump canister is surrounded by a dewar for the liquid nitrogen. Liquid nitrogen for the cryopump was stored in a large cryogenic storage sphere outside the test bay and was distributed to the individual cryopump dewars through the distribution manifold and the six cryogenic valves which are visible along the top of the cryopump assembly in Figure 26. A Varian 15.24 cm (6 in) high vacuum gate valve was installed between the cryopump and the laser cavity to isolate the cryopump so that the laser cavity side of the vacuum system could be brought up to atmospheric pressure during the initial one hour chill-down of the cryopump and between laser tests.

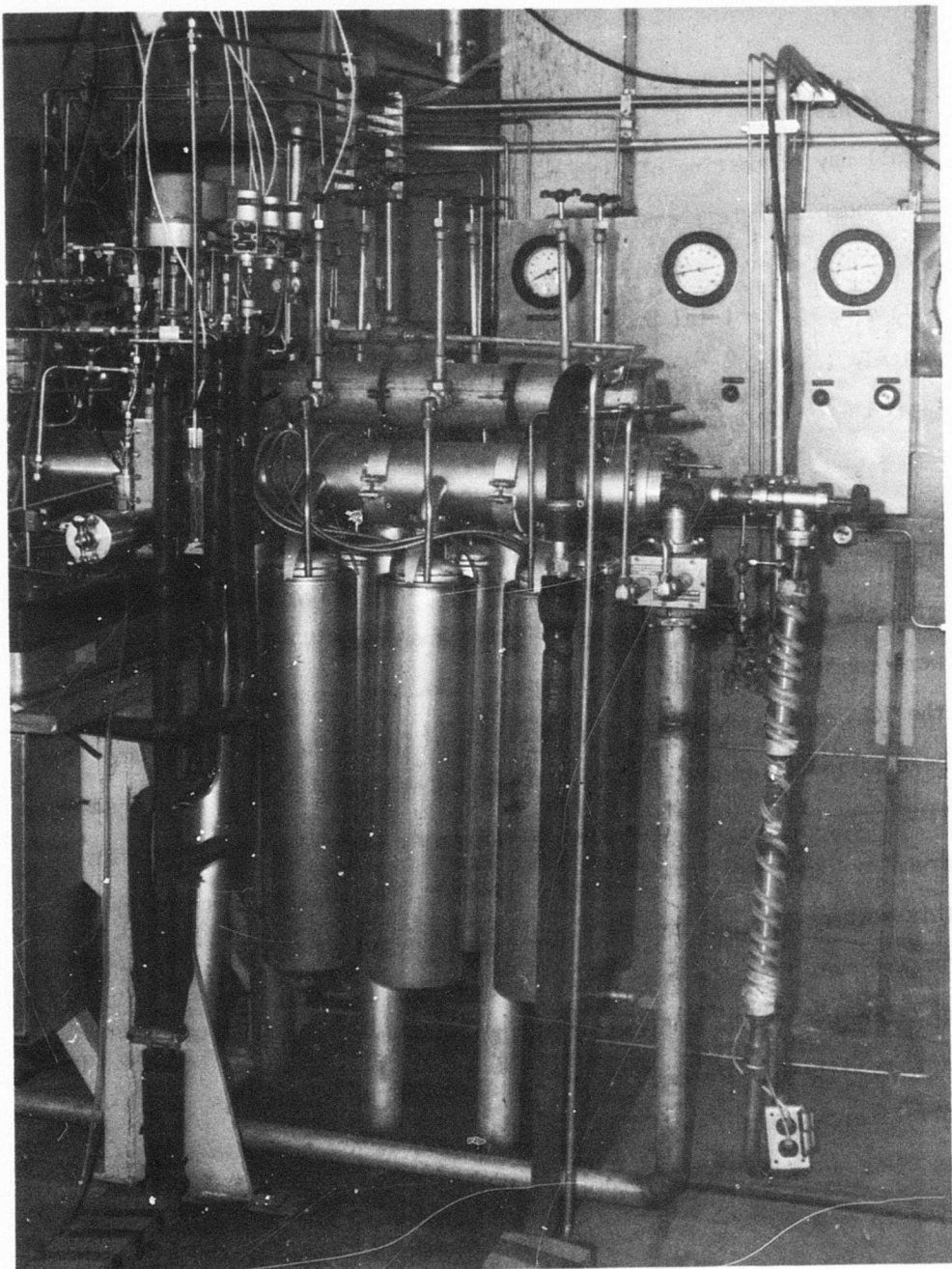


Figure 26. Cryopump System for AFRPL Laser Tests

This cryopump assembly provided sufficient adsorption capacity for a full day of testing of either of the AFRPL low power lasers. The six cryopump canisters contained a total of 20.4 kg of the Linde Type 5A Molecular Sieve. According to the Varian technical data sheets on these cryopumps, the total pumping capacity of the six pump system was approximately  $1.8 \times 10^6$  Torr-liters of nitrogen (or air), and the total pumping speed was approximately  $7.8 \times 10^4$  liters/sec at 20 Torr.

When this cryopump system was originally designed, all of the AFRPL laser testing was oriented toward nitrogen diluent, and all of the tests with the throat injection nozzle which are described in this section were conducted with nitrogen diluent. However, for some of the tests of the XCL5 nozzle which are described in Section V.C., the higher specific heat ratio ( $\gamma$ ) of a monatomic diluent was required. At 78°K, the adsorption capacity of the Linde Type 5A Molecular Sieve is even higher for argon or xenon than for nitrogen. However, the adsorption capacity of this sorbent for the lighter monatomic gases neon and helium is significantly lower than the adsorption capacity for nitrogen. As is discussed in Reference 16, for a pressure of  $10^{-2}$  Torr of the adsorbed gas in equilibrium with this sorbent at 78°K, the adsorption capacities in units of Torr-liters of adsorbed gas per gram of sorbent are as follows: nitrogen, 100; neon,  $\sim 9 \times 10^{-4}$ ; helium,  $\sim 8 \times 10^{-5}$ . Therefore, with this cryopump system, helium could not be used as the laser diluent because.

of excessive pressure increases in the laser cavity during a test. However, neon diluent was satisfactorily cryopumped at the low diluent flow rates required for the XCL5 laser. Following an XCL5 laser test, a residual pressure of 0.2 to 0.4 Torr of neon remained in the cryopump depending on the test duration and neon flow rate. To remove this residual neon, a Roots blower with a displacement of  $14.6 \text{ m}^3/\text{min}$  (516  $\text{ft}^3/\text{min}$ ) backed by a roughing pump with a displacement of  $1.42 \text{ m}^3/\text{min}$  (50  $\text{ft}^3/\text{min}$ )\* was coupled into the cryopump assembly. The 6.35 cm (2.5 in) diameter vacuum line to the blower is visible at the right end of the cryopump assembly in Figure 26. The liquid nitrogen cooled chevron baffle cold trap in this line is also visible. During the laser tests, a gate valve in this vacuum line isolated the blower from the cryopump system to prevent any toxic or corrosive combustion products from entering the mechanical pumping system. After a test, only neon and a trace of deuterium remained in the gas phase in the cryopump, and the valve to the blower was opened. Following a typical XCL5 laser test with neon diluent, the blower system reduced the residual neon pressure from 0.28 Torr to 0.04 Torr in less than 10 minutes. The deuterium adsorption capacity of the cryopump system was sufficient to adsorb the 19 grams of deuterium generated during each test of the Mod 2 high flow rate deuterium generators for up to three consecutive tests. The residual deuterium pressure in the cryopump following a single Mod 2 deuterium generator test was typically 0.11 Torr.

At the end of a test series, the cryopump was saturated with gaseous nitrogen. This massive addition of nitrogen heavily diluted the adsorbed HF and DF and excess D<sub>2</sub> from the laser tests. When the saturating flow of nitrogen had brought the cryopump pressure up to one atmosphere, the liquid nitrogen flow to the cryopump dewars was turned off, and the vent valve at the right end of the cryopump assembly in Figure 26 was opened. The stream of nitrogen with small concentrations of laser exhaust products which evolved from the cryopump as the Molecular Sieve warmed to ambient temperature was passed through three scrubber canisters before being vented to the atmosphere. The first heated canister contained aluminum oxide pellets to consume any reactive fluorides evolved from the cryopump, and the second and third canisters contained sodium fluoride pellets to remove the HF and DF from the cryopump exhaust stream. Dual electrical heaters clamped around each of the cryopump canisters were then turned on to heat the sorbent to the bakeout temperature of 250°C. The heaters were left on overnight to insure complete desorption of the gases adsorbed on the Molecular Sieve.

Two special requirements strongly influenced the selection of the nozzle design for the low power chemical laser used for the intial gas generator lasing tests at AFRPL. The first requirement was for a highly tolerant nozzle design capable of lasing over a wide range of off-design

reactant flow rates in order to simplify the task of matching the gas generator flow rates to the laser demands. The second requirement was for a nozzle design with a large throat gap in order to minimize the possibility of plugging of the nozzle by particulates ejected from nitrogen generator grains coupled directly to the laser combustor.

To satisfy these two special requirements for a laser to test the early solid propellant laser gas generators, an unconventional throat-injection nozzle design developed by Dr. Morsell of Boeing (Reference 17) for DF-CO<sub>2</sub> transfer chemical laser operation was selected. In this nozzle design, the D<sub>2</sub> and CO<sub>2</sub> secondary reactants are injected into the primary flow of diluent plus fluorine from the laser combustor through a row of secondary injection holes at the throat of the supersonic primary nozzle. In this laser configuration, a single, two-dimensional supersonic primary nozzle generated the laser gain medium, and the optical axis was parallel to the throat slit of this primary nozzle. A cross section of the AFRPL low power laser with this throat injection nozzle is shown in Figure 27.

The major features of the nozzle design used for this AFRPL laser were the same as for the nozzle designed and tested by Dr. Morsell (Reference 17). The nozzle throat gap was 1.0 mm (.0394 in), the half angle of the supersonic section of the nozzle was 14°, and the nozzle

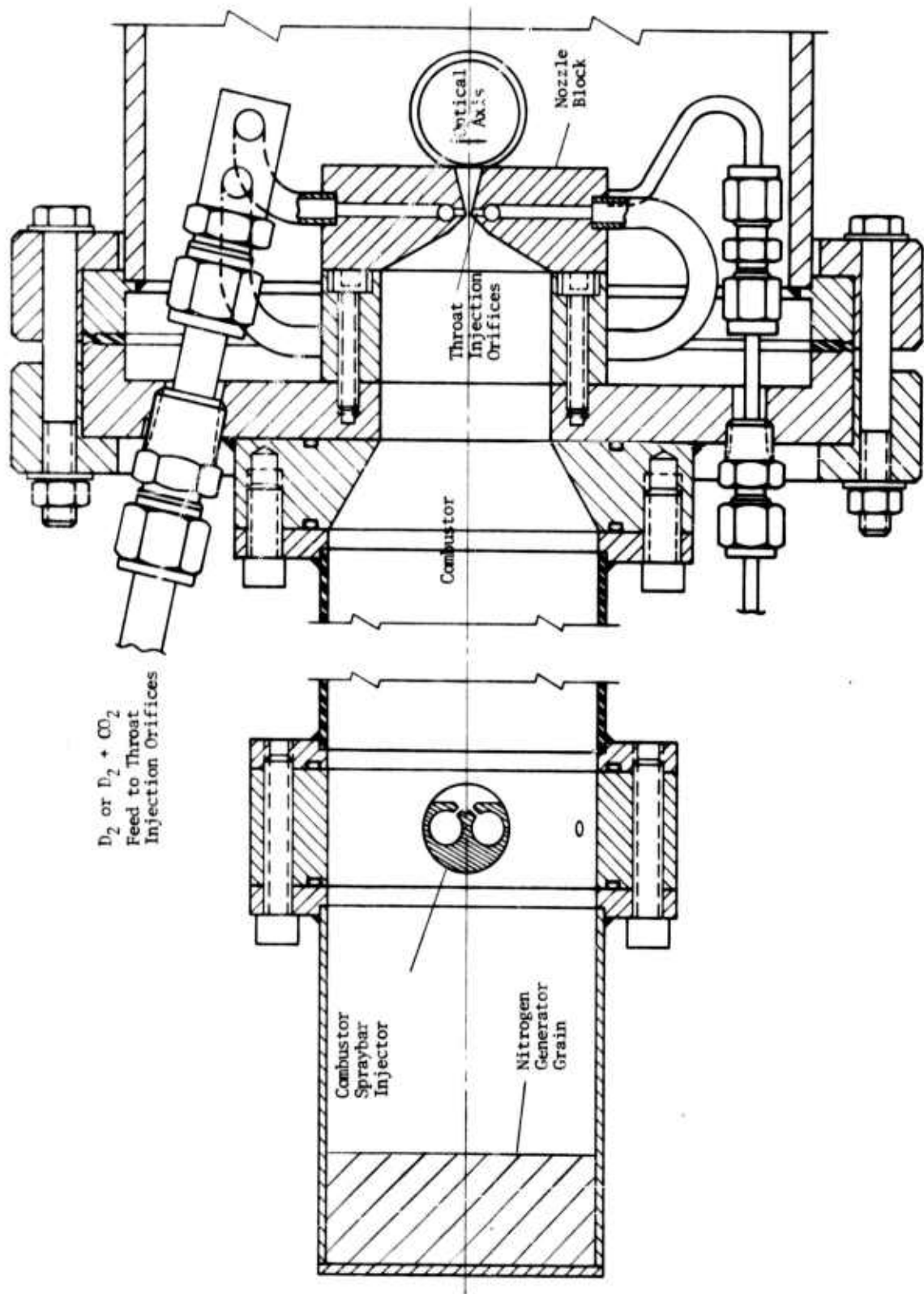


FIGURE 27. Cross Section of AFRL Low Power DF-CO<sub>2</sub> or DF Chemical Laser with Throat Injection Nozzle

width was 10.16 cm (4.000 in). The diameter of the secondary injection holes at the nozzle throat was 0.343 mm (.0135 in), and the hole spacing was 1.016 mm (0.040 in). The two uncooled half nozzle blocks which were bolted together to form the nozzle were fabricated from OFHC copper. A view of the throat injection nozzle assembly looking upstream toward the throat is shown in Figure 28. A close-up view of the row of secondary injection orifices along the throat of one of the half nozzle blocks is given in Figure 29. Streaks on the wall of the supersonic section of the nozzle generated by the reaction zones downstream of the secondary injection orifices are clearly visible in Figure 29.

Other details of this initial laser design are also shown in Figure 27. This laser was originally designed to use a nitrogen diluent generator grain coupled directly to the laser combustor. Therefore, a spraybar injector for the combustor oxidizer,  $\text{NF}_3$ , and the combustor fuel,  $\text{D}_2$ , was used so that the nitrogen from the solid grain could flow around the spraybar injector and then mix with the combustion products. A close-up of this spraybar injector which used unlike impinging injector orifices with a Nichrome hotwire for ignition is presented in Figure 30.

An external view of this laser system is shown in Figure 31. The specific laser configuration shown in this photograph differs in two

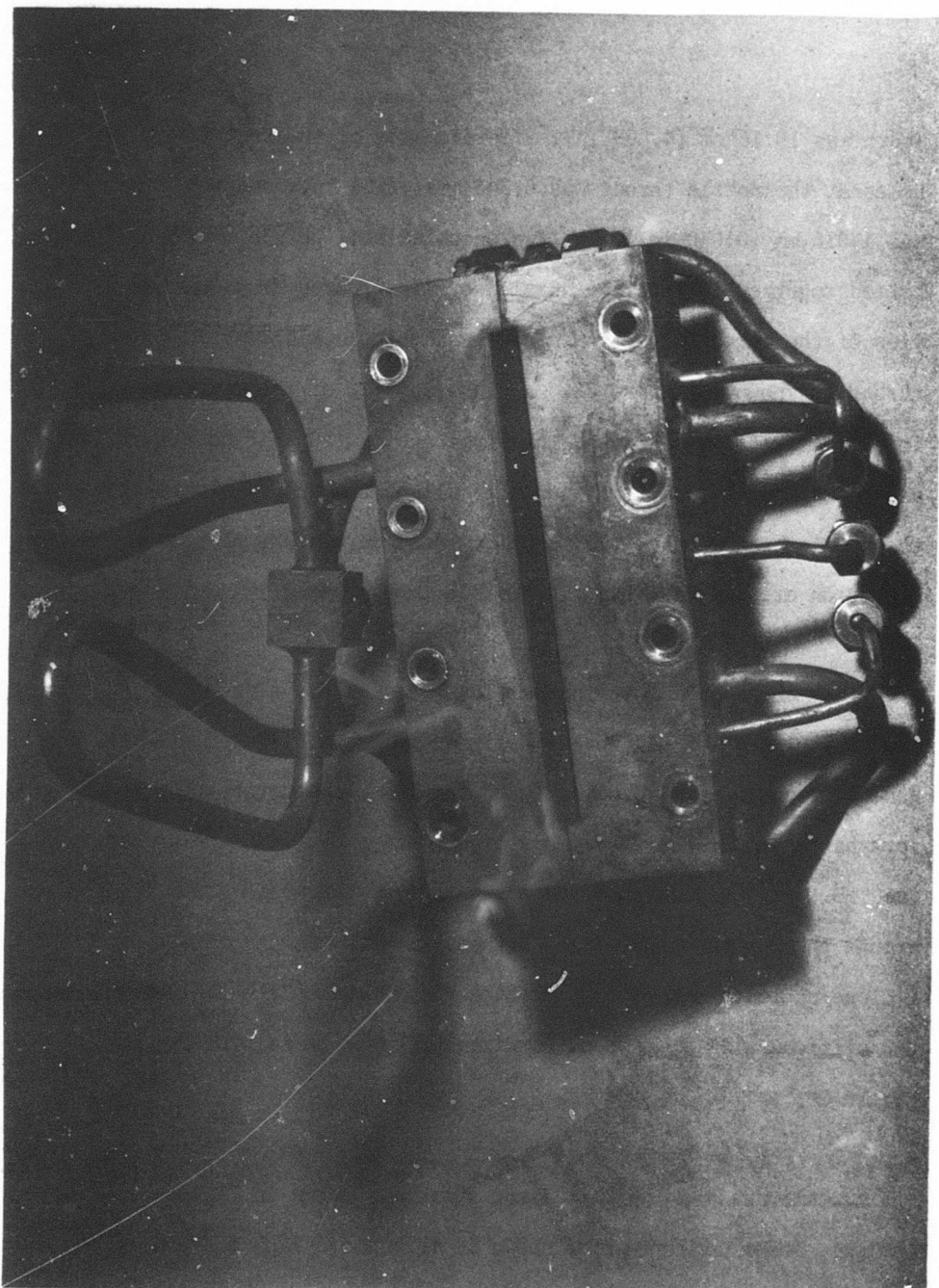
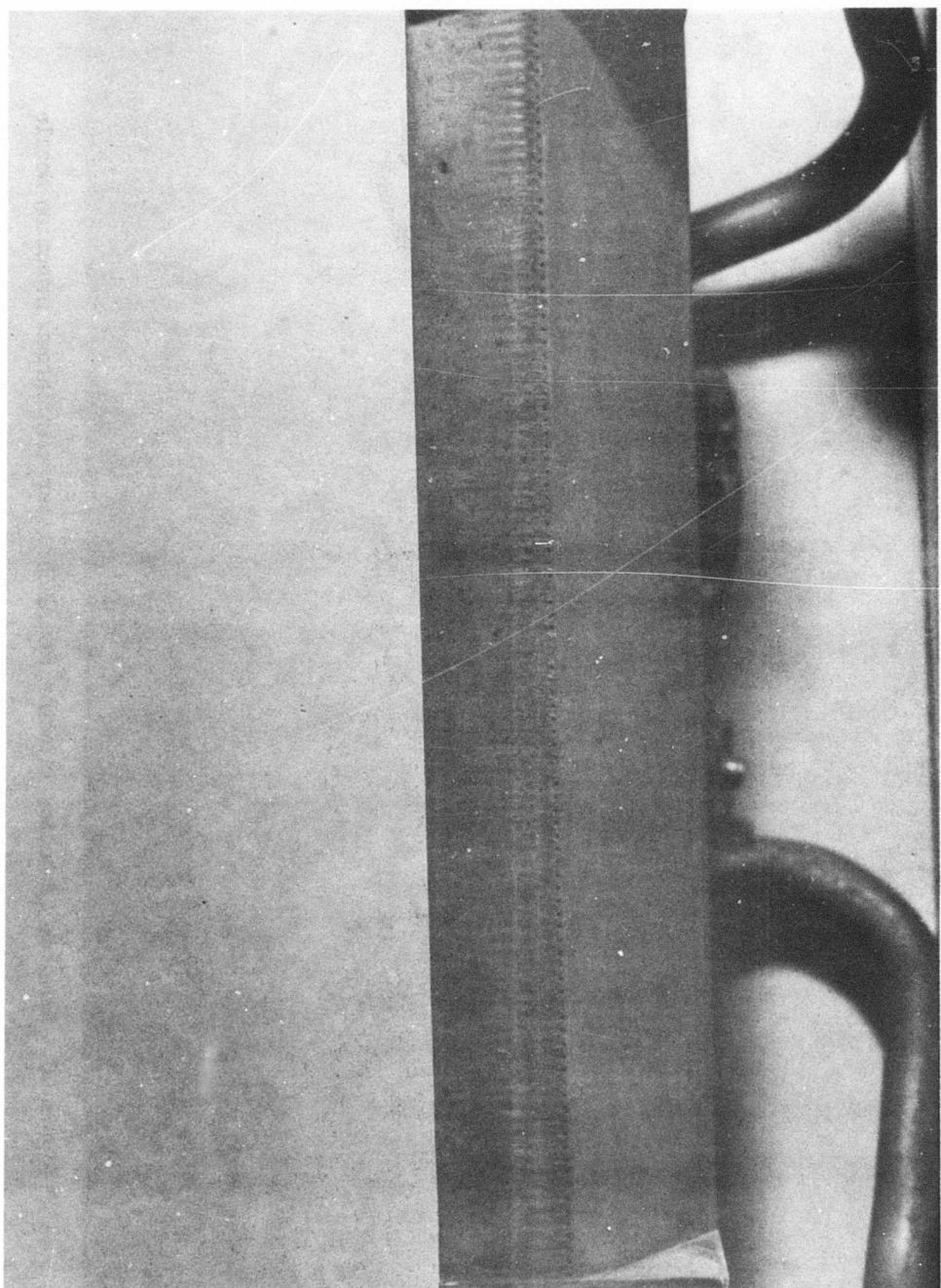


Figure 28. Throat Injection Nozzle Assembly Looking Upstream Toward Throat

Figure 29. Secondary Injection Orifices Along Nozzle Throat



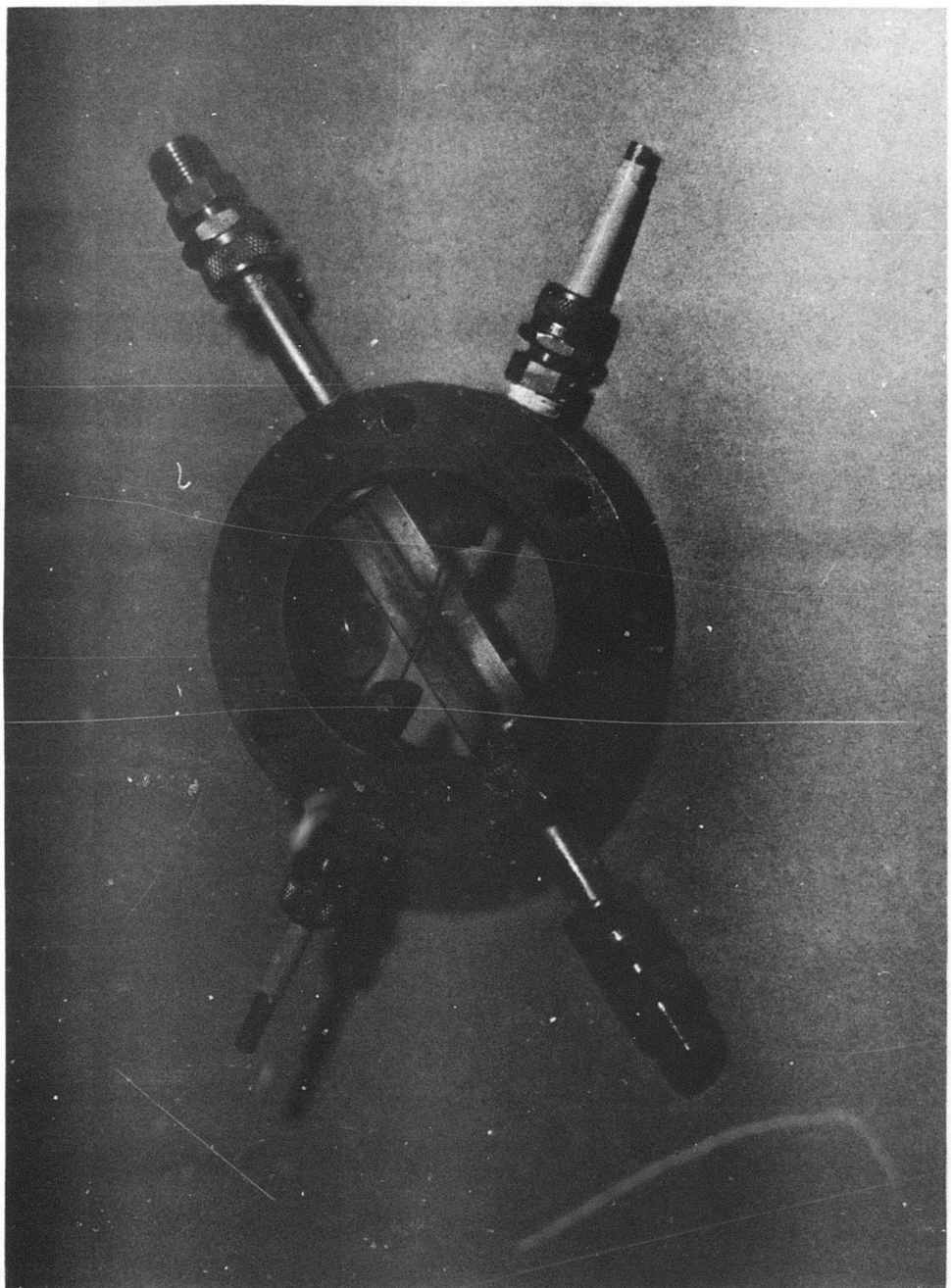


Figure 30. Spraybar Combustor Injector for AFRPL Laser with Throat Injection Nozzle

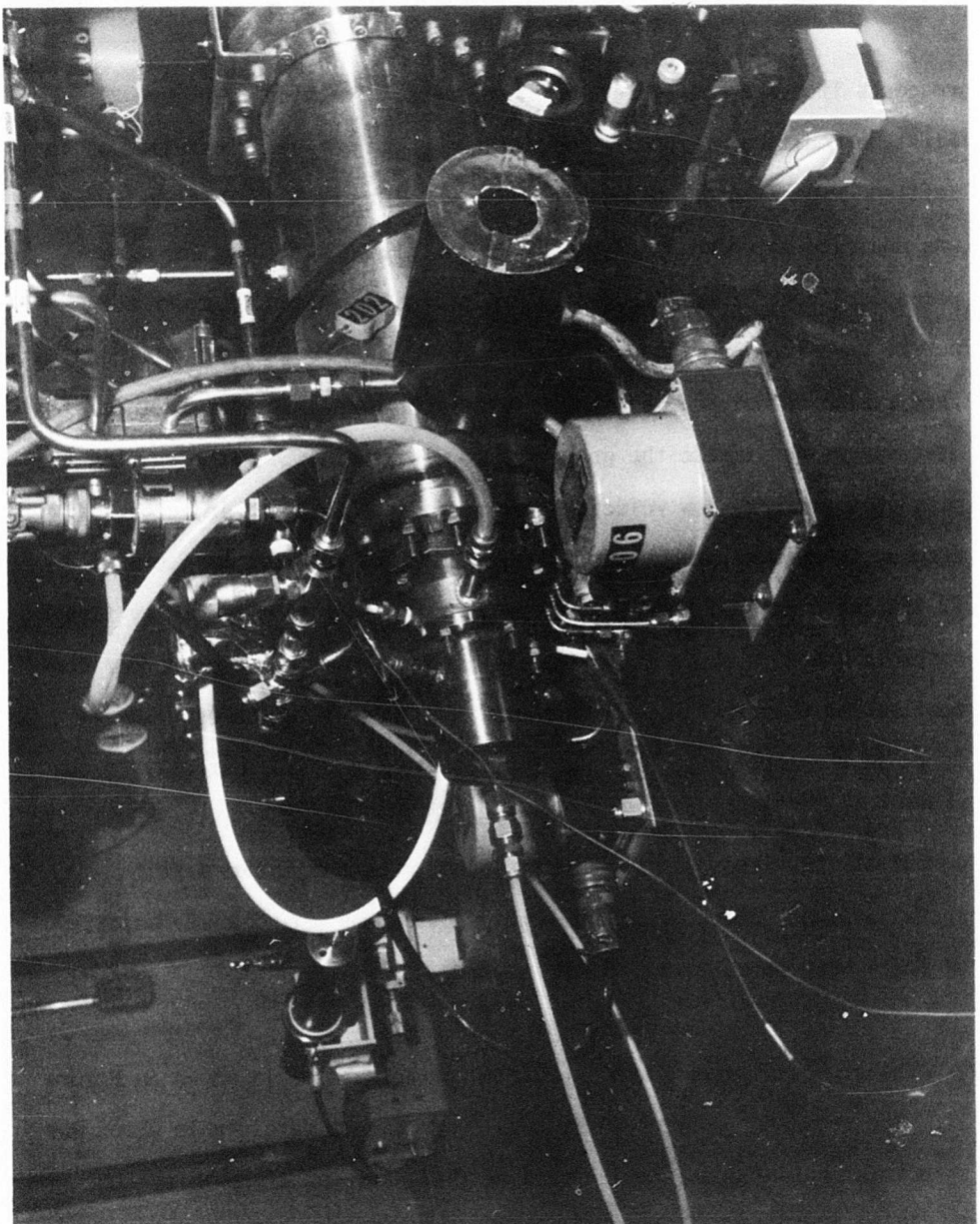


Figure 31. AFRLI Low Power DF-CO<sub>2</sub> or DF Laser with Throat Injection Nozzle

respects from the configuration shown in cross section in Figure 27.

First, a modified nitrogen generator grain can is shown installed on the left end of the laser combustor assembly in Figure 31. This grain can was modified as shown in Figure 31 by installing a fitting for a compressed nitrogen feed line on the end of the grain can in order to permit baseline laser tests using nitrogen from the facility nitrogen feed system rather than a nitrogen generator grain. A sintered nickel disc was welded inside the grain can to distribute the nitrogen flow and provide a uniform, low velocity flow around the spraybar injector.

Second, the nickel plenum section (12.7 cm (5.0 in) long by 6.033 cm (2.375 in) diameter) between the spraybar injector and the cavity flange assembly which is shown installed in Figure 27 had been removed for the test series when the photograph shown in Figure 31 was taken. Therefore, in the photograph the spraybar injector is bolted directly to the cavity flange assembly. For typical DF lasing conditions, the power output of this laser was 23 percent higher with the plenum section installed, and therefore, that configuration was used for the majority of tests with this laser.

The standard optical configuration for this laser is shown in Figure 31. The resonator optical system was mounted on a metal table which was structurally isolated from the rest of the laser and cryopump system. The laser combustor and nozzle assembly was cantilevered over the optical

table on one end of the laser cavity tube (14.285 cm (5.624 in) inside diameter) which was bolted at the other end to the gate valve at the inlet of the cryopump. Brewster-angle windows were installed on the end of optical tubes (9.068 cm (3.570 in) long by 2.223 cm (0.875 in) inside diameter) projecting from each side of the main cavity tube. A nitrogen purge flow (normally 10 liters/min) was injected into the optical tubes through a ring of purge orifices on the vacuum side of each Brewster window, and a separate, low velocity nitrogen purge flow was injected into the shroud tubes which are shown installed on the atmospheric pressure side of the Brewster windows. For the DF-CO<sub>2</sub> transfer chemical laser tests, sodium chloride windows were used, and for the HF and DF chemical laser tests, barium fluoride windows were used. The concave end mirror for the confocal resonator is shown in the right foreground in Figure 31, and the partially transmitting output coupler is on the other side of the laser cavity tube. In the left center of the photograph, the broadband laser power meter\* which was used to measure the outcoupled power is visible. The helium-neon alignment laser is in the left background of the photograph.

The flow rates for all of the reactants supplied to the laser from the facility compressed gas feed systems were set prior to the test using micrometer adjusting metering valves. The regulated supply pressure at each micrometering valve was monitored with a pressure transducer. Several techniques were used to establish the flow calibrations

for the micrometering valves. Electronic "Linear Mass Flowmeters" from Matheson\* and rotameter-type flowmeters from the same source were used for the "standard" gases  $N_2$ ,  $CO_2$ , and  $H_2$  for which factory calibrations for the flowmeters were available. To conserve  $NF_3$  (molecular weight 71.00), Freon 23\*\* ( $CHF_3$ , molecular weight 70.01) was used to calibrate the oxidizer micrometering valve. For both Freon 23 and deuterium, the primary flow calibrations were established from timed flows into a calibrated volume, and secondary flow calibrations for a Linear Mass Flowmeter were determined from the flow test data. Because the Linear Mass Flowmeters are calibrated in volumetric flow rate units of liters/min or  $cm^3/min$  at  $20^\circ C$  and 760 Torr, the laser flow rates presented in subsequent paragraphs will be given in those volumetric flow rate units.

The initial lasing demonstrations with the nitrogen and deuterium generator formulations were conducted with this laser operating in the DF- $CO_2$  transfer chemical laser mode and with the nitrogen generator grain cans coupled directly to the laser combustor as shown in Figure 27. Combustion of the nitrogen generator grains was irregular at the low laser combustor pressure of 27.6 to 48.3 kPa (4-7 PSIA), and partial clogging of the nozzle throat slit by particles ejected from the grain surface occurred during some tests. Therefore, the laser power varied during a test and from test to test at nominally identical conditions.

However, because this laser was very tolerant toward variations in  $N_2$  diluent flow rate when operating in the DF- $CO_2$  transfer laser mode, lasing demonstrations could be successfully conducted. The first lasing test with a nitrogen generator grain was conducted on 18 May 1973 (Test No. 132), and a peak power of 0.9 Watts was measured. By the time that the first lasing test with a deuterium gas generator was conducted on 21 June 1973, optimization of the reactant flow rates had increased the laser power to the 20 Watt range. For this first deuterium generator lasing test (No. 161), a 7.0 gram grain of  $3 LiAlD_4:1ND_4Cl$  formulation was combusted in the same gas generator used for the initial hydrogen generator tests at AFWL. During this test, the outcoupled power rose from 11 Watts to a final peak of 26 Watts. The reactant flow rates in units of liters/min were as follows:  $CO_2$ , 91;  $NF_3$ , 17.6;  $D_2$  (combustor), 15.2. The typical  $D_2$  flow rate from the gas generator to the throat injection orifices was 14.7 liters/min, but there were 30 percent variations in  $D_2$  flow rate during the 25 second gas generator burn. The optical axis was along the center plane of the nozzle (parallel to the nozzle throat slit) and 0.904 cm (0.356 in) downstream of the nozzle exit plane. The optical cavity length was 71 cm. One of the resonator mirrors was a 2.54 cm (1.0 in) diameter gold coated mirror with a radius of curvature of 1.0 m. The 93 percent reflectivity CdTe output coupler had a 1.0 m radius of curvature on the cavity side and a planar back face. During this test, the combustor pressure ranged from 41.4 to 48.3

kPa (6-7 PSIA), and the laser cavity pressure varied from 4 to 6 Torr. In the preceding test (No. 160) with 31.7 liters/min of  $D_2$  supplied to the throat injection orifices from the facility compressed  $D_2$  supply system, the laser power rose from an initial level of 14 Watts to a final peak of 26 Watts. The nitrogen generator grain formulation for both tests was 67.5 percent  $Fe_2O_3$  and 32.5 percent  $NaN_3$  by weight.

For subsequent tests of this laser in the HF and DF chemical laser modes which are less tolerant than the DF- $CO_2$  transfer laser mode toward variations in diluent flow rate, a more stable  $N_2$  diluent flow rate was required. Therefore, the modified grain can shown in Figure 31 was used to feed  $N_2$  into the laser combustor from a separate external  $N_2$  gas generator or from the facility  $N_2$  supply system. The first DF lasing demonstration using a solid  $D_2$  generating formulation was conducted with this laser configuration (Test 237, 30 Aug 73). The  $D_2$  gas generator used for this demonstration was the 3.810 cm (1.5 in) inside diameter version of the second generation design which is shown in the center left of Figure 10. The  $D_2$  generator grain was a 4  $LiAlD_4:1ND_4Cl$  formulation. During the middle of the gas generator burn, the  $D_2$  flow rate was up to 27 percent above the nominal 31.2 liters/min flow rate of the preceding baseline lasing test (No. 236) using  $D_2$  from the facility feed system, and the laser power of 5.6 Watts was lower than the baseline 7.0 Watts. However, during the gradual tailoff of the  $D_2$  generator grain,

the D<sub>2</sub> pressure at the metering valve matched the baseline 434 kPa (63 PSIA) D<sub>2</sub> supply pressure, and the laser output at that time matched the baseline 7.0 Watts. This identical laser performance at the same D<sub>2</sub> flow rate from either the gas generator or the facility D<sub>2</sub> supply system was anticipated because the gas sampling tests had previously demonstrated that the D<sub>2</sub> generator formulations without binder with LiAlD<sub>4</sub>: ND<sub>4</sub>Cl ratios of 3:1 to 4:1 produced very high purity D<sub>2</sub>. For both of these tests, the laser combustor flow rates in liters/min were as follows: NF<sub>3</sub>, 15.4; H<sub>2</sub> 16.9; and N<sub>2</sub>, 40.0. During both tests, the laser combustor pressure was 22.1 kPa (3.2 PSIA). The laser cavity pressure was 2.2 Torr for the baseline test and 2.4 Torr for the test with the D<sub>2</sub> gas generator because of the higher D<sub>2</sub> flow rate. The N<sub>2</sub> optics purge flow rate was 20 liters/min. For these two tests, the optical axis was located 0.730 cm (0.288 in) downstream of the nozzle exit plane, and the laser cavity length was 70 cm. The 5.08 cm (2.0 in) diameter germanium output coupler had a reflectivity of 93 percent and a radius of curvature of 4.0 m. The other resonator mirror was gold coated with a radius of curvature of 1.5 m and a diameter of 2.54 cm.

With this same laser configuration, a DF lasing demonstration using both a D<sub>2</sub> gas generator and an external N<sub>2</sub> gas generator was also conducted. Because the N<sub>2</sub> generator grains in the separate gas generator could operate at higher pressures near 517 kPa (75 PSIA), the grains combusted evenly, the N<sub>2</sub> flow rates were steady, and, therefore, the

laser power was also stable. During this test with both  $D_2$  and  $N_2$  gas generators (Test No. 276, 18 Oct 73), the laser power remained within 10 percent of its average value except during the gas generator ignition and tailoff transients.

V.C. NITROGEN TRIFLUORIDE PLUS FLUORINE, DEUTERIUM, HYDROGEN, AND NITROGEN GAS GENERATOR LASING DEMONSTRATIONS USING AFRPL XCL5 DF LASER

The AFRPL laser with the throat injection nozzle which was used for the lasing demonstrations described in the preceding section was replaced by a second low power DF laser design designated the 'XCL5'. The XCL5 laser used a conventional DF laser nozzle design in which the primary gas stream containing the fluorine atoms generated in the combustor and the secondary gas stream containing the deuterium cavity fuel flowed into the laser cavity through separate sets of two-dimensional supersonic nozzles as is shown schematically in Figure 1. The primary reason for changing the laser design was to reduce the oxidizer flow rate required for the laser combustor and thereby decrease the grain size required for lasing tests with the fluorine generator formulations. Because the XCL5 laser nozzle had been designed for DF or HF chemical laser operation, this laser could operate on only 25 percent of the  $NF_3$  flow rate required for the previous laser with the throat injection nozzle.

This second AFRPL low power DF laser was designated the "XCL5" because the set of three nozzle blades used for this laser was cut from the damaged CLV laser nozzle bank developed for AFWL by TRW (Reference 18). The original CLV nozzle bank was 2.54 cm (1.0 in) high by 20.32 cm (8.0 in) wide, but the nozzle blades at one end of the nozzle bank had been damaged by a cooling water failure during a laser test at TRW. A set of three nozzle blades containing two primary (fluorine) and three secondary (deuterium) nozzles was cut from this damaged nozzle bank by electric discharge machining. The original CLV nozzle design had throat gaps of 0.102 mm (0.004 in) for the primary nozzles and 0.076 mm for the secondary nozzles. The half angles for the primary and secondary nozzles were 12 degrees and 15 degrees, respectively. For CLV, the design geometric area ratios were 18.7 for the primary nozzles and 13.3 for the secondary nozzles. For the three used nozzle blades installed in the XCL5 laser, the average primary nozzle throat gap of 0.147 mm (0.0058 in) correspond to an average geometric area ratio of 13.8, and the average secondary nozzle throat gap of 0.0986 mm (0.00388 in) corresponded to an average geometric expansion ratio of 11.4.

A cross section of the XCL5 laser is shown in Figure 32. The set of three CLV nozzle blades was brazed to the end of a nickel 200 combustor body. The nozzle blades were water cooled, but the combustor body and nickel combustor injector were heat sink designs which were adequate for

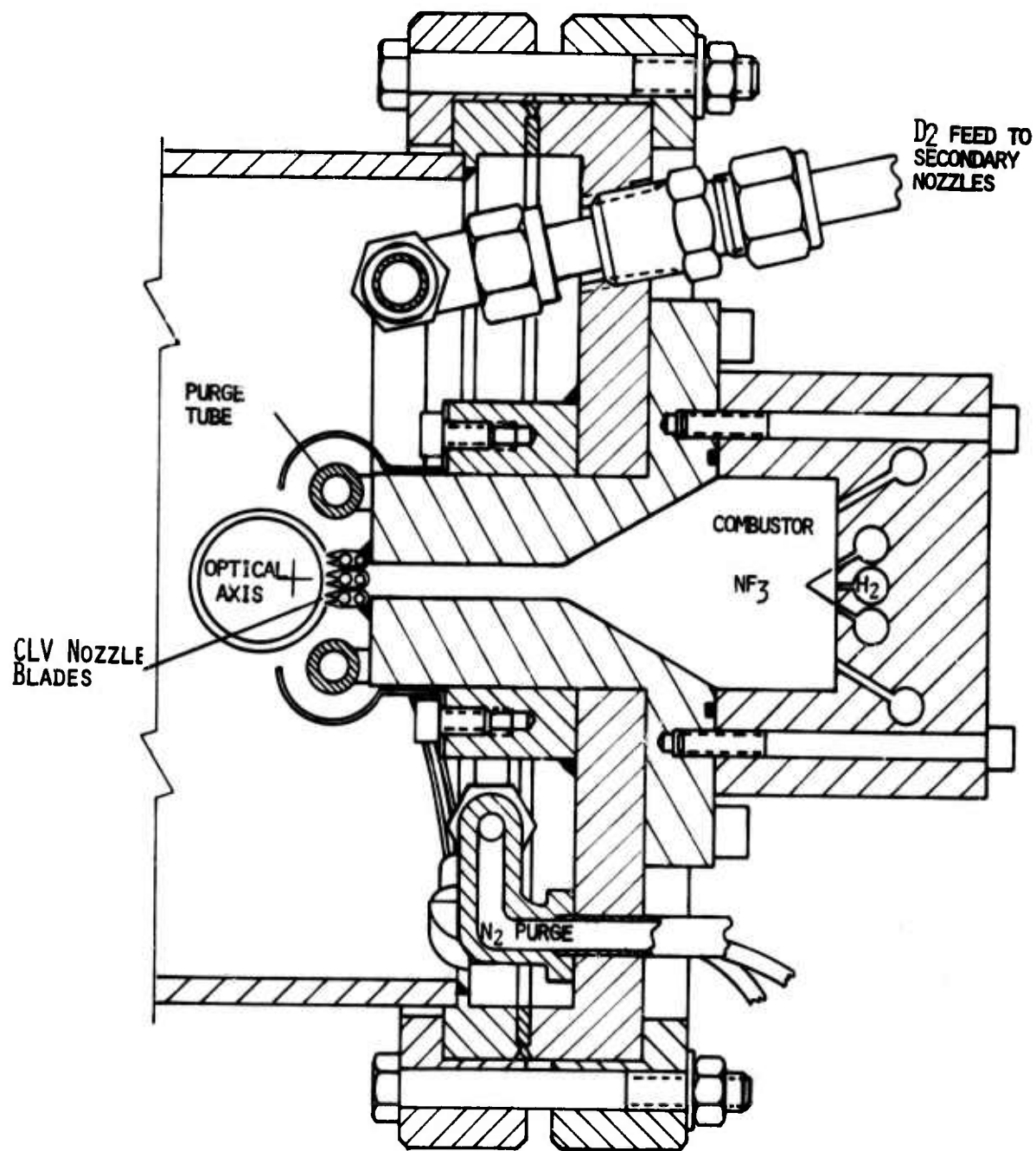


Figure 32. Cross Section of AFRPL "XCL5" Low Power DF Chemical Laser

the short duration (3-5 second) laser tests. In this laser design, the optical axis was parallel to the throat slits of the nozzle blades rather than at 90 degrees to the throat slits as is conventional for larger DF lasers such as the CLV. The optical axis was located downstream of the centerline of the middle secondary nozzle so that the mode volume would include both reaction zones between the flow from this center deuterium nozzle and the flows from the fluorine nozzles above and below it. With this unconventional orientation of the optical axis, the 2.54 cm (1.0 in) reaction zone length parallel to the optical axis provided sufficient gain for lasing, but the laser reactant flow rate requirements were very low. Sintered stainless steel purge tubes were installed both above and below the nozzle blades as is shown in Figure 32. The cavity pressure for the laser tests was varied by changing the nitrogen purge flow rate into these tubes and into the optical tubes on each side of the laser cavity tube. The feedthrough for the deuterium flow to the secondary nozzles is at the top of the laser mounting flange assembly, and the feedthroughs for the nitrogen purge and the nozzle cooling water are at the bottom of the flange.

A photograph of the XCL5 laser nozzle assembly taken from the laser cavity side of the mounting flange is shown in Figure 33. The individual deuterium feed tubes and cooling water tubes to both ends of each nozzle blade are visible. The nitrogen feed lines to the purge tubes above and below the nozzles are also shown.

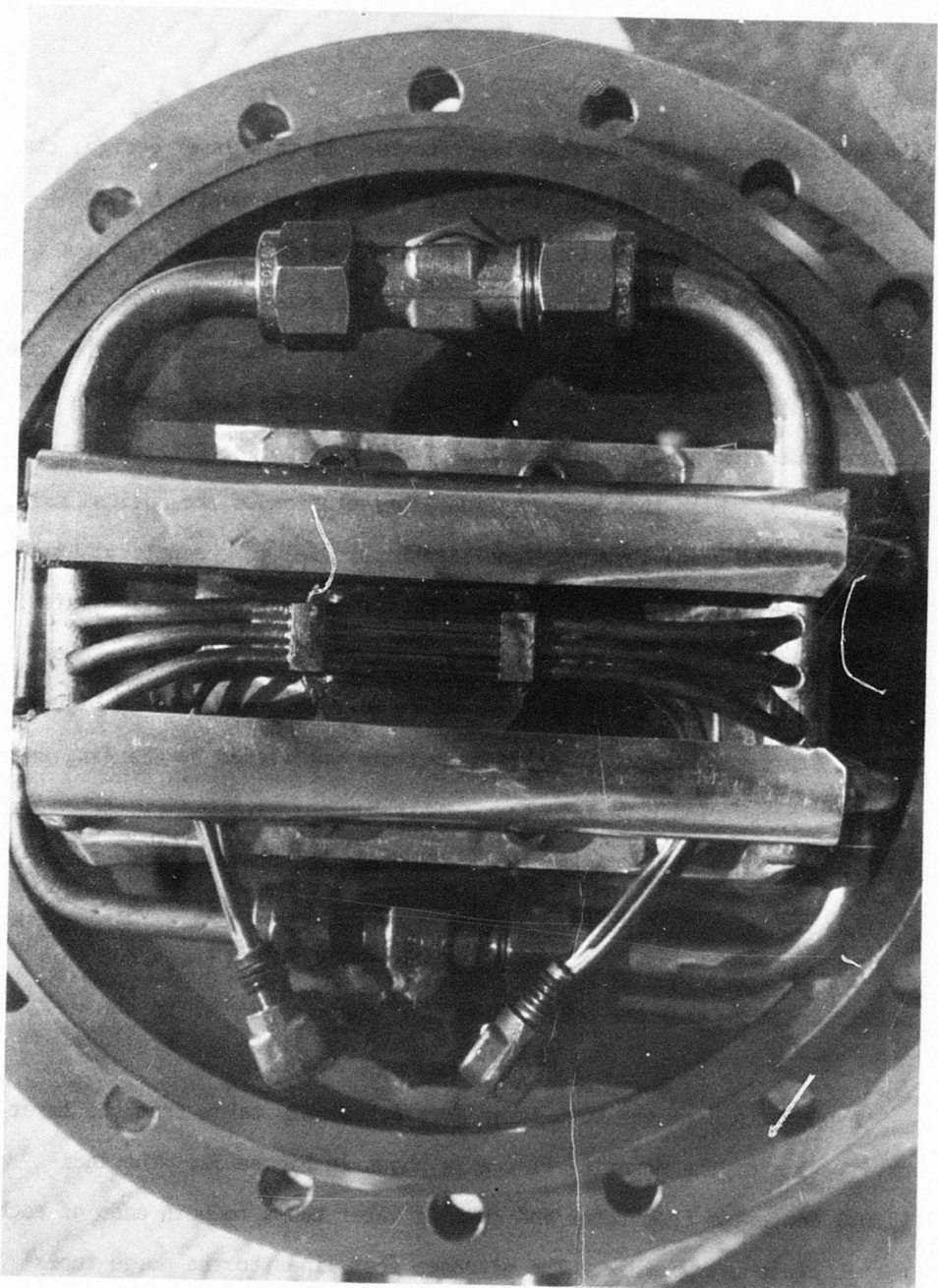


Figure 33. XCL5 Nozzle Assembly from Laser Cavity Side

In Figure 34, a photograph of the standard XCL5 combustor injector, the triplet injector pattern for the  $\text{NF}_3$  combustor oxidizer and the combustor fuel (normally  $\text{H}_2$ ) is apparent. The laser diluent could be injected along with the fuel or oxidizer or separately through the secondary injection orifices which are visible along the top and bottom of the injector face in this photograph and in the cross section in Figure 32. The combustor was ignited by an electric discharge generated by a corona discharge coil. The copper discharge electrode is visible on the right side of the combustor inner wall, and the alumina insulator extends out through the Swagelok fitting on the outer wall of the combustor.

In the overall view of the XCL5 laser system shown in Figure 35, all of the major optical system components are visible. For this photograph, the external shroud tubes which were normally installed over the Brewster windows were removed, and one of the barium fluoride window assemblies is visible on the end of the optical tube protruding from the right side of the laser cavity tube. The nitrogen feed line and injection ring for the optical tube purge are at the left end of the Brewster window assembly. The output coupler (germanium, 93 percent reflectivity, 4 meter radius of curvature, 5.08 cm (2.0 in) diameter) and the laser power meter are visible at the left side of the photograph, and the other cavity mirror (gold coated, 3 meter radius of curvature, 2.54 cm

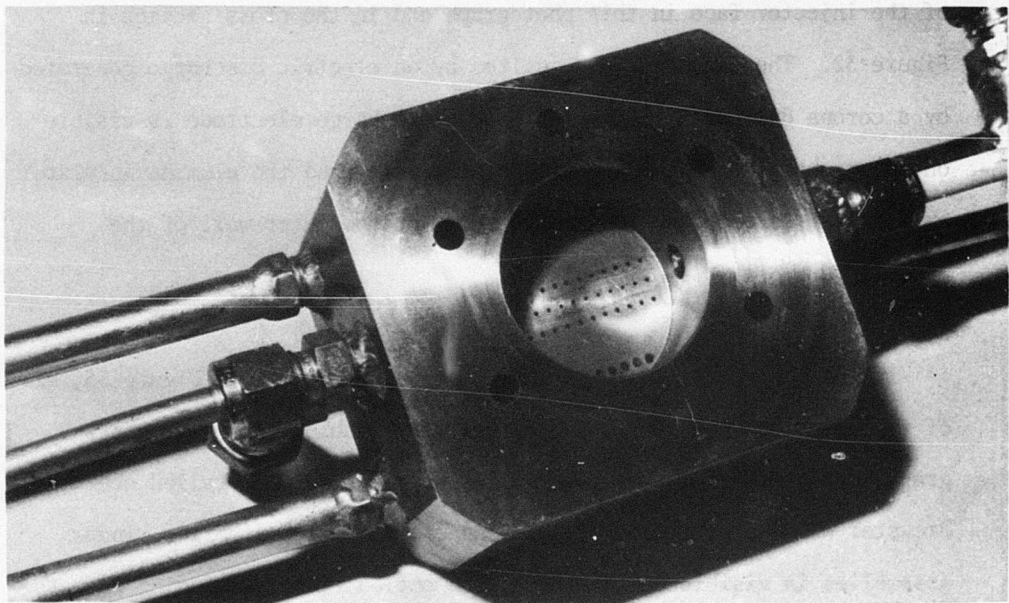


Figure 34. XCL5 Combustor Injector

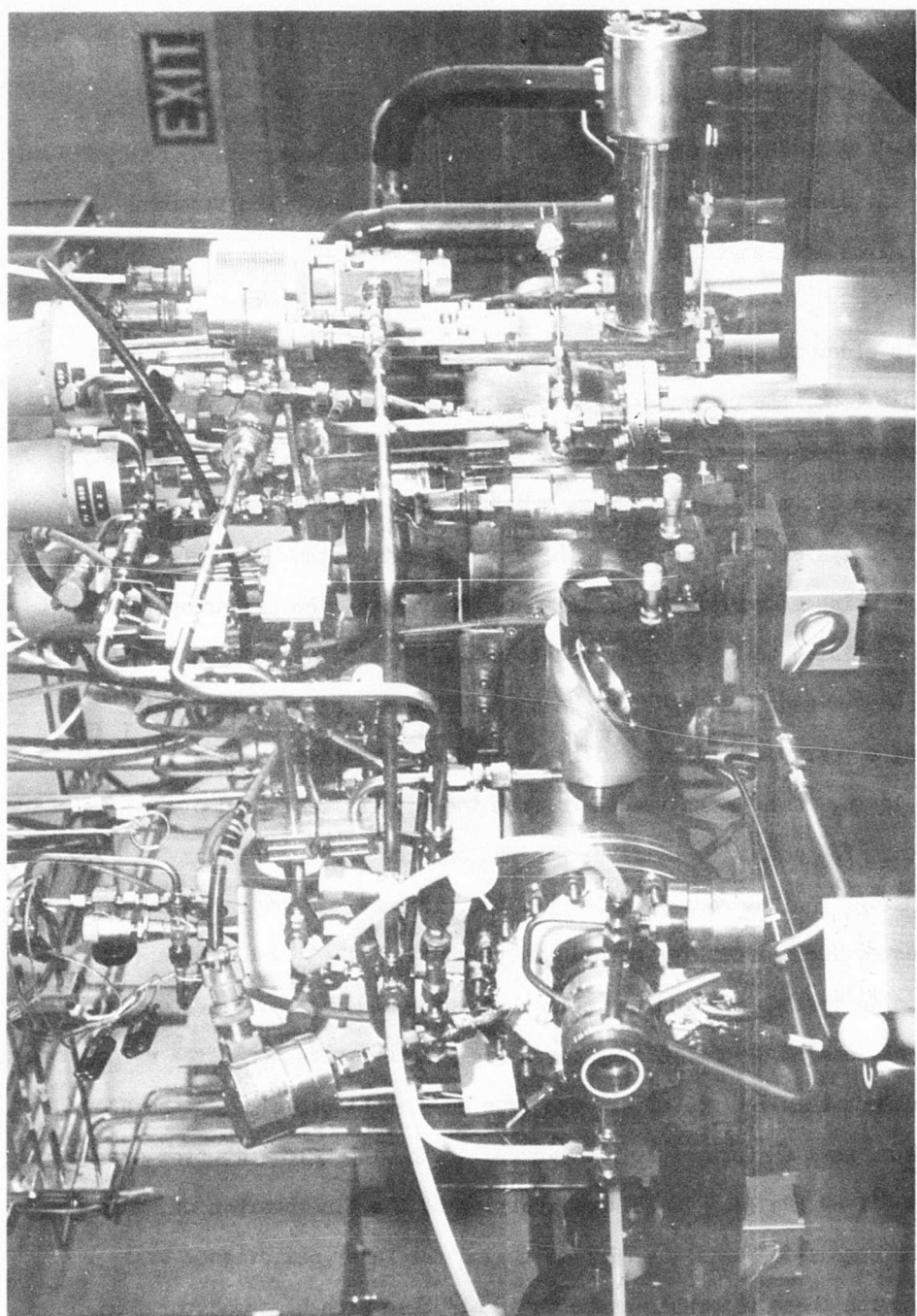


Figure 35. Overall View of XCL5 Laser System

(1.0 in) diameter) is in the right center foreground. The standard optical cavity length was 71.1 cm (28 in).

In order to simulate the combustion products from candidate solid formulations, the compressed gas reactant supply system for the XCL5 laser was designed to supply up to seven different gases simultaneously. In Figure 35, many of the valves and lines for these seven compressed gas feed systems are visible. The reactant flow rates were set prior to a test using micrometer adjusting metering valves, the gas pressures were regulated to a nominally constant level (344.7 kPa (50 PSIA) for all gases except  $N_2$ ), and the actual pressure at each metering valve during a test was monitored with a pressure transducer. For all of the XCL5 lasing tests using reactants from the compressed gas supply systems, the combustor oxidizer was  $NF_3$  and the cavity fuel was  $D_2$ . The combustor fuel was normally  $H_2$ , but fluorocarbon and hydrocarbon combustor fuels including octafluorocyclobutane ( $C_4F_8$ ) and ethane ( $C_2H_6$ ) were also tested. Extensive studies of the combustion of fluorocarbons with  $NF_3$  and  $F_2$  oxidizers at atmospheric pressure were conducted using the direct sampling molecular beam type mass spectrometer and laboratory scale burners (Reference 19). However, at the low XCL5 combustor pressures (31-69 kPa (4.5-10 PSIA)), ignition of the fluorocarbon or hydrocarbon combustor fuels was difficult, and the laser performance was lower with these alternate combustor fuels than with  $H_2$  combustor fuel.

Therefore, to simulate the  $CF_4$  content of the combustion products from fluorine atom generator formulations containing fluorocarbon or hydrocarbon polymers, a separate feed system to mix  $CF_4$  with the laser diluent was installed. The three independent diluent feed systems could supply nitrogen, argon, and neon or xenon.

In Figure 35, a Mod 1  $D_2$  gas generator is shown coupled into the  $D_2$  feed system for the laser secondary nozzles. In this photograph, thermocouples are installed in one of the tubing stubs on the side of the  $D_2$  generator and in a cross fitting in the outlet line from the gas generator. For tests of the  $D_2$ ,  $H_2$ , and  $N_2$  gas generators on the XCL5 laser system, the flow from the gas generators was fed to the laser through the same metering valves used for the tests with gases supplied from the facility compressed gas feed systems.

The combustor shown installed on the XCL5 laser in Figure 35 is a special combustor which was used rather than the standard XCL5 combustor injector (Figure 34) for the tests of the  $NF_4BF_4$ /polytetrafluoroethylene fluorine atom generator grains. During all of the tests with these grains, polymer fragments and solid contaminants ( $AgBF_4$ ) in the impure  $NF_4BF_4$  rapidly plugged the XCL5 fluorine nozzle throats, but the dual Nupro relief valves (which are shown installed in the vent lines leading from the combustor down along the optics table) successfully vented the

combustor flow directly into the cavity tube and thus prevented damage to the nozzle.

Tests with the XCL5 laser using mixtures of compressed gases to simulate the composition of the combustion products from the  $\text{XeF}_2$  or  $\text{NF}_4\text{BF}_4$ -oxidized fluorine atom generator formulations demonstrated that the laser performance was severely degraded by the high average molecular weights ( $M$ ) and low specific heat ratios ( $\gamma$ ) of the combustion products from those formulations. A comparison of the properties of the theoretical combustion products for the three oxidizers  $\text{F}_2$ ,  $\text{NF}_3$ , and  $\text{NF}_4\text{BF}_4$  is presented in Table 7. The same fuel,  $\text{CH}_2$  (with a heat of formation corresponding to polyethylene), was used for all of these equilibrium thermochemistry calculations. The molar ratios of oxidizer,  $\text{CH}_2$  fuel, and helium diluent were adjusted to achieve the same combustion temperature and combustion molar diluent-to-fluorine ratio,  $\Psi$ . The combustion temperatures listed in Table 7 are 73.13 percent of the adiabatic combustion temperature to account for combustor heat losses. For the combustion conditions shown in Table 7, the substitution of  $\text{NF}_4\text{BF}_4$  for  $\text{NF}_3$  oxidizer increases the  $M$  67 percent and decreases the  $\gamma$  9 percent. The effects of such large increases in  $M$  and decreases in  $\gamma$  on the power output of the XCL5 laser are illustrated in Table 8. For the small, low pressure XCL5 combustor, the heat loss from the combustor flow to the combustor walls was large. Typically, the effective average

TABLE 7  
COMPARISON OF COMBUSTION PRODUCT PROPERTIES  
FOR  $F_2$ ,  $NF_3$ , AND  $NF_4BF_4$  OXIDIZERS

<u>Reactants (Moles)</u>			<u>Combustion Products Properties</u>			
Oxidizer	Fuel (1)	Diluent	M	$\gamma$	T (2)	$\Psi$ (4)
1.885 $F_2$	.455 $CH_2$	8.0 He	10.58	1.481	1825	18.01
2.000 $NF_3$	.790 $CH_2$	8.0 He	14.67	1.405	1825	18.05
2.090 $NF_4BF_4$	1.455 $CH_2$	8.0 He	24.52	1.278	1827	18.02

(1) Polyethylene

(2) 26.87% Heat Loss

(3) 496 kPa (72 PSIA)

(4)  $\Psi = (X_{HF} + \sum X_{Diluents}) / (1/2 X_F + X_{F_2})$ ; X = Mole Fraction

TABLE 8  
EFFECT OF COMBUSTOR GAS PROPERTIES ON THE POWER OUTPUT  
OF THE XCL5 LASER

Test No.	Combustor Reactant Flow Rates (liters/minute)	Combustor Temperature (°K) (1)	M (g/mol)	γ	Ψ	Combustor Pressure (kPa/PSIA)	Laser Power (Watts)
450	4.136NF <sub>3</sub> /5.305H <sub>2</sub> /4.4Ne	1374	20.83	1.413	19.00	32.4/4.70	3.5
500-2	4.136NF <sub>3</sub> /5.305H <sub>2</sub> /5.71N <sub>2</sub>	1317	23.00	1.357	20.45	32.8/4.75	1.6
386	4.136NF <sub>3</sub> /4.713H <sub>2</sub> /1.612CF <sub>4</sub> /9.401Ar	980	33.82	1.359	14.05	59.6/8.65	0.56
433	4.136NF <sub>3</sub> /5.305H <sub>2</sub> /2.6CF <sub>4</sub> /7.6Ne	992	28.60	1.313	25.82	63.4/9.2	0.42
442	4.136NF <sub>3</sub> /5.305H <sub>2</sub> /4.0CF <sub>4</sub> /4.4Ne	971	33.64	1.255	24.01	62.7/9.10	0.35
393	4.136NF <sub>3</sub> /4.713H <sub>2</sub> /1.612CF <sub>4</sub> /8.401Ar/1.0Xe	980	37.63	1.359	15.74	60.3/8.75	0.32

FOOTNOTES

(1) 40 Percent of adiabatic combustion temperature  
 (2)  $\Psi = (\chi_{HF} + \sum X \text{ Diluents}) / (1/2X_F + X_{F_2})$ ; X = Mole Fraction

combustor temperatures calculated from the combustor pressures measured in hot flow tests and the nozzle throat area measured in cold flow tests were approximately 40 percent of the theoretical adiabatic combustion temperatures for the hot flow test conditions. Therefore, the combustor temperatures listed in Table 8 are 40 percent of the adiabatic combustion temperatures, and the other gas properties given in Table 8 also correspond to this reduced temperature. The  $NF_3$  flow rate was the same for all of these tests, but the power output for the highest  $M$  and lowest  $\gamma$  tests is an order of magnitude below the baseline power output of the laser with neon diluent. The power output was lower by a factor of two with nitrogen rather than neon diluent. The addition of  $CF_4$ , which increased the  $M$  and decreased the  $\gamma$ , severely degraded the power output, and the substitution of the heavier monatomic diluents argon and xenon for neon further degraded the laser performance. As was discussed in Section III.A., the laser performance degradation observed in these tests for the high  $M$ , low  $\gamma$  combustor compositions led to the termination of the development of fluorine atom generator formulations and the resumption of the development of clinker-type  $NF_3 + F_2$  generator formulations.

The oscillograph data traces for one of the compressed gas baseline tests of the XCL5 laser are shown in Figure 36. This test (No. 450, 30 Sep 1974) is the first entry in Table 8. For this test, the peak

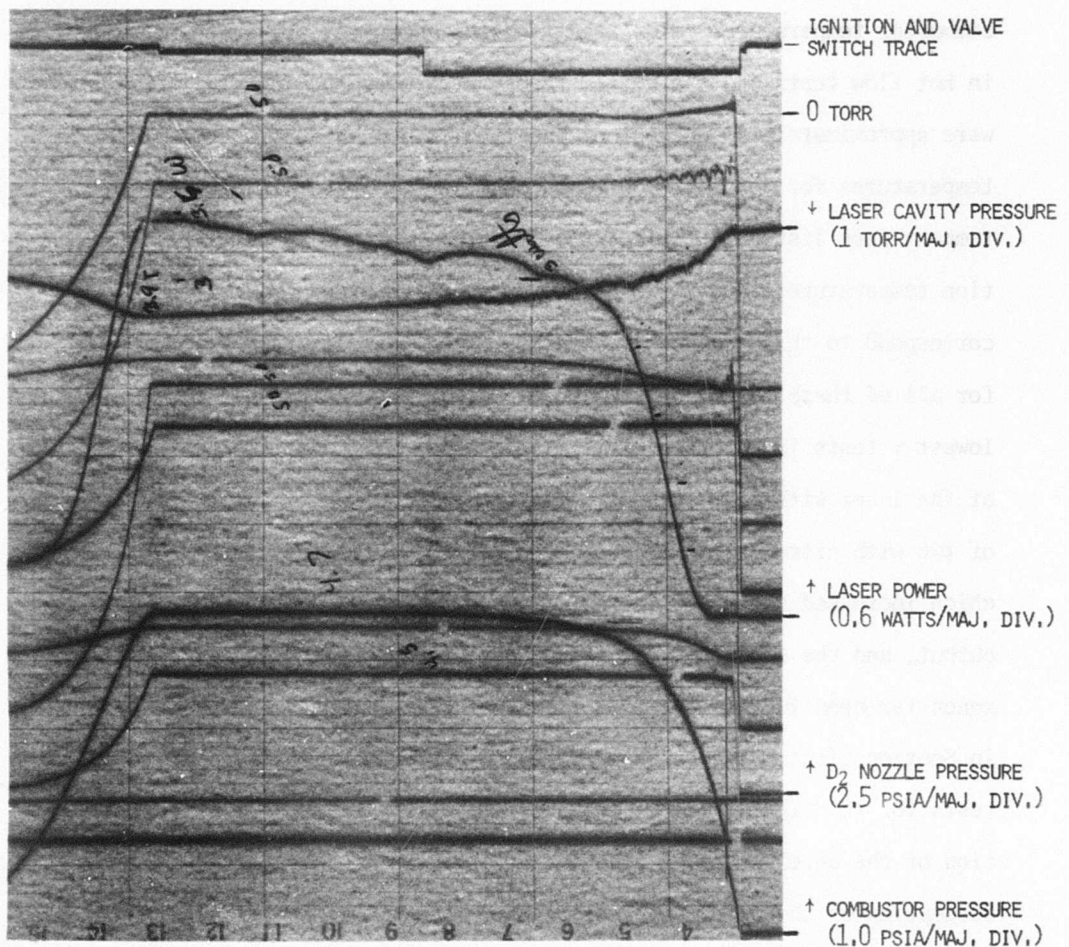


Figure 36. Oscillograph Data for XCL5 Compressed Gas Baseline Lasing Test No. 450

power of 3.5 Watts occurred at the end of the test at a cavity pressure of 2.9 Torr. The combustor pressure was steady at 32.4 kPa (4.7 PSIA) during the final 2.5 seconds of the test, and the D<sub>2</sub> nozzle supply pressure was steady at 31.0 kPa (4.5 PSIA), but the cavity pressure increased slowly as was typical for the cryopump system. Because of this gradual change in the relative pressures at the primary and secondary nozzle exits and in the laser cavity, for a particular test the relative pressure condition for maximum power could occur at any time during the test. For different laser operating conditions, the cavity pressure was adjusted to maximize the laser output power by varying the nitrogen purge flow rates. During the initial 2.3 seconds of the test while the corona discharge ignition switch was on, the cavity pressure trace shows that the capacitance manometer used to measure the cavity pressure picked up some low level electrical noise from the discharge, but none of the other data traces were affected. The combustor mass flow rate for this test was 0.272 g/sec, and the D<sub>2</sub> flow through the three secondary nozzles was 0.163 g/sec (58.4 liters/minute). The other traces on the oscillograph record are from the pressure transducers at the metering valves for the laser reactants.

Lasing tests were successfully conducted on the XCL5 laser with the nitrogen, "fluorine" (NF<sub>3</sub> + F<sub>2</sub>), deuterium, and hydrogen gas generators shown in Figure 37. Grain containers are shown beside the NF<sub>3</sub> + F<sub>2</sub>

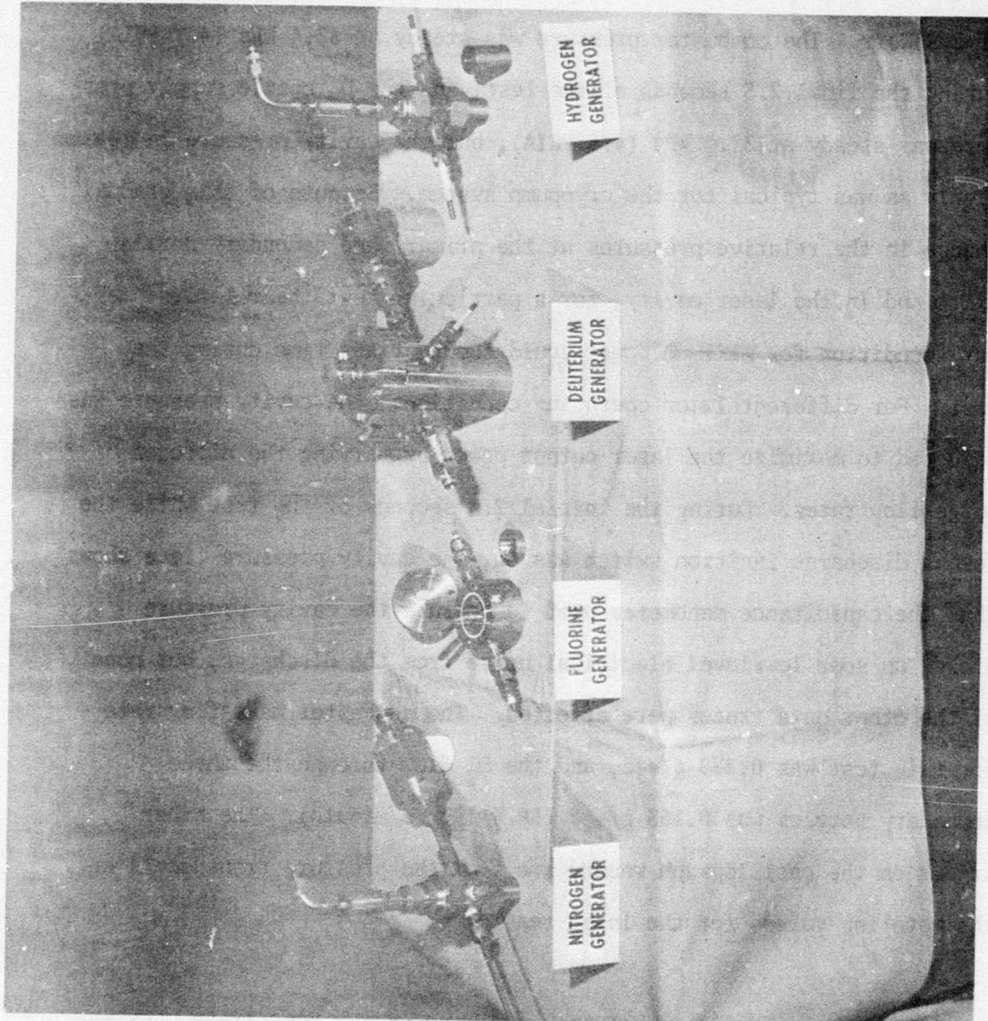


Figure 37. Nitrogen, "Fluorine" ( $NF_3 + F_2$ ), Deuterium, and Hydrogen Gas Generators Used for Lasing Demonstration on the XCL5 Laser

generator and the hydrogen generator, and pressure transducers are shown coupled to the nitrogen and deuterium gas generators. The hydrogen and nitrogen generators were identical except for the diameter and depth of the grain cavities bored into the ends of the grain containers.

The oscillograph record of the first lasing test with a Mod 1 deuterium generator coupled to the XCL5 laser is shown in Figure 38 (Test No. 451, 30 Sep 1974). The gas generator contained a 16.16 gram, center-perforated grain of  $4\text{LiAlD}_4:1\text{ND}_4\text{Cl}$  formulation with 4.2 weight percent Kraton binder plus Conco Oil plasticizer. Because of the center perforation in the grain, the  $\text{D}_2$  generator pressure was initially progressive and then regressive. The power output ranged from 1.56 Watts to a peak of 1.95 Watts late in the test at a cavity pressure of 3.15 Torr. As was discussed in Section II.C., the use of Conco Oil plasticizer in the deuterium generator formulations significantly degraded the purity of the deuterium evolved from the gas generator, and therefore, the power during this test was lower than the 3.0 to 3.5 Watts measured during the preceding baseline test (No. 450) using  $\text{D}_2$  from the facility  $\text{D}_2$  feed system. The combustor conditions for Test No. 451 were the same as those given in Table 8 for Test No. 450.

In Figure 39, the "fluorine" ( $\text{NF}_3 + \text{F}_2$ ) gas generator and a Mod 1 deuterium gas generator are shown coupled to the XCL5 laser. In this

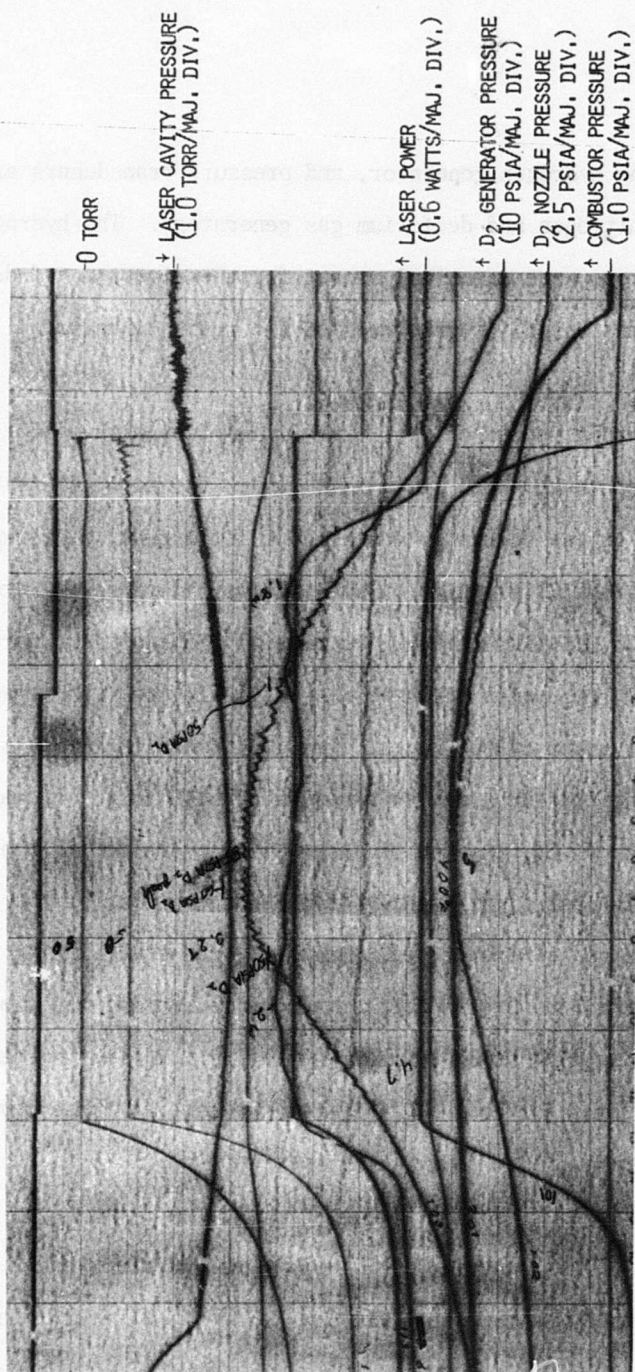


Figure 38. Oscillograph Record of XCL5 Lasing Test No. 451 with Mod 1 Deuterium Generator

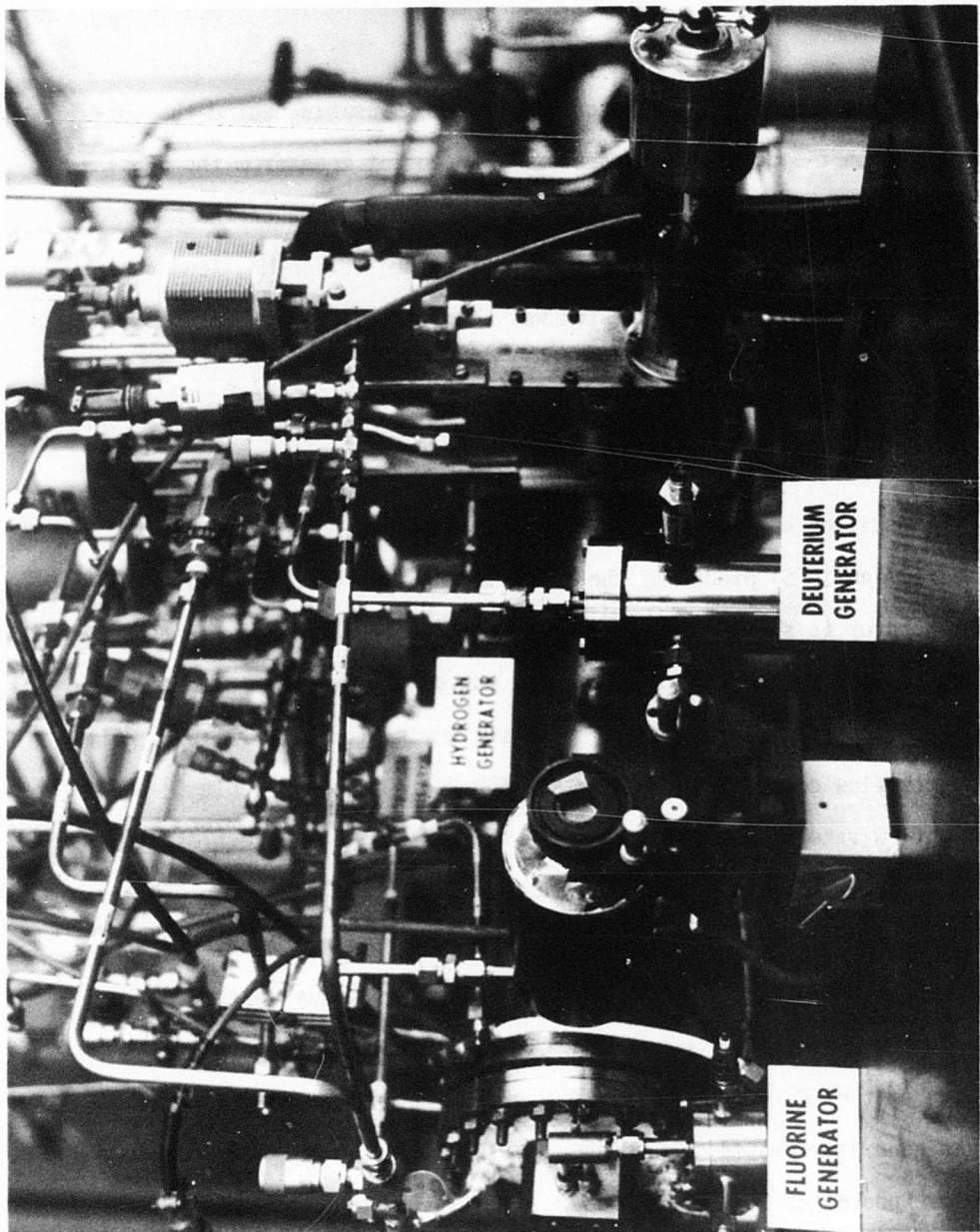


Figure 39. "Fluorine" ( $\text{NF}_3 + \text{F}_2$ ), Deuterium, and Hydrogen Gas Generators Coupled to XCL5 Laser

photograph, the hydrogen generator is partially visible behind the outlet tube from the deuterium generator. The outlet tube from the  $\text{NF}_3 + \text{F}_2$  gas generator is shown inserted into the same fitting on the  $\text{NF}_3$  manifold of the XCL5 combustor injector where the Teflon  $\text{NF}_3$  feed tube from the facility  $\text{NF}_3$  supply system was normally inserted. For the compressed gas baseline lasing tests preceding the  $\text{NF}_3 + \text{F}_2$  gas generator tests, the  $\text{N}_2$  feed line was coupled into the  $\text{NF}_3$  feed line so that the diluent and oxidizer were mixed prior to injection. In Figure 40, the oscillograph record from the compressed gas baseline test (No. 500-2, 17 Jan 1975) preceding the first lasing test with the  $\text{NF}_3 + \text{F}_2$  gas generator is shown. In this baseline test, the laser power steadily increased to 1.25 Watts at the time the gas supply valves closed and then rose to a transient peak of 1.6 Watts during the flow tailoff. The combustor flow conditions for Test No. 500-2 are given in Table 8, and the  $\text{D}_2$  flow rate through the secondary nozzles was 58.4 liters/minute. In Figure 41, the oscillograph record from Test No. 501 (17 Jan 1975), the first successful lasing test with the  $\text{NF}_3 + \text{F}_2$  gas generator, is shown. The peak laser power of 1.9 Watts occurred early in the test, and the power was nearly constant at  $1.0 \pm 0.5$  Watts during the final portion of the  $\text{NF}_3 + \text{F}_2$  gas generator burn. The pressure in the  $\text{NF}_3 + \text{F}_2$  gas generator peaked at 238 kPa (34.5 PSIA), and the laser combustor pressure peaked at 38 kPa (5.5 PSIA). At similar pressure conditions,

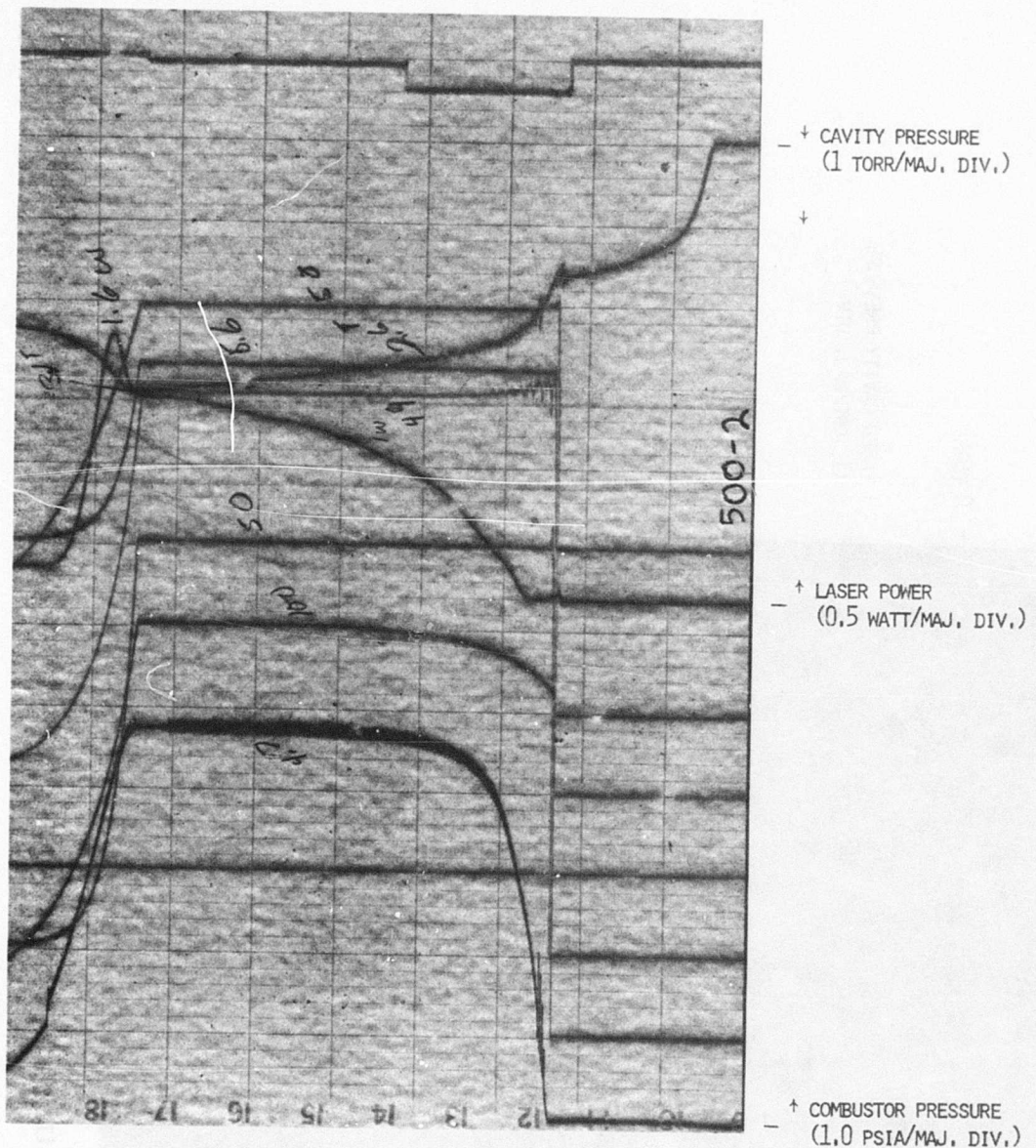


Figure 40. Oscillograph Record of XCL5 Compressed Gas Baseline Lasing Test No. 500-2

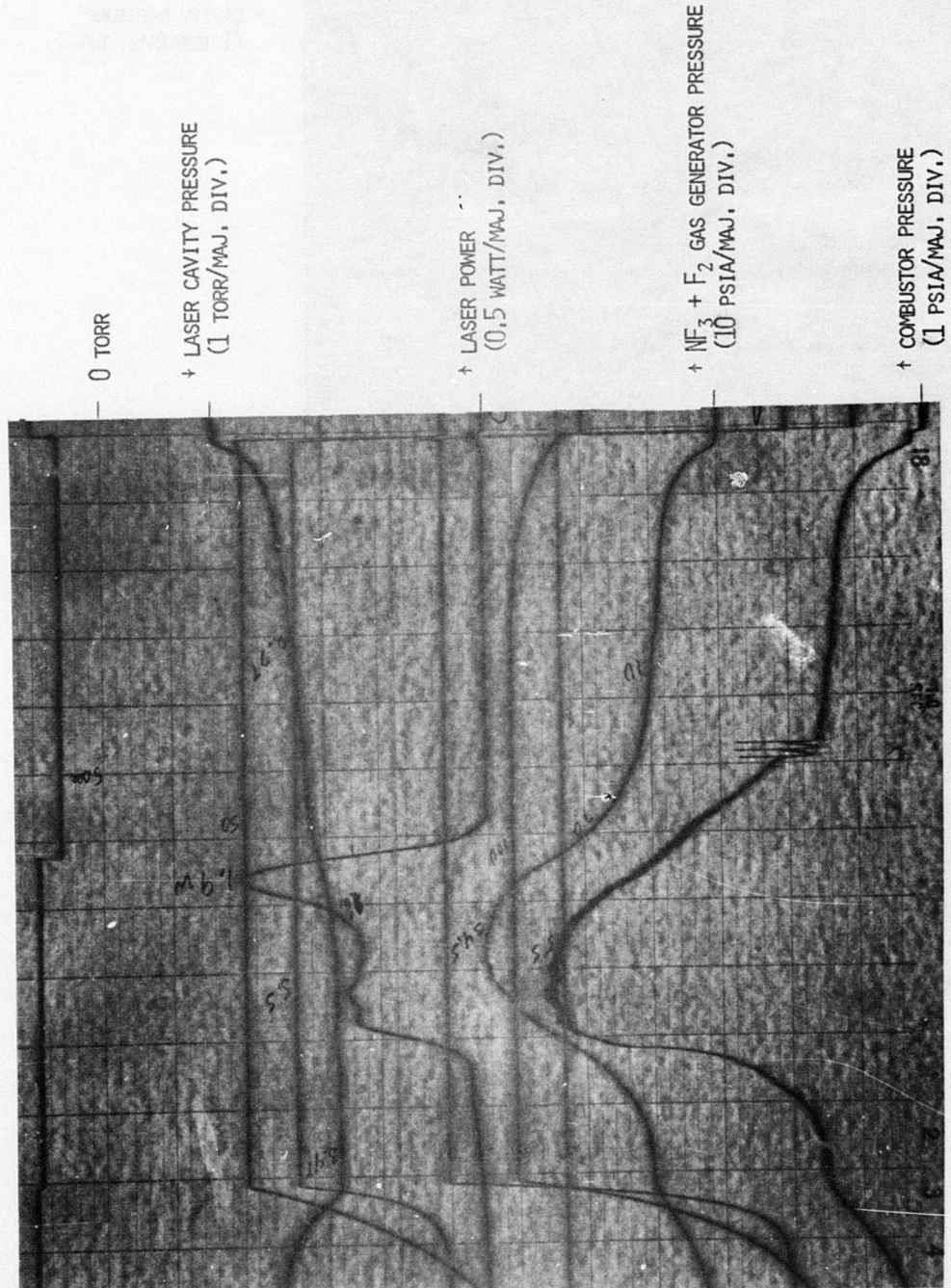


Figure 41. Oscillograph Record of First Lasing Test with  $\text{NF}_3 + \text{F}_2$  Gas Generator (Test No. 501)

the laser power output observed during Test No. 501 with the  $\text{NF}_3 + \text{F}_2$  gas generator was very close to the power output measured during the baseline test (Test No. 500-2). At seven seconds after the master switches were turned on in Test No. 501, the laser power was 1.3 Watts at a combustor pressure of 33 kPa (4.8 PSIA) and a cavity pressure of 3.2 Torr. This laser performance was 4 percent higher than the 1.25 Watt power output at the end of the baseline test (Test No. 500-2) at a combustor pressure of 32.8 kPa (4.75 PSIA) and a cavity pressure of 3.1 Torr.

Lasing tests with multiple gas generators were also conducted with the XCL5 laser, and lasing was demonstrated with up to three of the four laser reactants supplied simultaneously from the solid propellant gas generators. Lasing with the deuterium, hydrogen, and nitrogen all supplied from gas generators was demonstrated (Test No. 498, 3 Jan 1975). In that test, the laser power had reached 1.0 Watts when the hydrogen generator grain container popped out of the gas generator housing and terminated the test. Seven attempts were made to complete an "all solids" lasing demonstration with all four of the laser reactants supplied from gas generators. However, a series of experimental problems prevented lasing in these initial "all solids" tests, and the transfer of Capt Channell and Capt O'Pray in July 1975 terminated the test program before these problems could be corrected. The most

frequent problem in the multiple gas generator tests was poor combustion of the small nitrogen gas generator grains. As was discussed in Section IV.C., the small nitrogen generator grains pressed into cavities in the relatively massive stainless steel grain containers were difficult to ignite and, if they ignited, they frequently extinguished before they burned to the end of the grain. During one of the "all solids" tests, the small hydrogen generator grain extinguished prematurely in a similar manner. In two other tests, the orifice in the  $\text{NF}_3 + \text{F}_2$  gas generator cover plugged, and the grain combustion products were vented into the cryopump through the Nupro pressure relief valve. Sequencing failures which delayed the ignition of one or more of the gas generators prevented lasing in the remaining "all solids" tests. The oscillograph record of one of these tests (No. 542, 5 May 1975) is shown in Figure 42. The hydrogen generator pressure was stable at  $400 \pm 13.8 \text{ kPa}$  ( $58 \pm 2 \text{ PSIA}$ ) for 10 seconds, and the  $\text{NF}_3 + \text{F}_2$  gas generator pressure was  $165 \pm 13.8 \text{ kPa}$  ( $24 \pm 2 \text{ PSIA}$ ) for 3.5 seconds. However, in this test, the nitrogen generator grain failed to ignite which disrupted the planned ignition sequence and delayed the ignition of the  $\text{NF}_3 + \text{F}_2$  gas generator until after the  $\text{D}_2$  generator grain had burned out.

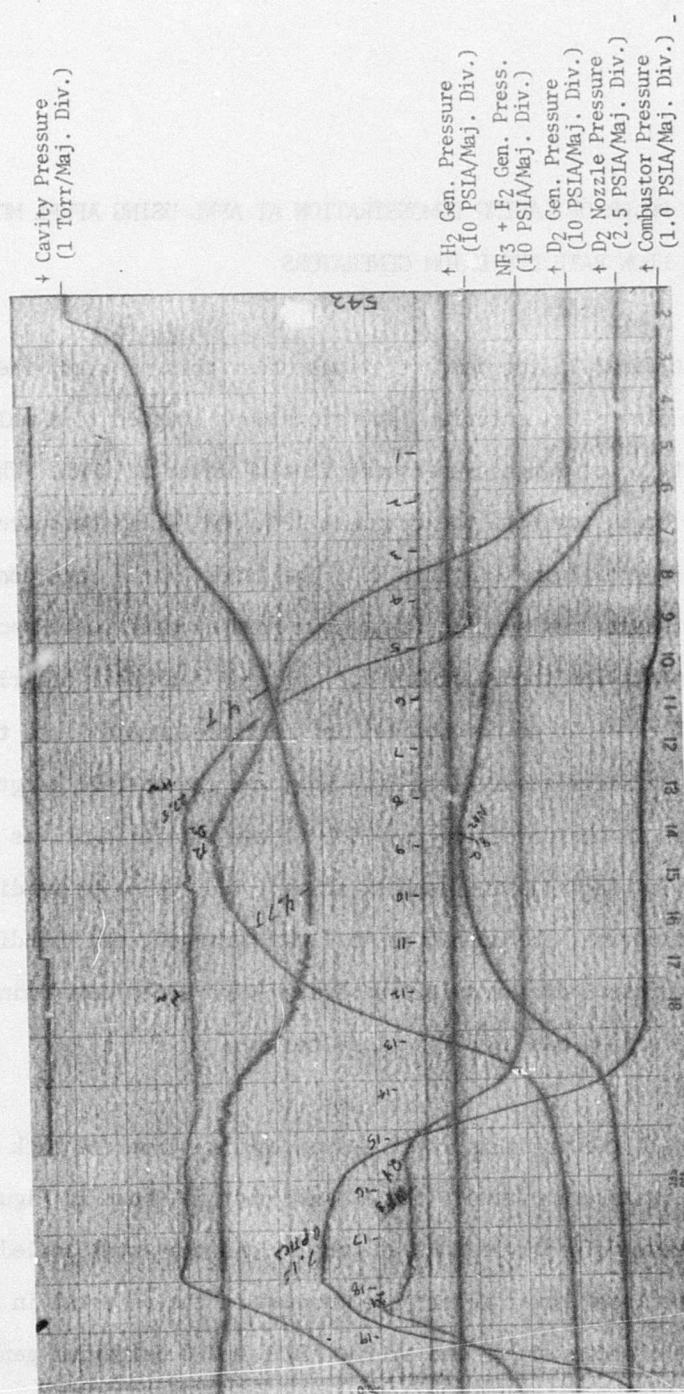


Figure 42. Oscillograph Record of Multiple Gas Generator Test No. 542

V.D. HIGH POWER DF LASING DEMONSTRATION AT AFWL USING AFRPL MOD 2  
HIGH FLOW RATE DEUTERIUM GENERATORS

For the final lasing demonstrations under this program, the AFRPL Mod 2 high flow rate deuterium generators were coupled to a multi-hundred watt power range, supersonic flow DF laser at AFWL. The laser nozzle and combustor were the original AFWL/TRW "CLII" hardware which is described in detail in Reference 20. The laser nozzle bank consisted of an array of contoured supersonic primary nozzles with sonic secondary injection slits for the  $D_2$  cavity fuel between each pair of primary nozzles. The height of the nozzles in the direction parallel to the nozzle throat slits was 1.27 cm (0.5 in), and the overall length of the nozzle array in the direction parallel to the optical axis was 17.78 cm (7.0 in). For these lasing demonstrations, the combustor oxidizer was elemental fluorine, the combustor fuel was hydrogen, and the diluent was helium. A digital data acquisition system with a dedicated minicomputer for data reduction was used for these tests.

An overall view of this laser system looking from the back side of the combustor assembly toward the exhaust duct is shown in Figure 43. The 90 percent reflectivity output coupler and the water cooled sensing head for the laser power meter\* are mounted on the pedestal in the right center of the photograph. One of the AFRPL Mod 2 deuterium generators

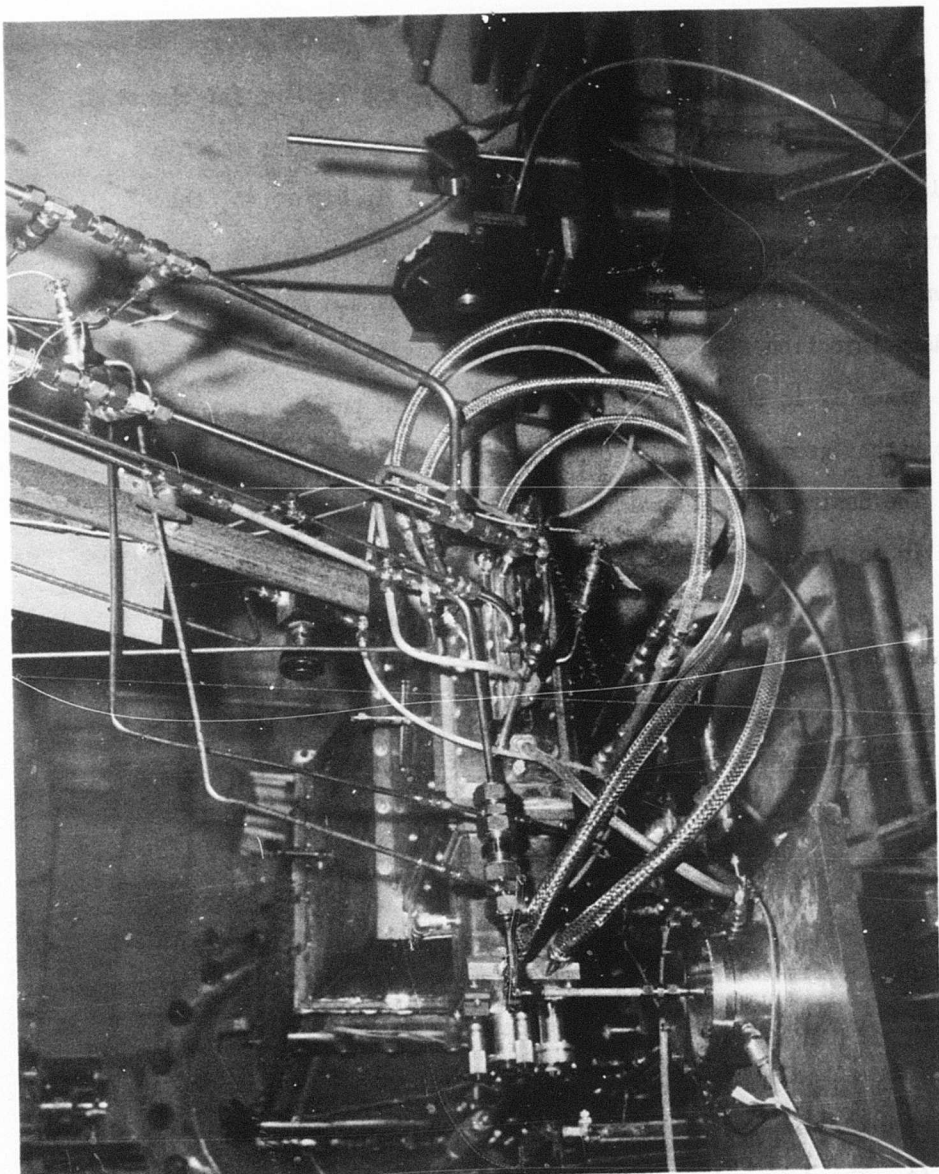


Figure 43. AFRPL Mod 2 Deuterium Generator Coupled to AFWL Supersonic Flow DF Laser for High Power Lasing Demonstration

is on the pedestal in the left foreground, and the housing for the other laser cavity mirror with its micrometer adjusting knobs is visible behind the outlet tube from the gas generator. In Figure 43, the deuterium metering nozzle assembly is shown installed in the line between the deuterium generator and the feed manifold for the laser secondary injection slits. A detailed cross section of this metering nozzle assembly is shown in Figure 13. For these tests, a metering nozzle with a geometric throat diameter of 2.527 mm (0.0995 in.) was used. The design and calibration of these metering nozzles are discussed in detail in Reference 7.

The deuterium generator grains for these tests were the standard 144 gram grains of the 3LAD2 formulation which are described in Section II.C. A photograph of a disassembled Mod 2 gas generator with one of these grains in the protective plastic bag in the foreground is shown in Figure 17.

During the first test with a deuterium generator coupled to the laser on 2 July 1975, a peak of 369.8 Watts of outcoupled power was measured at a  $D_2$  flow rate of 1.909 grams per second. The laser output power and deuterium mass flow rate histories for this test are shown in Figure 44. The data points plotted in Figure 44 are averages over 250 millisecond intervals computed by the digital data reduction system. As was typical for the grains of the 3LAD2 formulation prepared from the

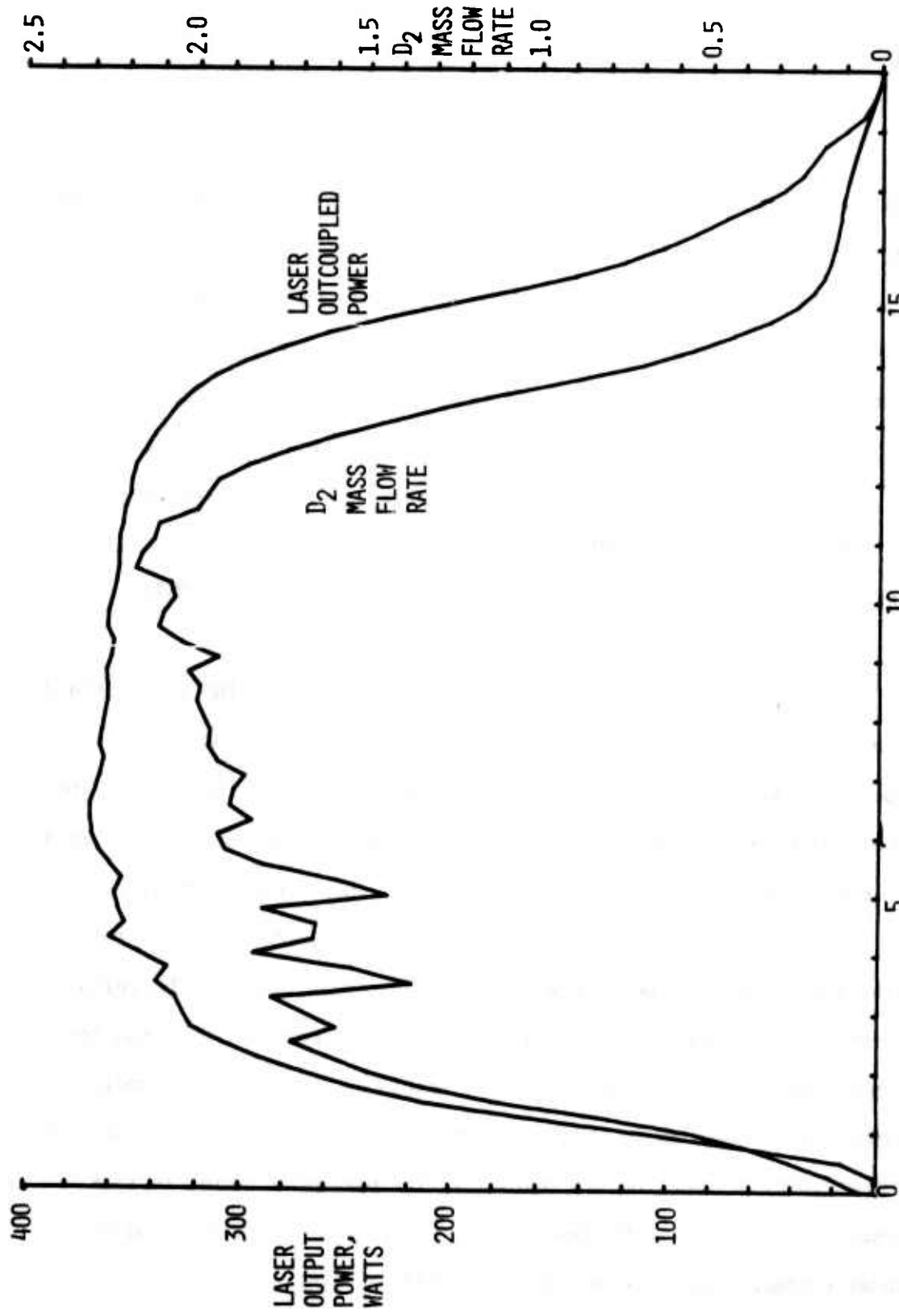


FIGURE 44. LASER POWER AND DEUTERIUM MASS FLOW RATE HISTORIES FOR THE FIRST MOD 2 DEUTERIUM GENERATOR LASING TEST ON THE AEM OF LASER

coarser ingredients (< 105  $\mu\text{m}$ ), there were several perturbations in the  $\text{D}_2$  mass flow rate early in the burn, but later in the test the  $\text{D}_2$  mass flow rate stabilized. The oscillograph data traces from a test of the same type of grain at AFRPL which are shown in Figure 18, exhibit similar initial irregularities. In Figure 44, the relatively slow time response of the laser power meter dampens the effect on the laser power of the initial variation in the  $\text{D}_2$  flow rate. At the peak power point in this initial gas generator lasing test, the cavity pressure was 5.38 Torr, and the laser combustor pressure was 103.8 kPa (15.06 PSIA).

Immediately following this initial lasing demonstration with a Mod 2 deuterium generator, a baseline lasing test using deuterium from the facility compressed gaseous deuterium supply system was conducted. The peak laser power measured during this baseline test was 385.2 Watts at a  $\text{D}_2$  mass flow rate of 2.00 grams per second. The 4.16 percent difference in outcoupled power between this baseline test and the preceding test with the deuterium generator was within the normal range of the variations in power (approximately plus or minus five percent) from run-to-run or within a run for this laser. Therefore, no definitive conclusions can be drawn as to whether there was any significant difference in output power between the two tests. At the peak power point in this baseline lasing test, the laser cavity pressure was 4.15 Torr and the laser combustor pressure was 100.5 kPa (14.58 PSIA).

Three additional tests with the Mod 2 deuterium generators were conducted at AFWL on 3 July 1975. On that day, during the initial baseline tests using deuterium from the facility feed system, the laser performance was found to be degraded. The laser power was lower than on the previous day, and the power varied by up to twenty percent during a baseline run at nominally constant conditions. During the limited test time available, the cause of this degradation in the laser baseline performance could not be identified and corrected. Therefore, the final three deuterium generator tests were conducted with the laser performance degraded. The peak output power during the second gas generator test was 251 Watts, and the peak power during the fourth test was 230 Watts. During the third gas generator test, the deuterium generator itself ignited and burned normally. However, no laser power was generated in this test because one of the safety interlocks in the facility fluorine supply system had been inadvertently left in the "safe" position, and, therefore, the oxidizer flow to the laser combustor was never initiated.

### REFERENCES

1. Doughty, J.R., O'Pray, J.E., and Channell, R.E., "Solid Propellants for Chemical Lasers", Proceedings of the First DOD Conference on High Energy Laser Technology, IRIA Center, Ann Arbor, MI, Dec 1974.
2. Goshgarian, B., and Solomon, W., AFRPL-TR-72-30, Apr 1972.
3. Love, D., Dengel, O., Pallay, B., Gotzmer, C., Greendale, A., Barber, W., Pisacane, F., Adams, C., Lee, R., and Winkler, E., "Development of Solid Propellant Gas Generators for Chemical Lasers", 11th JANNAF Combustion Meeting, Pasadena, CA, Sep 1974.
4. Dengel, O.H., Barber, W.H., and Bowen, R.E., "Solid Hydrogen/Deuterium Gas Generators for Chemical Lasers", 12th JANNAF Combustion Meeting, Newport, RI, CPIA Publication 273, Dec 1975.
5. Selph, C., and Hall, R., "USAF Rocket Propulsion Laboratory Theoretical ISP Program", AFRPL, Edwards AFB, CA, Sep 1974.
6. Hurd, D.T., An Introduction to the Chemistry of the Hydrides, John Wiley & Sons, Inc., New York, 1952.
7. Powell, M.F., and Bornhorst, B.R., Design and Experimental Evaluation of a Direct Combustion HF Chemical Laser (DCL-II), AFRPL-TR-72-67, Aug 1973.
8. Spencer, D., Mirels, H., and Duran, D., "Performance of a CW HF Chemical Laser with N<sub>2</sub> or He Diluent", Journal of Applied Physics, Vol. 43, p 1151, 1972.
9. Flanagan, J., Solid Propellant Laser Fuel Generator, AFWL-TR-73-195, Nov 1973.
10. Fluorine Generator Solid Ingredient Development, AFRPL-TR-75-49, Final Report, Contract F04611-74-C-0035, Rocketdyne, Sep 1975.
11. Hyman, H., Noble Gas Compounds, University of Chicago Press, Chicago, 1963.
12. Malm, J.G., and Appelman, E.H., "The Chemical Compounds of Xenon and Other Noble Gases", Atomic Energy Review, Vol. 7, No. 3, p 3, Oct 1969.
13. Dynamic Compatibility of Halogen Propellants, AFRPL-TR-72-118, Jan 1973.

14. United Technologies Corp., Chemical Systems Division, Contract DAAH03-76-M-3037, Army Missile Command, Redstone Arsenal, AL.
15. Falk, T.J., Parametric Studies of the DF-CO<sub>2</sub> Chemical Transfer Laser, AFWL-TR-71-96, Jun 1972.
16. Turner, F.T., and Feinleib, M., "Performance Criteria for Sorption Pumps", presented at the Eighth Annual Symposium of the American Vacuum Society, Washington, D.C., Oct 16-19, 1961.
17. Private communication, Dr. D. McClure, Boeing.
18. HF/DF Chemical Laser Technology Studies, AFWL-TR-74-150, Oct 1974.
19. Goshgarian, B., Selph, C., and O'Pray, J.E., 'Mass Spectrometric Investigation of Fluorocarbon Flames', paper presented at the AIAA/SAE 10th Propulsion Conference, San Diego, CA, Oct 21-23, 1974.
20. Hydrogen Fluoride Laser Technology Study, AFWL-TR-72-28, Feb 1972.